THE STATISTICS OF FINITE ROTATIONS IN PLATE TECTONICS

by

STEVEN J. HELLINGER

B.S., Massachusetts Institute of Technology
(1973)

SUBMITTED IN PARTIAL FULFILLMENT
OF THE REQUIREMENTS FOR THE
DEGREE OF

DOCTOR OF PHILOSOPHY

at the

MASSACHUSETTS INSTITUTE OF TECHNOLOGY

(May, 1979)

Signature of Author.....
Department of Earth and Planetary Sciences
May 4, 1979

Certified by.....
Thesis Supervisor

Accepted by.....
Chairman, Departmental Committee on Graduate Students

THE STATISTICS OF FINITE ROTATIONS IN PLATE TECTONICS

by

STEVEN J. HELLINGER

Submitted to the Department of Earth and Planetary Sciences on May 4, 1979 in partial fulfillment of the requirements for the Degree of Doctor of Philosophy

ABSTRACT

Incomplete knowledge of the pattern of magnetic lineations and fossil transform faults represented by sea floor spreading data on two plates generated by the same spreading center leads to uncertainties in a reconstruction of the past relative configuration of the plates. Such uncertainties may be treated mathematically using a finite rotation to describe one configuration relative to another. Part I of this paper presents the statistical formulation of the problem of uncertainty in the finite rotation. The error in a given data point is assumed to obey a spherical analogue of a truncated bivariate-normal probability distribution. The method of reconstruction reflects this assumption and the fundamental tenets of plate tectonics. The construction of a confidence region for the rotation tensor is considered in detail. The method of construction is shown to depend upon both the kind

of data set being examined and the assumptions that are made about uncertainties in the data. Several methods of construction are given, each of which is appropriate for a particular kind of data set and a particular set of assumptions about the uncertainties. The propagation of errors through a sequence of finite rotations is examined, and the uncertainty in a reconstruction of the relative configuration of two plates via reconstructions of intermediate pairs of plates is obtained.

Part II of this paper shows how the theory of Part I may be used to study the uncertainties of reconstructions in the South Pacific for the times of anomalies 13 and 18.

Name and Title of Thesis Supervisor: Peter Molnar

Associate Professor
of Earth Sciences

Table of Contents

THE STATISTICS OF FINITE ROTATIONS IN PLATE TECTONICS

Part II:
An Application to the Evolution of the South Pacific

CHAPTER I: INTRODUCTION

The first comprehensive presentation of the concept of continental drift was published by Taylor (1910), closely followed by Wegener (1929) and further elaborated by du Toit (1937) and others (see du Toit, 1937, pp. 11-36). The hypothesis of plate tectonics grew from the synthesis of this concept with the ideas of sea-floor spreading and transform faults (Hess, 1962; Wilson, 1965), and the contributions of many others (see Le Pichon et al., 1973, Chapter I). This hypothesis states that the strong outer layer of the earth is composed of a small number of large rigid plates. It is the interaction of these rigid plates at their boundaries that accounts for most of the present-day tectonic activity (Morgan, 1968; McKenzie and Parker, 1967; Isacks et al., 1968; see Le Pichon et al., 1973, Chapter II).

Material may be added, conserved, or consumed at a point on the instantaneous boundary between two rigid plates in relative motion. Oceanic crust is created at an oceanic ridge crest, conserved along a transform fault and destroyed in a trench. The creation of oceanic crust at an oceanic ridge crest establishes a geologic record of the accreting margin of the instantaneous boundary between the two plates. This record can be discerned from the linear magnetic anomalies which are established simultaneously with the creation of oceanic crust and thereafter borne away on either side of this accreting plate margin (Vine, 1966). Some of the newly-created oceanic crust may be destroyed or altered

during subsequent changes in relative motion. The relative shear of two sections of oceanic crust on opposite sides of a transform fault leaves a fossil trace, called a fracture zone, in the plates. The morphology of a section of fracture zones depends on the history of relative motion between the two plates at the succession of instantaneous plate boundaries since the time that the oldest part of this section moved beyond the transform fault. The relation between the transform fault at the time of interest (the instantaneous conserving plate boundary) and the segment of fracture zone which developed from it can thus be deduced only if the history of relative motion for appropriate times at relevent places on the plate boundary is known. Trenches are useless for reconstructions as oceanic crust is destroyed after it enters them.

The quantitative description of relative motions of rigid plates on a sphere is based on a well-known theorem due to Euler (see Bullard et al., 1965; see discussion in Le Pichon et. al., 1973, pp. 28-39):

> The general displacement of a rigid body with one point fixed is a rotation about some axis passing through the fixed point.

In the case of rigid plates constrained to move on the surface of a spherical earth, the motions can be described as rotations about an axis passing through the center. The points at which this axis intersects the sphere are

poles of rotation. The instantaneous relative motion of two rigid plates, represented by an infinitesimal rotation, may thus be completely described by a vector in the direction of the rotation axis with magnitude equal to the angular velocity. This description has several important implications for the geometry of boundaries between rigid plates in relative motion.

A transform fault must be a small-circle around the pole of rotation that describes the instantaneous relative motion between a pair of rigid plates (see Le Pichon et al., 1973, p. 29). If the pole of rotation remained fixed with respect to the pair of plates for a finite time, then the trend of the transform fault would not change during this period (see Le Pichon et al., 1973, p. 33). The trend of the fracture zone developed from the transform fault during this finite time would follow the same small-circle path. This relation is rarely observed. Further, all plates cannot rotate through finite angles about instantaneous relative rotation axes fixed with respect to the pairs of plates (McKenzie and Morgan, 1969; see Le Pichon et al., 1973, pp. 20,33,34,108). Although there is no geometric constraint on the shape of a segment of ridge axis, the ridge is often observed to be nearly perpendicular to the direction of spreading (see Le Pichon et al., 1973, pp. 20,21,24,26,27). These facts establish the kinematic framework within which the question of uncertainty in a reconstruction

must be discussed.

The Eulerian description of a finite rotation may be formulated as a 3x3 orthogonal tensor Λ which depends upon the latitude and longitude of the pole of rotation, (θ, ϕ), and the angle of rotation ψ. Inferences about Λ are thus seen to be inferences about (θ, ϕ, ψ). The necessity for such inferences arises from the important question of estimation of the relative finite motion of two plates via estimates of the relative finite motions of several intermediate pairs of plates. The ultimate goal of this work is to estimate the parameters and associated uncertainties of the Λ_i, $i = 1, 2, .., N-1$ which are necessary to describe uniquely the finite relative motions of (N-1) plates with respect to one plate taken fixed. This paper discusses in detail the problem of estimation of the parameters of a finite rotation from sea-floor spreading data.

CHAPTER II: FORMULATION OF THE PROBLEM

II.1 Uncertainties in Sea-Floor Spreading Data

The linear magnetic anomalies carried away from oceanic ridge crests are presumed to delineate oceanic crust of constant age formed at a past accreting plate margin. If a pair of plates has remained completely rigid since the lineations of a given age were developed, then the rotation which restores the original relative positions of these lineations will also restore the plates to their past relative position. This rotation may not precisely align the segments of the formerly active transform faults along corresponding offsets of the lineations because the morphology of a fracture zone may evolve during the history of relative motion between the two plates (see discussion in Chapter I). A reconstruction, however, may not let a magnetic lineation cross a fracture zone.

The former plate boundary is defined at a finite number of discrete points where ship tracks cross the features. Systematic differences among crossings that are presumed to represent the same segment of the former plate boundary may arise in several ways. An unmapped fracture zone may exist between magnetic anomaly crossings that are assumed to be part of the same lineation. Crossings of corresponding plate boundaries that have been assumed to lie on the same fracture zone may actually lie on different fracture zones. The part of a magnetic anomaly profile that represents oceanic crust of a given age is not precisely known. We

do not know exactly where the transform fault was within the fracture zone, and if there has been subsequent deformation we cannot know where it was. Thus there are uncertainties of position, due to ignorance, which may lead to systematic errors, and another possible error due to deformation (see discussion in: Le Pichon et al., 1973, pp. 65,66,103-114). Further, there are errors of location associated with the navigational record of the ship. The basic assumption to be made here is that any systematic error will be small compared with the uncertainty assigned to the position of the magnetic lineation or transform fault.

II.2 Geologic Uncertainty and Statistical Uncertainty

In evaluating the correctness of a reconstruction of two plates that share an oceanic ridge there are a number of uncertainties to be considered. The information in the extant geologic record relevant to the reconstruction may be insufficient to constrain the reconstruction uniquely because the geologic record may be incomplete. Thus there may be a range of reconstructions that are consistent with the extant geologic record. Even if the geologic record is complete the geology may have been altered since the time it was laid down. Moreover, we have only a limited sampling of the extant geologic record and our interpretation of this data is strongly influenced by assumptions about the kinds of geologic processes that have been active in the

past. It is therefore often difficult to provide a quantitative interpretation of geologic uncertainties.

Not all geologic questions of uncertainty can be treated by statistical methods. To pose the geologic problem as a statistical problem we use the following definitions:

(1) The error in a datum is specified by the Cartesian components of the difference between the datum and its true position.

(2) The error in a rotation tensor is specified by the components of the difference between the rotation tensor and the true rotation tensor (in the 9-dimensional Euclidean space of real 3x3 matrices).

We make the following assumptions:

(1) Geologic information would be sufficient to yield the correct reconstruction if data were correctly interpreted and without uncertainties of location.

(2) The errors in the data are mutually independent and obey a law of probability that may be described by a probability density function. The particular form of the probability distribution for the error in a single data point is a spherical analogue of a truncated bivariate-normal probability distribution (Chapter III).

A technique to estimate the rotation tensor that specifies the reconstruction will be introduced (Chapter III) based on these two assumptions.

These assumptions and the technique of estimation

provide for a functional relation between the error in the estimated rotation tensor and both the true positions of the data and the errors in the data. There will be no error in the estimated rotation tensor if there are no errors in the data.

With the given assumptions the methods of statistical theory will furnish a rational means for expressing the uncertainty in the reconstruction by means of a confidence region for the rotation tensor. The method by which a confidence region is obtained is described in part (3) of section III.6 of this paper (see, e.g., Kendall and Stuart, 1973, pp. 103-136; Fisher, 1959, pp.37-44; Cramér, 1974, pp. 507-524 for discussions of confidence intervals and regions).

II.3 Assumptions About the Geologic Record

The following assumptions will be made about the geologic record:

(1) A pair of corresponding lineations lies between the same pair of fracture zones. There is no fracture zone between the pair of fracture zones that are at the ends of the lineations.

(2) If lineation data were without error then we could obtain the exact shapes and positions of the lineations. The unique correct reconstruction would cause the pairs of corresponding lineations to overlie precisely.

(3) Fracture zones may or may not line up precisely in the correct reconstruction, and the position of the transform fault within the fracture zone may have been systematically altered. These details depend upon the history of relative motion between the two plates.

(4) The shape of a lineation between a pair of fracture zones or a segment of transform fault between a pair of offset lineations can be well-approximated by one or more great-circle arcs. By well-approximated we mean that any difference between the actual shape and approximate shape is small compared to the uncertainties of position associated with the data.

II.4 Methods of Reconstruction

Consider the simple but relevant problem in Figure I. We have data $\hat{s}_{ijk}$, $i=1,2; j=1,2; 1 \leq k \leq n_{ij}$, for corresponding lineations on a pair of rigid plates. Here the index i denotes the plate, the index j denotes a particular lineation on the plate, and the index k denotes a particular data point of the n_{ij} points for lineation j on plate i. If $\hat{s}_{ijk}$ were without error its position would be s_{ijk}. Assume plate 1 is fixed and that Λ is the rotation tensor that restores plate 2 to its past position with respect to plate 1. Each lineation is assumed to follow an arc of a great-circle. Each great-circle can be specified by a unit vector that is normal to the plane that contains the great-circle. These are denoted by $p_{11}, p_{12}, p_{21}, p_{22}$, chosen so

that $p_{11}=\Lambda p_{21}, p_{12}=\Lambda p_{22}$. The first task is to derive a good reconstruction from the data. Figure Ib shows such a reconstruction.

There are two criteria of fit that have been used in making reconstructions. Bullard et al. (1965) fit together the digitized contours of continental margins on opposite sides of the Atlantic Ocean. For a given fitting pole they computed the angle of rotation that minimized the sum of squares of angular misfits along small circles between the two contours. The fitting pole for which this sum was an absolute minimum was found by search methods. This criterion is not appropriate to the present problem for several reasons:

(1) The data consists of a small number of well-separated points with assigned standard deviations of error, not a set of contours.

(2) The criterion suffers from two major limitations pointed out by McKenzie et al. (1970): The criterion does not perform well if parts of each contour form a small circle about the fitting pole; further, it weighs misfits near the fitting pole more heavily than those near the equator relative to this pole.

(3) The criterion takes no account of the uncertainties in the data. Suppose the likely errors in $[\hat{s}_{12k}, 1\leq k\leq 3]$ were decreased by a factor of 10. The fit of the two lower lineations ought to be weighted more heavily in making a reconstruction. Bullard et al.'s criterion does not include

this.

To avoid some of the problems of Bullard et al.'s method, McKenzie et al.(1970) minimized the misfit area between two contours. To obtain a good estimate of the misfit area, McKenzie et al. (1970) and McKenzie and Sclater (1971) represented each contour by a sequence of points α_i,β_i on the unit sphere. The α_i are rotated by trial rotation T to resultant points denoted by γ_i, where $\gamma_i=T\alpha_i$. Taking each γ_i in turn, the nearest point β_j is found and a measure of the misfit area is provided by the triple scalar product $\gamma_i \cdot \beta_j x \beta_{j+1}$. The first and third objections to Bullard et al.'s criterion are also valid objections to the use of this criterion for the present problem.

The method of reconstruction proposed here is as follows:

(1) We refer to Figure I. A preliminary reconstruction will be found. Let $\hat{\Lambda}$ denote the rotation tensor for this reconstruction.

(2) We refer to Figure II. The rotated $\hat{s}_{2jk}$ are $\hat{\Lambda}\hat{s}_{2jk}$. The great-circle that fits each of the combined datasets $[\hat{s}_{111},\hat{s}_{112},\hat{s}_{113},\hat{\Lambda}\hat{s}_{211},\hat{\Lambda}\hat{s}_{212}]$, $[\hat{s}_{121},\hat{s}_{122},\hat{s}_{123},\hat{\Lambda}\hat{s}_{221},$ $\hat{\Lambda}\hat{s}_{222},\hat{\Lambda}\hat{s}_{223}]$ is estimated by least-squares methods (see section III.4). Let $\hat{p}_1,\hat{p}_2$ denote the unit vectors through the origin that are normal to the planes of these great-circles.

The distance of each point in the first combined

dataset from the plane normal to $\hat{p}_1$ is calculated. Each of these distances is virtually identical to the distance of the associated point from the estimated great-circle measured along a meridian through the point and $\hat{p}_1$ when this distance is small. The distance of each point is then divided by the standard deviation of error that was assigned to the point. The sum of squares of the weighted distances is computed. A similar sum of squares is computed for the second combined dataset. The sum of the two resultant sums is taken as the measure of fit of the data.

The angle that minimizes the measure of fit for the pole of $\hat{\Lambda}$ is found. This is accomplished as follows:

Let $\hat{\psi}$ be the angle of $\hat{\Lambda}$. The initial angle is $\hat{\psi}$. The measure of fit is computed for each angle $\hat{\psi}+na$, $-N \leq n \leq N$, where n is an integer, $a>0$ is a chosen increment and Na represents the half-range of search. Let $\hat{\psi}+n_0 a$ represent the angle of this group for which the measure of fit is a minimum. The measure of fit is then examined for each angle $\hat{\psi}+n_0 a+mb$, $-M \leq m \leq M$, $b=a/M$. Let $\hat{\psi}+n_0 a+m_0 b$ represent the angle of this group for which the measure of fit is a minimum. This angle is chosen as the angle that minimizes the measure of fit.

This task is then repeated for a number of poles of rotation at a chosen distance from the trial pole. The pole for which the measure of fit is a minimum is selected as the new starting point. If no pole is better than the

initial pole then the chosen distance is decreased by a multiplicative factor. The process is repeated until a reconstruction is obtained that minimizes the measure of fit within an acceptable approximation. This reconstruction will be chosen as the most acceptable reconstruction.

II.5 Caveats in the Use of the Methods Herein Proposed

The method of reconstruction utilizes a least-squares analysis of errors. As with all least-squares approaches, the reconstruction becomes quite sensitive to data that depart from the assumptions of the method (e.g., misplaced data points; points that were assigned standard deviations of error much smaller than the actual standard deviations of error). The mathematical structure will provide sensible results if the standard deviations of error assigned to the data are small and if there are a number of significant changes in trend among the various sections of data.

CHAPTER III: THE STATISTICS OF FINITE ROTATIONS

III.1 Introduction

We begin with a definition of coordinates. In a right-handed orthonormal system of coordinates (x,y,z) let a unit vector s have coordinates (a,b,c), $|c|\neq 1$. Let the polar coordinates (θ_0, ϕ_0) of s be defined by the relations:

$$\theta_0=\sin^{-1}c, \; -\frac{\pi}{2} < \sin^{-1}c < \frac{\pi}{2}$$

$$\phi_0=\tan^{-1}(b/a) + m\pi + 2n\pi \text{ for } a\neq 0, \; -\frac{\pi}{2} < \tan^{-1}(b/a) < \frac{\pi}{2}$$

n= any integer, $m = \begin{cases} 0 & a>0 \\ 1 & a<0 \end{cases}$. For a=0, b>0 we have $\phi_0=\pi/2 + 2n\pi$. For a=0, b<0 we have $\phi_0= -\pi/2 + 2n\pi$.

Then the Cartesian coordinates of s satisfy the relation

$$(a,b,c) = (\cos\theta_0\cos\phi_0, \cos\theta_0\sin\phi_0, \sin\theta_0)$$

Let ' denote the transpose of a vector. Let the index i (i=1,2) denote the plate and let j ($1\leq j\leq J$, $J>1$) denote a particular segment (lineation or fossil transform section) for plate i. We possess data $(\hat{s}_{ijk}, \; 1\leq k\leq n_{ij})$ for n_{ij} crossings of segment ij. The associated points without error are $(s_{ijk}, \; 1\leq k\leq n_{ij})$. These points satisfy $\hat{s}'_{ijk}\hat{s}_{ijk}=1$ and $s'_{ijk}s_{ijk}=1$ respectively. The Cartesian coordinates of $\hat{s}_{ijk}$ are $(\hat{x}_{ijk}, \hat{y}_{ijk}, \hat{z}_{ijk})$ and the polar coordinates are $(\hat{\theta}_{ijk}, \hat{\phi}_{ijk})$. The analogous coordinates for s_{ijk} are $(x_{ijk}, y_{ijk}, z_{ijk})$ and $(\theta_{ijk}, \phi_{ijk})$.

III.2 How the Statistical Uncertainty in a Point on the Unit Sphere Will be Specified

We refer to Figure III. Let s be a reference point on the unit sphere and let $\hat{s}$ be an observation of s. Let K denote the plane normal to s through the origin. If $\hat{s}$ is required to be in the hemisphere centered at s then $\hat{s}$ is unambiguously specified by its projection onto K. The projection of $\hat{s}$ onto K, rather than $\hat{s}$ itself, will be used in analysis of the error in $\hat{s}$. The probability that the projection of $\hat{s}$ is contained by the portion of K within the unit sphere is one. The statistical distribution of $\hat{s}$ can be represented by a statistical distribution of vectors in K if the probability assigned to the portion of K within the unit sphere is one. If nearly all of this probability is concentrated near the origin then the probability found in the vicinity of the intersection of K with the unit sphere will have little effect upon the analysis. If some of the latter probability were distributed in a reasonable manner over the part of K outside the unit sphere then it would still have little effect upon the analysis. In this case the distribution of $\hat{s}$ could be approximately represented by a statistical distribution of vectors in all of K. This approximation will be made in the analysis to follow.

III.3 The Statistical Distribution of Errors in the Data

We refer to Figure III. Let q,r be unit vectors in K such that [q,r,s] form a right-handed orthonormal basis. Let $\hat{s} = s + e$ where $e'=(u,v,w)$ and $\hat{s}'\hat{s} = 1$. Then

$$\hat{s} = (q'e)q + (r'e)r + s + (s'e)s$$

As $(s+e)'(s+e) = 1$ we have $e's = -(e'e)/2$ and

$$\hat{s} = (q'e)q + (r'e)r + s - ((e'e)/2)s$$

Let r be chosen as a unit vector in the (x,y) plane. Let $q=r \times s$ where '$\times$' denotes the vector product. If $s' \neq (0,0,1)$ then the vectors q and r are determined by s up to sign, $(q,r) = \pm(q(s),r(s))$, where

$$\begin{bmatrix} q'(s) \\ r'(s) \end{bmatrix} = \pm \begin{bmatrix} -ac/(1-c^2)^{1/2}, & -bc/(1-c^2)^{1/2}, & (1-c^2)^{1/2} \\ b/(1-c^2)^{1/2}, & -a/(1-c^2)^{1/2}, & 0 \end{bmatrix}$$

In polar coordinates

$$\begin{bmatrix} q'(s) \\ r'(s) \end{bmatrix} = \pm \begin{bmatrix} -\cos\phi_0 \sin\theta_0, & -\sin\phi_0 \sin\theta_0, & \cos\theta_0 \\ \sin\phi_0, & -\cos\phi_0, & 0 \end{bmatrix}$$

Let $O(\varepsilon)$ represent a quantity d (vector or scalar) such that $|d| \leq C|\varepsilon|$ for all ε sufficiently small and some finite constant C. Choose $\hat{s}$ close to s, $e'e \ll 1$, $a \neq 0$. For $|u| < |a|/2$ we have

$$\begin{aligned} \phi(\hat{s}) &= \tan^{-1}((b+v)/(a+u)) + m\pi + 2n\pi \\ &= \phi(s) + (av-bu)/(a^2+b^2) + (u/a)(bu-av)/(a^2+b^2) \\ &\quad -(b/a)(av-bu)^2/(a^2+b^2)^2 + O(|e|^3)/a^2 \end{aligned}$$

For a=0 we use

$$\hat{\phi(s)}=\cot^{-1}(u/(b+v)) + m\pi + 2n\pi,\ -\frac{\pi}{2} <\cot^{-1}(u/(b+v))< \frac{\pi}{2},$$

m,n are as defined in section III.1 .

Then for $|v|<|b|/2$ we have

$$\hat{\phi(s)}=\phi(s) - u/(b+v) + (u/(b+v))^3/3 - O((u/b)^5)$$

For $|w|<(1-|c|)/2$ we have

$$\hat{\theta(s)}=\sin^{-1}(c+w) = \theta(s) + w/(1-c^2)^{1/2} + (c/2)w^2/(1-c^2)^{3/2} + O(w^3)/(1-c^2)^{5/2}$$

We have

$$\begin{matrix} q'e \\ r'e \end{matrix} = \pm \begin{matrix} (-acu-bcv+w(1-c^2))/(1-c^2)^{1/2} \\ (bu-av)/(1-c^2)^{1/2} \end{matrix}$$

As s'e=au+bv+cw = -(e'e)/2 we have

$$\begin{matrix} q'e \\ r'e \end{matrix} = \pm \begin{matrix} w/(1-c^2)^{1/2} -(c/2)(e'e)/(1-c^2)^{1/2} \\ (bu-av)/(1-c^2)^{1/2} \end{matrix}$$

Therefore

$$\begin{matrix} q'e \\ r'e \end{matrix} = \pm \begin{matrix} \hat{\theta(s)}-\theta(s) + O(e'e)/(1-c^2)^{3/2} \\ -(\hat{\phi(s)}-\phi(s))\cos\theta_0 + O(e'e)/a \end{matrix}$$

where the terms O(e'e) in this expression can be determined directly from the expansions for $\hat{\theta(s)}$ and $\hat{\phi(s)}$ given above. In this case q'e represents the change in latitude to the first order in $|e|$ and r'e represents the component of e along the parallel of latitude θ_0 to the first order in $|e|$.

Define w_1=q'e, w_2=r'e, w'=(w_1,w_2). We assume w to have a bivariate-normal distribution with mean 0 and probability density given by (see Morrison, 1967, Chapter 3; Cramér,

1974, pp. 287-288):

$$(\det(A))^{-1/2}(2\pi)^{-1}\exp(-\tfrac{1}{2}w'A^{-1}w)$$

where A is a positive definite covariance matrix and det(.) is the determinant function. Further, we will assume $A=\sigma^2 I$ where I is the identity matrix and σ is a positive scalar, $\sigma<<1$. This distribution, for errors small in relation to the diameter of the earth, is a close approximation to distributions often assumed for spherical data such as those of Fisher and Bingham (Mardia, 1972, Chapters 8,9). The contours of constant probability density are circles in K of the form $w'A^{-1}w = \sigma^{-2}w'w$ = constant. We can incorporate information about the approximate magnitude of error within this formal structure. To extend to all data, it will be assumed that the error in $\hat{s}_{ijk}$ is of this form with covariance matrix $H_{ijk}=\sigma^2_{ijk}I$.

III.4 Estimation of Great-Circles

Let p_{ij} be a unit vector. The scalar product $p'_{ij}\hat{s}_{ijk}$ gives the distance of $\hat{s}_{ijk}$ from the plane perpendicular to p_{ij}. When this distance is small it is virtually identical to the distance of $\hat{s}_{ijk}$ from the great-circle associated with this plane measured along a meridian through $\hat{s}_{ijk}$ and p_{ij}. The distance weighted by the standard deviation of error assigned to s_{ijk} is $p'_{ij}\hat{s}_{ijk}/\sigma_{ijk}$. The sum of squares of the weighted distances of the $\hat{s}_{ijk}$ from this plane for $1\leq k\leq n_{ij}$ is

$$\sum_{1\leq k\leq n_{ij}} (p'_{ij}\hat{s}_{ijk})^2/\sigma^2_{ijk} = p'_{ij}\hat{B}_{ij}p_{ij}$$

where $\hat{B}_{ij}$ is the 3x3 weighted covariance matrix

$$\hat{B}_{ij} = \sum_{1\leq k\leq n_{ij}} \sigma^{-2}_{ijk} \begin{bmatrix} \hat{x}^2_{ijk} & \hat{x}_{ijk}\hat{y}_{ijk} & \hat{x}_{ijk}\hat{z}_{ijk} \\ \hat{y}_{ijk}\hat{x}_{ijk} & \hat{y}^2_{ijk} & \hat{y}_{ijk}\hat{z}_{ijk} \\ \hat{z}_{ijk}\hat{x}_{ijk} & \hat{z}_{ijk}\hat{y}_{ijk} & \hat{z}^2_{ijk} \end{bmatrix}$$

To find the plane that gives the arc segment with best weighted least-squares fit to the data is equivalent to finding an eigenvector $\hat{p}_{ij}$ associated with the smallest eigenvalue of the positive semidefinite symmetric matrix $\hat{B}_{ij}$: $\hat{B}_{ij}\hat{p}_{ij}=\tau\hat{p}_{ij}$, τ minimal. Let $\hat{\alpha}_{ij},\hat{\beta}_{ij},\hat{\gamma}_{ij}$ be the eigenvalues of $\hat{B}_{ij}$. We assume $\hat{\alpha}_{ij}>\hat{\beta}_{ij}>\hat{\gamma}_{ij}\geq 0$. Let $\hat{q}_{ij},\hat{r}_{ij},\hat{p}_{ij}$ be the respective associated eigenvectors of unit length (there are two such eigenvectors for each eigenvalue but they differ only in sign), chosen so that $\hat{q}_{ij} \times \hat{r}_{ij}=\hat{p}_{ij}$ where 'x' denotes the vector product.

If $\hat{s}_{ijk}=s_{ijk}$, $1\leq k\leq n_{ij}$, we define $\hat{B}_{ij}=B_{ij}$, $\hat{p}_{ij}=p_{ij}$, $\hat{q}_{ij}=q_{ij}$, $\hat{r}_{ij}=r_{ij}$, $\hat{\alpha}_{ij}=\alpha_{ij}$, $\hat{\beta}_{ij}=\beta_{ij}$, $\hat{\gamma}_{ij}=\gamma_{ij}=0$. These quantities represent the eigenvectors and eigenvalues of $\hat{B}_{ij}$ if there were no errors in the data. Hence p_{ij} defines the great-circle through the true points that correspond to the actual observations.

III.5 Criterion of Fit

Let $\hat{\Lambda}$ be the rotation tensor associated with a chosen reconstruction. Let $\hat{B}_j$, $1 \leq j \leq J$, be the weighted covariance matrix (defined in section III.4) for the combined data $[\hat{s}_{1jk},\ 1 \leq k \leq n_{1j};\ \hat{\Lambda}\hat{s}_{2jk},\ 1 \leq k \leq n_{2j}]$. Let $\hat{\alpha}_j, \hat{\beta}_j, \hat{\gamma}_j$ be the eigenvalues of $\hat{B}_j$. We assume $\alpha_j > \beta_j > \gamma_j \geq 0$. Let $\hat{q}_j, \hat{r}_j, \hat{p}_j$ be the respective associated eigenvectors, chosen so that $\hat{q}_j \times \hat{r}_j = \hat{p}_j$. Let $\hat{K}_j$ denote the plane normal to $\hat{p}_j$. Let t_{1jk} denote the point that is the intersection of a great-circle through $\hat{s}_{1jk}$ and $\hat{p}_j$ with the great-circle defined by $\hat{K}_j$ (there are two such points of intersection but the point of interest is that point which is closest to $\hat{s}_{1jk}$). Let t_{2jk} be the analogous point for $\hat{\Lambda}\hat{s}_{2jk}$ (see Figure II).

In the j th section the sum of squares of the weighted distances of the fixed and rotated points from $\hat{K}_j$ is $\hat{\gamma}_j$. The measure of fit to be used is

$$\Phi_0 = \sum_{1 \leq j \leq J} \hat{\gamma}_j$$

This criterion of fit has an interpretation in terms of classical statistical theory. Given the statistical assumptions of section III.3, the likelihood function (Kendall and Stuart, 1973, Chapter 18; Cramér, 1974, pp. 498-499; Morrison, 1967, p. 14) for the set of observations $[\hat{s}_{ijk}]$ is proportional to

$$\prod_{i,j,k} \exp\{\tfrac{1}{2}(s'_{ijk}\hat{s}_{ijk}/\sigma_{ijk})^2\} \qquad (1)$$

The points $[s_{ijk},\ 1 \leq k \leq n_{ij}]$ satisfy $p'_{ij}s_{ijk}=0$ (section III.4). For any rotation tensor Λ expression (1) equals

$$\prod_{j,k} \exp\{\tfrac{1}{2}(s'_{1jk}\hat{s}_{1jk}/\sigma_{1jk})^2\} \prod_{j,k} \exp\{\tfrac{1}{2}[(\Lambda s_{2jk})'\hat{\Lambda s}_{2jk}/\sigma_{2jk}]^2\} \qquad (2)$$

The object is to find estimates of the unknowns s_{ijk}, Λ such that expression (2) is maximized subject to $p'_{1j}s_{1jk} = (\Lambda p_{2j})'\Lambda s_{2jk} = 0$ and $p_{1j}=\Lambda p_{2j}$ (or $p_{1j}= -\Lambda p_{2j}$ if the signs are opposite). Discussions of maximum likelihood estimation can be found in: Kendall and Stuart, 1973, Chapter 18; Cramér, 1974, pp. 498-506; Morrison, 1967, pp. 14-17; Fisher, 1959, Chapter 6). This problem is equivalent to

$$\max_{s_{ijk},\Lambda} \{ \sum_{j,k} (s'_{1jk}\hat{s}_{1jk}/\sigma_{1jk})^2 + \sum_{j,k} [(\Lambda s_{2jk})'\hat{\Lambda s}_{2jk}/\sigma_{2jk}]^2 \} \qquad (3)$$

where $s'_{1jk}p_{1j} = (\Lambda s_{2jk})'p_{1j} = 0$ for all j and k.

The maximum of expression (3) occurs when $s_{1jk}=t_{1jk}\perp p_{1j}$, $s_{2jk}=t_{2jk}\perp p_{1j}$. Then p_{1j}, $\hat{s}_{1jk}$, t_{1jk} are coplanar and

$$(t'_{1jk}\hat{s}_{1jk})^2 = 1 - (p'_{1j}\hat{s}_{1jk})^2$$

Similarly $(t'_{2jk}\Lambda\hat{s}_{2jk})^2 = 1 - (p'_{1j}\Lambda\hat{s}_{2jk})^2$. Thus the given problem is equivalent to

$$\min_{p_{1j},\Lambda} \{ \sum_{j,k} (p'_{1j}\hat{s}_{1jk}/\sigma_{1jk})^2 + \sum_{j,k} (p'_{1j}\Lambda\hat{s}_{2jk}/\sigma_{2jk})^2 \}$$

(4)

Expression (4) is quadratic in the components of each of p_{1j} and Λ. For fixed Λ the expression is quadratic in p_{1j} and there are 3J unknown components. These 3J components satisfy the following J quadratic conditions:

$$p'_{1j}p_{1j}-1=0, \quad 1\leq j\leq J \qquad (5)$$

Hence for fixed Λ we can obtain linear equations in the 3J unknown components with J Lagrange multipliers. In this case (4) reduces to J separate eigenvalue equations of the kind discussed in section III.4 . The j th equation involves only p_{1j}, Λ, and the relevant data.

With Λ unknown (4) is fourth-order in the components of both p_{1j} and Λ. There are 3J+9 unknown components. Let $\lambda_1,\lambda_2,\lambda_3$ be the respective column vectors of Λ. The 3J+9 unknown components satisfy the J quadratic conditions of (5) and also the following 6 quadratic conditions:

$$\lambda'_i\lambda_i-1=0, \quad i=1,2,3 \; ; \; \lambda'_i\lambda_j=0, \quad i\neq j, \quad 1\leq i,j\leq 3$$

Therefore we can obtain non-linear equations in the 3J+9

unknown components with J+6 Lagrange multipliers. This yields a non-linear system with 4J+15 unknown quantities. The non-linearity of the system necessitates the use of a numerical method for its solution. In virtually all cases it will be computationally impractical to obtain an accurate solution of (4) by a numerical approach because the dimensionality of the system will be quite large.

We consider the accuracy of an approximate solution of this system as follows:

Let $\hat{u}$ denote the pole of rotation of the most acceptable rotation tensor $\hat{\Lambda}$. Let $\hat{\Phi}$ be the associated measure of fit. For a given pole u_* in the vicinity of $\hat{u}$ we calculate the angle that minimizes the measure of fit by the method discussed in section II.4 . This pole and angle specify a measure of fit denoted by Φ_*. For most datasets there will be a region of u_* in the vicinity of $\hat{u}$ for which Φ_* is only slightly different from $\hat{\Phi}$. This region will be very narrow in one direction and very long in the direction that is normal to the first direction (see, e.g., discussion in Appendix I). If u_* is far from $\hat{u}$ but u_* lies within the region along the long axis then the system will appear to have a reasonable solution. If u_* is close to $\hat{u}$ but u_* lies along the short axis then the system will appear to have a poor solution. This implies that the accuracy of an approximate solution is hard to judge from the degree of agreement of the terms in (4); hence an approximate

solution of the system is likely to be unreliable and we need to know the dimensions of the region to check the accuracy of an approximate solution.

For the reasons given above the non-linear system with Lagrange multipliers is not a useful representation of the problem.

We consider the rate of convergence and reliability of a numerical method to search for $\hat{\Lambda}$ based on the gradient of Φ_*. Let ∇_* denote the gradient with respect to the elements of u_*. Consider the vector projection of $\nabla_*\Phi_*$ onto the plane tangent to the unit sphere at u_*. This vector can be decomposed into a component in the direction of the long axis of the region and a component in the direction normal to the long axis. The magnitude of the former component will be very small because Φ_* changes very little for u_* along the long axis. The magnitude of the latter component will be much larger than the magnitude of the former component when u_* is a small distance from the long axis. These observations imply that the direction of the gradient of the measure of fit is not a reliable indicator of the direction in which the numerical method should iterate and that the magnitude of the gradient is not a reliable indicator of how far the approximate solution is from the desired solution. Hence the rate of convergence of any such method will be slow and the accuracy of the approximate solution obtained after a certain number of iterations will

be hard to judge.

The problem will be solved by the procedure outlined in section II.4 because of the above considerations. The step-by-step progress of the search can be visually monitored by following the sequence of poles of rotation. This provides a simple and reliable means to understand the behavior of the measure of fit as a function of the rotation tensor.

III.6 Construction of an Uncertainty Region

The maximum likelihood estimate of the rotation tensor is almost surely not equal to the true rotation tensor. We wish to find a region of rotation tensors that includes the maximum likelihood estimate of the rotation tensor and other rotation tensors that are acceptable by reasonable criteria. We want to exclude from this region any rotation tensor for which the associated reconstruction is not reasonable in the light of the data and assigned standard deviations of error. It will then be reasonable to believe that the true rotation tensor is somewhere within the region. This region will be called an uncertainty region for the unknown true rotation tensor Λ. The construction of an uncertainty region depends upon the conceptual framework within which the data's uncertainties are treated. We consider three cases:

(1) If no assumptions are made about the errors in the data beyond upper bounds for the magnitudes of such errors then the set of acceptable reconstructions is limited only by the requirement that the reconstructed plate boundary could have existed within the limits of error for the data. For example, it may be impossible to locate a previously active transform fault within its associated fracture zone. A consequent constraint on an acceptable reconstruction is that magnetic lineations may not cross this fracture zone because the previously active transform fault must be common to the two overlapping sections of fracture zone in the reconstruction. In this case the section-by-section configur-

ation of the data with respect to the estimated common great-circle arc must be examined to determine the acceptability of the reconstruction.

(2) The assumptions about errors in the data may have two parts:

a. There are upper bounds for the magnitudes of the errors.

b. Probability distributions are assumed for the errors. Of course, the probability distributions must be consistent with the limits imposed by part a.

Given these assumptions there will be reconstructions for which the configuration of the data with respect to the estimated common great-circle arcs seems intuitively acceptable and other reconstructions that seem unacceptable. A reasonable quantitative means to distinguish such acceptable reconstructions from unacceptable reconstructions may require that the contribution of each section to the measure of fit for the reconstruction be less than a chosen value for the section. For example, we may stipulate that the root-mean-square deviation of the data points from the estimated common great-circle arc for each section of an acceptable reconstruction may not exceed c_j, where c_j is a positive scalar. This condition is equivalent to $(\hat{\gamma}_j/(n_{1j}+n_{2j}))^{1/2} \leq c_j$, $1 \leq j \leq J$ (see sections III.4 and II.4 for definitions of $\hat{\gamma}_j$, n_{1j} and n_{2j} respectively).

(3) We assume that the error in each data point has the probability distribution specified in section III.3 of this paper. Let $n_j=n_{1j}+n_{2j}-2$, where n_{ij} is defined in section II.4 of this paper. By results in Appendix II, if Λ is the true rotation tensor then each $\hat{\gamma}_j$ has approximately a χ^2 distribution with n_j degrees of freedom. The distributions of $\hat{\gamma}_j$, $1\leq j\leq J$, are mutually independent. Let $\chi^2_{\alpha;n_j}$ be the positive scalar such that the probability that a χ^2 random variable with n_j degrees of freedom exceeds $\chi^2_{\alpha;n_j}$ is α. This number can be obtained from standard statistical tables (see, e.g., Morrison, 1967). The region of rotation tensors $\hat{\Lambda}$ such that the associated $\hat{\gamma}_j\leq\chi^2_{\alpha;n_j}$, $j=1,\ldots,J$ is then a confidence region for Λ of significance level $1-(1-\alpha)^J$.

III.7 The Uncertainty in the Resultant of a Sequence of Finite Rotations

Let $\Lambda_1,\Lambda_2,\Lambda_3$ be rotation tensors such that $\Lambda_3=\Lambda_2\Lambda_1$. Let $u_1,u_2,u_3,\psi_1,\psi_2,\psi_3$ denote the respective poles of rotation and angles of rotation associated with $\Lambda_1,\Lambda_2,\Lambda_3$. u_3 is an eigenvector of Λ_3 with eigenvalue = 1. There are two such eigenvectors of unit length but they differ only in sign. ψ_3 is determined up to sign by $1+2\cos\psi_3 = \text{Trace}(\Lambda_3)$, $-\pi\leq\psi_3\leq\pi$. Let R_3 be a rotation tensor such that $R_3'u_3=(0,0,1)'$. Let $T_3=R_3'\Lambda_3R_3$. Then

$$T_3 = \begin{bmatrix} \cos\psi_3 & \sin\psi_3 & 0 \\ -\sin\psi_3 & \cos\psi_3 & 0 \\ 0 & 0 & 1 \end{bmatrix}$$

and the sign of ψ_3 is determined.

Let Δ be a matrix such that $(T_3+\Delta)'(T_3+\Delta) = I$ and $\det(T_3+\Delta) = 1$. Hence $T_3+\Delta$ is a rotation matrix. Let δ_{ij}, $1\leq i,j\leq 3$ be the elements of Δ. Let u_3+v_3 be the pole of rotation and let $\psi_3+\lambda_3$ be the angle of rotation for $T_3+\Delta$. Δ is a perturbation of T_3 when $|\delta_{ij}|\ll 1$ and $|\delta_{ij}|\ll|\psi_3|$. In this case $|v_3|\ll 1$. Then the coordinates of $R_3'(u_3+v_3)$ through first order in δ_{ij} are given by (see Appendix III):

$$\left[\frac{1}{2}(\delta_{13}+\delta_{23}\sin\psi_3/(1-\cos\psi_3)),\ \frac{1}{2}(\delta_{23}-\delta_{13}\sin\psi_3/(1-\cos\psi_3)),\ 1\right]$$

We also have

$$\lambda_3 = -(\delta_{11}+\delta_{22}+\delta_{33})/2\sin\psi_3$$

through first order in δ_{ij} (Appendix II). When the conditions $|\delta_{ij}|<<1$ and $|\delta_{ij}|<<|\psi_3|$ are not met the relation between either $R_3'(u_3+\nu_3)$ or λ_3 and δ_{ij} is no longer well-approximated by a linear relation.

Let Δ_i be a perturbation in Λ_i, i=1,2. We have $(\Lambda_i+\Delta_i)'(\Lambda_i+\Delta_i) = I$ and $\det(\Lambda_i+\Delta_i) = 1$. Let the associated poles and angles be $u_i+\nu_i, \psi_i+\lambda_i$, i=1,2 respectively. From $T_3=R_3'\Lambda_3R_3$ and $\Lambda_3=\Lambda_2\Lambda_1$ we obtain $T_3=R_3'\Lambda_2\Lambda_1R_3$. Then $T_3+\Delta = R_3'(\Lambda_2+\Delta_2)(\Lambda_1+\Delta_1)R_3$ whence

$$\Delta = R_3'(\Lambda_2\Delta_1+\Delta_2\Lambda_1+\Delta_2\Delta_1)R_3$$

The magnitudes of uncertainties in poles and angles of rotation suggests that the non-linear term $\Delta_2\Delta_1$ may be too large relative to the linear terms to be neglected in the analysis of propagation of errors in many cases. For example, when $|\psi_2|<<1$ and u_2 is close to the data there can be a very large uncertainty in u_2 and ψ_2. The reason is that we can find angle changes λ_2 for a large range of poles $u_2+\nu_2$ such that $u_2+\nu_2$, $\psi_2+\lambda_2$ provides a reasonable reconstruction. The result will be $|\lambda_2|>>|\psi_2|$ for many poles $u_2+\nu_2$. This implies $\Delta_2\Delta_1$ is significant compared to $\Lambda_2\Delta_1$. Furthermore, this also suggests that the functional dependence of Δ_2 upon u_2,ψ_2, ν_2,λ_2 may have significant non-linearity in ν_2 and λ_2. In this case linear theory is inadequate for the study of propagation of errors.

CHAPTER IV

The Effect of Errors in the Data on the Estimated Rotation Tensor

IV.1 Introduction

For the purposes of this chapter let Φ designate Φ_0. Much of the terminology in sections 1-4 of this chapter follows that in Rudin (1964). Let R^m denote a Euclidean vector space of dimension m, m>0. We have data $\hat{s}_{ijk} = s_{ijk} + e_{ijk}$ where

$$|\hat{s}_{ijk}| = 1, \quad |s_{ijk}| = 1, \quad |e_{ijk}| \leq \sqrt{2} \qquad (1)$$

The condition $|e_{ijk}| \leq \sqrt{2}$ confines $\hat{s}_{ijk}$ to the hemisphere centered at s_{ijk}. Let

$$\hat{S}_i' = (\hat{s}_{ij1}', .., \hat{s}_{ijn_{i1}}', .., \hat{s}_{ij1}', .., \hat{s}_{ijn_{ij}}', .., \hat{s}_{iJ1}', .., \hat{s}_{iJn_{iJ}}').$$

$i=1,2;\ j=1,..,J.$

$$\hat{S}' = (\hat{S}_1', \hat{S}_2') \qquad (2)$$

Let S be the vector $\hat{S}$ when $\hat{s}_{ijk} = s_{ijk}$ for all i,j,k.

Let S^2 be the unit sphere in R^3: $S^2 = \{s \varepsilon R^3 : s's=1\}$. Let $u \varepsilon S^2$. Let $H^2(u)$ be the unit hemisphere in R^3 centered at u: $H^2(u) = \{s \varepsilon S^2 : 0 \leq u's \leq 1\}$. $H^2(u)$ is bounded because $|s|=1$ if $s \varepsilon H^2(u)$. Let $v,s \varepsilon R^3$. v'v, v's are continuous functions of v on R^3. Thus $H^2(u)$ is closed in R^3.

Let $N = \sum_{i,j} n_{ij}$. Let W be the subset of R^{3N} specified by (1) and (2). For each $\hat{S}\varepsilon W$ we have $\hat{s}_{ijk}\varepsilon H^2(s_{ijk})$ for all i,j,k. This implies that W is a closed and bounded subset of R^{3N}. Hence W is compact in R^{3N} (see Rudin, 1964, Chapter 2).

Let Λ_* be a rotation tensor with elements λ_{ij}, $1\leq i,j\leq 3$. The true rotation tensor is Λ. Let $L\subset R^9$ be the set of rotation tensors. If I is the identity matrix and det(.) denotes the determinant function then $\Lambda_*'\Lambda_*=I$ and $\det(\Lambda_*)=1$ if and only if $\Lambda_*\varepsilon L$. L is bounded because $\sum_{i,j}\lambda_{ij}^2 = 3$ for any $\Lambda_*\varepsilon L$. Let A be a real 3x3 matrix. L is closed in R^9 because A'A and det(A) are continuous functions of A. L is compact in R^9 because L is closed and bounded in R^9 (see Rudin, 1964, Chapter 2).

We write $\Phi=\Phi(\hat{S},\Lambda_*)$ for $\hat{S}\varepsilon W\subset R^{3N}$ and $\Lambda_*\varepsilon L\subset R^9$. We have $\Phi(\hat{S}=S,\Lambda_*=\Lambda)=0$. Let M=3N+9. We have $(\hat{S},\Lambda_*)\varepsilon R^M$. Φ is continuous on R^M because $\hat{\gamma}_j$ is continuous on R^M. Φ has continuous derivatives of all orders at any point in R^M such that $\hat{\gamma}_j\neq\hat{\beta}_j$, j=1,..,J because $\hat{\gamma}_j$ has continuous derivatives of all orders at any point in R^M such that $\hat{\gamma}_j\neq\hat{\beta}_j$ (see, e.g., discussion in Wilkinson, 1965, Chapter 2, pp. 62-68). The continuity of $\hat{\gamma}_j$ and $\hat{\beta}_j$ on R^M implies that $\hat{\gamma}_j\neq\hat{\beta}_j$ in a neighborhood of $(\hat{S},\Lambda_*)$ in R^M if $\hat{\gamma}_j\neq\hat{\beta}_j$ at $(\hat{S},\Lambda_*)$. Hence $\hat{\gamma}_j$ has continuous derivatives of all orders in a neighborhood of $(\hat{S},\Lambda_*)$ in R^M if $\hat{\gamma}_j\neq\hat{\beta}_j$ at $(\hat{S},\Lambda_*)$.

IV.2 Existence of Rotation Tensors That Minimize the Measure of Fit

Let Δ be the set of scalars $\Phi(\hat{S},\Lambda_*)$ for $\Lambda_*\varepsilon L$ and given $\hat{S}$. Δ is compact in R^1 because Φ is a continuous mapping from L into R^1 (see Rudin, 1964, p. 77, Thm. 4.14). Hence there exists at least one $\hat{\Lambda}_*\varepsilon L$ such that

$$\Phi(\hat{S},\hat{\Lambda}_*) = \inf_{\Lambda_*\varepsilon L} \Phi(\hat{S},\Lambda_*)$$

IV.3 The Equation of Estimation in R^9

Assume $\hat{\gamma}_j \neq \hat{\beta}_j$, $1 \leq j \leq J$ at $\hat{S},\hat{\Lambda}_*$. Let A be a real 3x3 matrix with elements a_{ij}, $1 \leq i,j \leq 3$. Let N_r be a neighborhood of $\hat{\Lambda}_*$ in R^9 of radius $r>0$ such that $\hat{\gamma}_j \neq \hat{\beta}_j$ for $A\varepsilon N_r$. Define the operator

$$\partial/\partial a_k = [\partial/\partial a_{1k}, \partial/\partial a_{2k}, \partial/\partial a_{3k}] \quad , \quad k=1,2,3$$

Then ∇, the gradient operator in R^9, may be represented by

$$\nabla' = [\partial/\partial a_1, \partial/\partial a_2, \partial/\partial a_3]$$

$\nabla\Phi(\hat{S},A)$ exists and is continuous for $A\varepsilon N_r$ (see section IV.1). Let $a_k' = (a_{1k}, a_{2k}, a_{3k})$, $k=1,2,3$. The condition $A'A=I$ defines nine constraints of the form

$$a_i' a_j = \delta_{ij} \quad , \quad 1 \leq i,j \leq 3$$

where δ_{ij} is the Kronecker δ: $\delta_{ij}=1$ if $i=j$, $\delta_{ij}=0$ otherwise.

Among the nine are found six independent constraints which will be denoted by g_k, k=1,..,6. We define

$$g_k = a_k'a_k - 1 = 0, \quad k=1,2,3$$
$$g_4 = a_1'a_2 = 0$$
$$g_5 = a_1'a_3 = 0$$
$$g_6 = a_2'a_3 = 0$$

Let τ_k, k=1,2,..,6 be scalars. Let $\tau' = (\tau_1,\tau_2,..,\tau_6)$. For $A \varepsilon N_r$ define

$$F(\hat{S},A,\tau) = \nabla\Phi(\hat{S},A) - \sum_{1\leq k\leq 6} \tau_k \nabla g_k$$

In N_r, $\hat{\Lambda}_*$ is a solution of

$$F(\hat{S},A,\tau) = 0, \quad A'A = I, \quad \det(A) = 1 \qquad (1)$$

Other solutions of (1), if any, may represent local minima or local maxima of Φ within N_r as well as more complicated behavior. The vector τ that corresponds to a particular $\hat{\Lambda}_*$ is uniquely defined by

$$F(\hat{S},\hat{\Lambda}_*,\tau) = 0 \qquad (2)$$

The reason that τ is unique is as follows: We have

$$\begin{aligned}
\nabla' g_1 &= (2a_1', 0, 0) \\
\nabla' g_2 &= (0, 2a_2', 0) \\
\nabla' g_3 &= (0, 0, 2a_3') \\
\nabla' g_4 &= (a_2', a_1', 0) \\
\nabla' g_5 &= (a_3', 0, a_1') \\
\nabla' g_6 &= (0, a_3', a_2')
\end{aligned} \qquad (3)$$

For $A = \hat{\Lambda}_*$ the vectors a_1,a_2,a_3 are orthonormal vectors.

Then (3) implies that ∇g_k, k=1,..,6 are mutually orthogonal vectors in R^9. Hence the components of $\nabla\Phi$ with respect to the basis (∇g_k, k=1,..,6) are unique and these components are τ_k, k=1,..,6.

From (3) we have

$$\nabla g_m' \nabla g_m = 4, \quad m=1,2,3$$
$$= 2, \quad m=4,5,6$$
$$\nabla g_m' \nabla g_n = 0, \quad m\neq n, \quad 1\leq m,n\leq 6.$$

Let G be a 6x6 matrix with elements $(G)_{mn}$. Let

$$(G)_{mn} = \nabla g_m' \nabla g_n, \quad 1\leq m,n\leq 6.$$

Let Y be the column vector whose m th entry is $\nabla g_m' \nabla\Phi$, m=1,..,6. Premultiplying (2) by $\nabla' g_m$, m=1,..,6 in succession we obtain $G\tau = Y$. Hence $\tau = G^{-1}Y$.

IV.4 Analysis of the Equation of Estimation in R^3

To analyze the equation of estimation it is necessary to represent both the set of rotation tensors and the set of possible data by open sets. For this purpose it is useful to express the data in polar coordinates and to represent a rotation tensor by the polar coordinates of a pole of rotation and an angle of rotation associated with the pole.

Let u be the pole of rotation associated with Λ. u is an eigenvector of Λ with eigenvalue = 1 and $|u| = 1$. There are two such eigenvectors but they differ only in sign. Let ψ_0 be the angle of rotation of Λ. ψ_0 is determined up to sign by

$$1 + 2\cos\psi_0 = \text{Trace}(\Lambda) \ , \ -\pi \leq \psi_0 \leq \pi .$$

The sign of ψ_0 for given u can be determined by the procedure discussed in section III.7 . Let θ_0, ϕ_0 be the polar coordinates of u. The parameters θ_0, ϕ_0, ψ_0 specify Λ but they are determined by Λ only up to sign.

Let Λ_* be a rotation tensor and let u_* be the pole of rotation for Λ_*. We assume without loss of generality that $u_* \varepsilon H^2(u)$ so that u_* is in the hemisphere centered at u. If u_* represents the pole of an estimated rotation tensor then u_* is almost certainly in a small neighborhood of u in $H^2(u)$ because the likely errors in the data are very small. If we restrict u_* to this neighborhood then the analysis of the equation of estimation will not be significantly affected.

Let $0<c<1$. Let $H_c(u) = \{s\varepsilon H^2(u): c<s'u\leq 1\}$. We will assume $1-c << 1$ and $u_*\varepsilon H_c(u)$. For example, if the maximum great-circle distance between u and u_* is 5^o of arc then 1-c is approximately 4×10^{-3}.

Let θ, ϕ be the polar coordinates of u_*. Let $F_c(u) = \{(\theta,\phi): u_*\varepsilon H_c(u)\}$. θ is continuous on S^2. ϕ is continuous at $u_*\varepsilon S^2$ except at $u_*' = \pm(0,0,1)$, where ϕ is not defined, and at those u_* for which $\phi = -\pi/2$ when ϕ is restricted to the range $-\pi/2\leq\phi<3\pi/2$. Let

$$\theta_{max} = \sup_{u_*\varepsilon H_c(u)} \theta \quad , \quad \phi_{max} = \sup_{u_*\varepsilon H_c(u)} \phi$$

$$\theta_{min} = \inf_{u_*\varepsilon H_c(u)} \theta \quad , \quad \phi_{min} = \inf_{u_*\varepsilon H_c(u)} \phi$$

We may assume without loss of generality that

$$-\pi/2<\theta_{min}<\theta_{max}<\pi/2, \quad -\pi/2<\phi_{min}<\phi_{max}<3\pi/2 \qquad (1)$$

because these relations will hold for any c, $0<c<1$, if we transform the coordinates of u_* to a coordinate system where u lies in the x-y plane and the y-coordinate of u is ≥ 0. As $H_c(u)$ is open in S^2 and θ is continuous on S^2 there is no $u_*\varepsilon H_c(u)$ such that $\theta(u_*) = \theta_{max}$ when $\theta_{max} < \pi/2$. Similar conclusions hold for θ_{min}, ϕ_{min}, ϕ_{max} under the conditions in (1). Thus $F_c(u)$ is open in R^2.

Let ψ be the angle of rotation of Λ_* associated with u_*. We will assume that $-\pi<\psi<\pi$ because a rotation angle of magnitude as large as π is excluded by the data. Let $P' = (\theta,\phi,\psi)$. Let $X = \{P: (\theta,\phi)\varepsilon F_c(u), -\pi<\psi<\pi\}$. Then X is

open in R^3. Let $P_0' = (\theta_0, \phi_0, \psi_0)$. Then $P_0 \varepsilon X$.

The polar coordinates of $\hat{s}_{ijk}$ are $\hat{\theta}_{ijk}, \hat{\phi}_{ijk}$ and the polar coordinates of s_{ijk} are θ_{ijk}, ϕ_{ijk}. $\hat{s}_{ijk}$ is almost certainly in a small neighborhood of s_{ijk} in S^2 because the likely errors are very small. If we restrict $\hat{s}_{ijk}$ to this neighborhood then the analysis of the equation of estimation will not be significantly affected. The covariance matrix of the error in $\hat{s}_{ijk}$ is $\sigma_{ijk}^2 I$ (see section III.3) where $0<\sigma_{ijk}<<1$. Let k_{ijk} be a positive constant such that $k_{ijk}\sigma_{ijk}<<1$. Let

$$G_{ijk} = \{s \varepsilon S^2 : \cos(k_{ijk}\sigma_{ijk}) < s' s_{ijk} \leq 1\}.$$

We assume $\hat{s}_{ijk} \varepsilon G_{ijk}$ (for example, if $k_{ijk} = 5$ then we assume that $\hat{s}_{ijk}$ is restricted to a spherical cap of approximate half-width $5\sigma_{ijk}$). G_{ijk} is open in S^2. Let

$$F_{ijk} = \{(\theta, \phi) : s \varepsilon G_{ijk}\}.$$

If there are any F_{ijk} for which a relation similar to (1) does not hold then we assume that we can transform the coordinates of the data to a coordinate system where all F_{ijk} satisfy such a relation. Thus F_{ijk} is open in R^2 for all i,j,k. We also assume that relation (1) holds in this coordinate system.

Let $\hat{p}_{ijk}' = (\hat{\theta}_{ijk}, \hat{\phi}_{ijk})$ for all i,j,k. Let

$$\hat{D}_i' = (\hat{p}_{ill}', \ldots, \hat{p}_{iln_{il}}', \ldots, \hat{p}_{ijl}', \ldots, \hat{p}_{ijn_{ij}}', \ldots, \hat{p}_{iJl}', \ldots, \hat{p}_{iJn_{iJ}}')$$

$$i=1,2;\ j=1,2,\ldots,J$$

Let $\hat{D}' = (\hat{D}_1', \hat{D}_2')$. Hence $\hat{D} \epsilon R^{2N}$ (see section IV.1 for definition of N). Let D be the vector $\hat{D}$ when $\hat{s}_{ijk} = s_{ijk}$ for all i,j,k. Let $Y = \{\hat{D}: \hat{p}_{ijk} \epsilon F_{ijk}$ for all i,j,k$\}$. Then Y is open in R^{2N}. Let $Z = \{(\hat{D},P): \hat{D} \epsilon Y, P \epsilon X\}$. Then Z is open in R^{2N+3}. We assume $\hat{\gamma}_j \neq \hat{\beta}_j$, j=1,..,J for any $(\hat{D},P) \epsilon Z$.

We write $\Phi = \Phi(\hat{D},P)$ where $\Phi(\hat{D}=D, P=P_0) = 0$ and Φ has continuous derivatives of all orders in Z (see discussion in section IV.3). Let

$$\nabla' = (\partial/\partial\theta, \partial/\partial\phi, \partial/\partial\psi)$$

Let

$$f(P,\hat{D}) = \nabla\Phi(\hat{D},P)$$

$f \epsilon R^3$ and f has continuous derivatives of all orders in Z. Let $f' = (f_1, f_2, f_3)$. Let $\hat{P}$ be that P which minimizes Φ for given $\hat{D} \epsilon Y$. We assume $\hat{P} \epsilon X$. $\hat{P}$ is a solution of

$$f(P,\hat{D}) = 0 \qquad (2)$$

Other solutions of (2), if any, may represent local minima or local maxima of $\Phi(\hat{D},P)$ as well as more complicated behavior. Assume $\hat{P}$ is the unique solution of (2). Let K be a 3x3 real matrix and let the i <u>th</u> row vector of K be $\nabla' f_i$, i=1,2,3. Let K_0 be the value of K when $P = P_0$ and $\hat{D} = D$. If $\det(K_0) \neq 0$ then the Implicit Function Theorem (see Rudin, 1964, pp. 195-197, Thm. 9.18) shows that (2) provides for a relation

$$\hat{P} = \Psi(\hat{D})$$

for $\hat{D}$ in a neighborhood of D, where Ψ is continuously differentiable in that neighborhood.

Let ψ_i, i=1,2,3 be the components of Ψ. Let d_j be the

j th component of D, j=1,..,2N. Let C be a 3x2N matrix with elements c_{ij}, i=1,2,3; j=1,..,2N. Let

$$c_{ij} = \partial\psi_i/\partial d_j$$

Let o(a) denote a quantity such that $o(a)/|a| \to 0$ as $|a| \to 0$. In the neighborhood of $\hat{D} = D$ we have the expansion

$$\Psi(\hat{D}) = \Psi(D) + C(\hat{D}-D) + o(\hat{D}-D)$$

where $\Psi(D) = P_0$.

IV.5 Perturbation Analysis of the Equation of Estimation

We have data $\hat{s}_{ijk} = s_{ijk} + e_{ijk}$ where e_{ijk} is the error in $\hat{s}_{ijk}$, $|\hat{s}_{ijk}| = |s_{ijk}| = 1$ and $\hat{s}_{ijk}$ is effectively restricted to a small neighborhood of s_{ijk} on the unit sphere (see sections III.3, IV.4).

Let $\hat{B}_{j*}$ be the 3x3 symmetric positive semidefinite matrix defined by

$$\hat{B}_{j*} = \sum_{1\le k\le n_{1j}} \sigma_{1jk}^{-2} \hat{s}_{1jk}\hat{s}_{1jk}' + \sum_{1\le k\le n_{2j}} \sigma_{1jk}^{-2} (\Lambda_* \hat{s}_{2jk})(\Lambda_* \hat{s}_{2jk})'$$

Let $\hat{B}_j$ be the value of $\hat{B}_{j*}$ when $\Lambda_* = \Lambda$. Let B_j be the value of $\hat{B}_{j*}$ when $\hat{s}_{ijk} = s_{ijk}$ for all i,j,k and $\Lambda_* = \Lambda$. Let $\alpha_j, \beta_j, \gamma_j = 0$ be the eigenvalues of B_j. We assume $\alpha_j > \beta_j > \gamma_j$. Let q_j, r_j, p_j be the eigenvectors of unit length associated with $\alpha_j, \beta_j, \gamma_j$ respectively. There are two such eigenvectors for each eigenvalue but they differ only in sign. As the eigenvalues are distinct q_j, r_j, p_j form an orthonormal basis. We assume $q_j \times r_j = p_j$ where 'x' denotes the vector product.

Let $\hat{\gamma}_{j*}$ be the minimum eigenvalue of $\hat{B}_{j*}$. We assume $\hat{\gamma}_{j*}$ is distinct. Let $\hat{p}_{j*}$ be an eigenvector of unit length associated with $\hat{\gamma}_{j*}$. Of the two such eigenvectors choose the one closest to p_j. Then $\hat{p}_{j*} = p_j + v_{j*}$ where $|v_{j*}|$ is small. Similarly, let $\hat{p}_j$ be the eigenvector of unit length associated with the distinct minimum eigenvalue $\hat{\gamma}_j$ of $\hat{B}_j$ such that $\hat{p}_j = p_j + v_j$ where $|v_j|$ is small.

The measure of fit for the points $\hat{s}_{ijk}$ and rotation

tensor Λ_* is

$$\Phi = \sum_{1 \le j \le J} \hat{\gamma}_{j*} \qquad (1)$$

Assume that Λ_* is in a neighborhood of Λ. We have

$$\Lambda_* \simeq (I+E)\Lambda \qquad (2)$$

where E is an antisymmetric perturbation matrix as defined in Appendix I. Let $\varepsilon_1, \varepsilon_2, \varepsilon_3$ be the independent elements of E. Let $\varepsilon' = (\varepsilon_1, \varepsilon_2, \varepsilon_3)$. Using (2) in (1) we can obtain an approximate expression for Φ that depends upon the data $\hat{s}_{ijk}$, Λ and ε. Let $\tilde{\Phi}$ denote this approximate expression. We seek a vector $\hat{\varepsilon}$ such that $\tilde{\Phi}$ is minimized. To this $\hat{\varepsilon}$ there will correspond a rotation tensor $\hat{\Lambda}$. We assume that $\hat{\Lambda}$ is in a neighborhood of Λ. Let

$$\nabla' = (\partial/\partial\varepsilon_1, \partial/\partial\varepsilon_2, \partial/\partial\varepsilon_3).$$

Then $\hat{\varepsilon}$ is a solution of

$$\nabla\tilde{\Phi} = 0 \qquad (3)$$

We would like to compare the magnitudes of the terms in (3) that are linear in ε and e_{ijk} with the other terms given representative values of σ_{ijk} and typical sets of points s_{ijk}. The purpose of this comparison is to see whether the functional relation between $\hat{\varepsilon}$ and the s_{ijk} and e_{ijk} is well-approximated by a relation that is linear in e_{ijk} (Of course, we assume that a functional relation exists; see discussion in section IV.4). The result will be that the relation between $\hat{\varepsilon}$ and e_{ijk} is not well-approximated by a linear rela-

tion. This conclusion will be obtained from each of two different lines of argument.

Let $(\xi_{1jk},\eta_{1jk},\zeta_{1jk})$ be the coordinates of s_{1jk} in the orthonormal basis (q_j,r_j,p_j). Let $(\xi_{2jk},\eta_{2jk},\zeta_{2jk})$ be the coordinates of Λs_{2jk} in the same basis. We have

$$\zeta_{1jk} = p_j's_{1jk} = 0,\ \zeta_{2jk} = p_j'\Lambda s_{2jk} = 0$$

and $\xi_{ijk}^2 + \eta_{ijk}^2 = 1$. We also have

$$\alpha_j = \sum_{i,k} \xi_{ijk}^2/\sigma_{ijk}^2\ ,\ \beta_j = \sum_{i,k} \eta_{ijk}^2/\sigma_{ijk}^2\ ,$$

$$\sum_{i,k} \xi_{ijk}\eta_{ijk}/\sigma_{ijk}^2 = 0$$

(4)

Let the coordinates of e_{1jk} in this basis be $(u_{1jk},v_{1jk},w_{1jk})$. Let the coordinates of Λe_{2jk} in this basis be $(u_{2jk},v_{2jk},w_{2jk})$. Let $\delta_{1jk} = e_{1jk}$, $\delta_{2jk} = \Lambda e_{2jk} + E\Lambda(s_{2jk}+e_{2jk})$. Let the coordinates of $E\Lambda s_{2jk}$ and $E\Lambda e_{2jk}$ in this basis be, respectively, $(a_{2jk},b_{2jk},c_{2jk})$ and $(f_{2jk},g_{2jk},h_{2jk})$. The former components are linear in ε and the latter components are not linear in ε and e_{2jk}.

We refer to Figure IV. For our representative set of points we assume $\sigma_{ijk} = \sigma$, $0<\sigma<<1$. Then (4) yields

$$\alpha_j = \sigma^{-2} \sum_{i,k} \xi_{ijk}^2,\ \beta_j = \sigma^{-2} \sum_{i,k} \eta_{ijk}^2,\ \sum_{i,k} \xi_{ijk}\eta_{ijk} = 0$$

(5)

Furthermore, we assume max $|\eta_{ijk}| = 10\sigma$ and $\xi_{ijk} > 0$ for all i,j,k (for example, if σ is equivalent to 10 km then max $|\eta_{ijk}|$ is equivalent to 100 km and the great-circle arc along which the points lie is approximately 200 km in length). The relation max $|\eta_{ijk}| = 10\sigma$ is equivalent to max $\eta_{ijk}^2 = 100\sigma^2$ and min $\xi_{ijk}^2 = 1 - 100\sigma^2$. Therefore

$$\xi_{ijk}^2 >> \eta_{ijk}^2 \tag{6}$$

for all i,j,k (for example, if σ is equivalent to 10 km then $\sigma \simeq 1.5 \times 10^{-3}$ and $100\sigma^2 \simeq 2.25 \times 10^{-4}$). Using (6) in (5) we obtain

$$\alpha_j >> \beta_j, \quad j=1,..,J \tag{7}$$

Argument 1: With the results of Appendix II we obtain

$$\hat{\gamma}_{j*} \simeq c_j - a_j^2/\alpha_j - b_j^2/\beta_j$$

where

$$c_j = \sigma^{-2}\Big[\sum_{1\le k\le n_{1j}} w_{2jk}^2 + \sum_{1\le k\le n_{2j}} (w_{2jk} + c_{2jk} + h_{2jk})^2\Big]$$

$$a_j = \sigma^{-2}\Big[\sum_{1\le k\le n_{1j}} (\xi_{1jk} + u_{1jk})w_{1jk} +$$

$$\sum_{1\le k\le n_{2j}} (\xi_{2jk} + u_{2jk} + a_{2jk} + f_{2jk})(w_{2jk} + c_{2jk} + h_{2jk})\Big]$$

$$b_j = \sigma^{-2}\Big[\sum_{1\le k\le n_{1j}} (\eta_{1jk} + v_{1jk})w_{1jk} +$$

$$\sum_{1\le k\le n_{2j}} (\eta_{2jk} + v_{2jk} + b_{2jk} + g_{2jk})(w_{2jk} + c_{2jk} + h_{2jk})]$$

With these expressions (3) is equivalent to

$$\sum_{1\le j\le J} \nabla c_j - 2 \sum_{1\le j\le J} a_j \nabla a_j/\alpha_j - 2 \sum_{1\le j\le J} b_j \nabla b_j/\beta_j = 0$$

(8)

We have max $|\eta_{2jk}| = 10\sigma$ and $\mathrm{Var}(v_{2jk}) = \sigma^2$ where Var(.) denotes the variance of a scalar random variable. Thus $[\mathrm{Var}(v_{2jk})]^{1/2}$ is not insignificant compared to $|\eta_{2jk}|$ for any j,k. This implies that $b_j \nabla b_j$ has terms $O(e'_{2jk} e_{2jk})$ that are significant compared to terms $O(\eta_{2jk} e_{2jk})$. Moreover b_{2jk}, which depends only on ε and Λs_{2jk}, is probably significant relative to v_{2jk}. Thus $b_j \nabla b_j$ may also have significant terms that are $O(\varepsilon' e_{2jk})$ and $O(\varepsilon'\varepsilon)$.

From (5) we have

$$\sum_{i,k} (\xi_{ijk}/\alpha_j^{1/2})^2 = \sum_{i,k} (\eta_{ijk}/\beta_j^{1/2})^2 = \sigma^2, \quad \sum_{i,k} \xi_{ijk}\eta_{ijk} = 0$$

Let

$$U' = (\xi_{1j1}, \cdots, \xi_{1jn_{1j}}, \xi_{2j1}, \cdots, \xi_{2jn_{2j}})/\alpha_j^{1/2}$$

$$V' = (\eta_{1j1}, \cdots, \eta_{1jn_{1j}}, \eta_{2j1}, \cdots, \eta_{2jn_{2j}})/\beta_j^{1/2}$$

Then $U'U = V'V = \sigma^2$ and $U'V = 0$. Thus U and V are orthogonal vectors of magnitude σ. Let

$$W' = (w_{1j1}, \cdots, w_{1jn_{1j}}, w_{2j1}, \cdots, w_{2jn_{2j}})$$

Then

$$U'W = \sum_{i,k} \xi_{ijk} w_{ijk}, \quad V'W = \sum_{i,k} \eta_{ijk} w_{ijk}$$

We have

$$a_j \simeq \sigma^{-2} \alpha_j^{1/2} U'W, \quad b_j \simeq \sigma^{-2} \beta_j^{1/2} V'W$$

As $|h_{2jk}| << |c_{2jk}|$ we have

$$\nabla a_j / \alpha_j^{1/2} \simeq \sigma^{-2} \sum_{1 \le k \le n_{2j}} (\xi_{2jk} / \alpha_j^{1/2}) \nabla c_{2jk}$$

$$\nabla b_j / \beta_j^{1/2} \simeq \sigma^{-2} \sum_{1 \le k \le n_{2j}} (\eta_{2jk} / \beta_j^{1/2}) \nabla c_{2jk}$$

Thus

$$\begin{aligned} a_j \nabla a_j / \alpha_j &\simeq \sigma^{-4} U'W \sum_{1 \le k \le n_{2j}} (\xi_{2jk} / \alpha_j^{1/2}) \nabla c_{2jk} \\ b_j \nabla b_j / \beta_j &\simeq \sigma^{-4} V'W \sum_{1 \le k \le n_{2j}} (\eta_{2jk} / \beta_j^{1/2}) \nabla c_{2jk} \end{aligned} \tag{9}$$

These relations suggest that both both $a_j \nabla a_j / \alpha_j$ and $b_j \nabla b_j / \beta_j$ are equally significant terms in (8). We have

$$\nabla c_j \simeq 2\sigma^{-2} \sum_{1 \le k \le n_{2j}} (w_{2jk} + c_{2jk}) \nabla c_{2jk} \tag{10}$$

The coefficient of ∇c_{2jk} in (10) is $2\sigma^{-2}(w_{2jk} + c_{2jk})$. For Λ_* in a neighborhood of Λ we assume that $|c_{2jk}|$ is not large compared to $|w_{2jk}|$. We write

$$\left| \sum_{1 \le k \le n_{2j}} (w_{2jk} + c_{2jk}) \right| \simeq k_1 |W|$$

where k_1 is moderate (e.g., $10^{-1} < k_1 < 10^1$).

$\xi_{2jk}/\alpha_j^{1/2}$ is a component of U and $|U| = \sigma$. Also $\eta_{2jk}/\beta_j^{1/2}$ is a component of V and $|V| = \sigma$. Furthermore V and U are orthogonal. These results and (9) suggest that

$$\sigma^{-2}\left|U'W \sum_{1\le k\le n_{2j}} (\xi_{2jk}/\alpha_j^{1/2}) + V'W \sum_{1\le k\le n_{2j}} (\eta_{2jk}/\beta_j^{1/2})\right| = k_2|W|$$

where k_2 is a constant, $0<k_2<2$ and k_2 is not close to 0. The magnitudes of k_1 and k_2 suggest that all terms in (8) are important. Now, $b_j \nabla b_j$ has significant terms that are not linear in ε and e_{ijk}. From this argument we suggest that (8) is not well-approximated by ignoring the terms that are not linear in ε and e_{ijk}. By well-approximated we mean that the solution of the approximate system of equations (without non-linear terms) is close to the solution of the full system of equations (with all terms present). The suggestion that (8) is not well-approximated by a linear system is a reflection of the fact that good agreement of the terms in the linear system does not necessarily imply that the solution of the linear system is close to the solution of the full system (see discussion in section III.5).

Argument 2: Another approximate expression for Φ for the points $\hat{s}_{ijk}$ and Λ_* in a neighborhood of Λ is

$$\tilde{\Phi} = \sum_{j,k} \sigma_{1jk}^{-2} (\hat{p}_{j*}' \hat{s}_{1jk})^2 + \sum_{j,k} \sigma_{2jk}^{-2} [\hat{p}_{j*}' (I + E) \Lambda \hat{s}_{2jk}]^2$$

We have

$$p_j' \Lambda s_{2jk} = p_j' s_{1jk} = 0, \quad \nabla (p_j' e_{1jk}) = \nabla (p_j' e_{2jk}) = 0$$

We have $\sigma_{ijk} = \sigma$. Let

$$d_{1jk} = v_{j*}' (s_{1jk} + e_{1jk})$$

$$d_{2jk} = [p_j' E \Lambda + v_{j*}' (I + E) \Lambda] (s_{2jk} + e_{2jk})$$

With the above expression for $\tilde{\Phi}$ (3) is then equivalent to

$$\sum_{j,k} \sigma^{-2} (p_j' e_{1jk} + d_{1jk}) \nabla d_{1jk} + \sum_{j,k} \sigma^{-2} (p_j' e_{2jk} + d_{2jk}) \nabla d_{2jk} = 0 \qquad (11)$$

The vector v_{j*} is functionally related to the points $\{s_{1jk}, k=1,..,n_{1j}; \Lambda s_{2jk}, k=1,..,n_{2j}\}$ and the perturbations $\{\delta_{ijk}, i=1,2;\ k=1,..,n_{ij}\}$. When $|\delta_{ijk}| << 1$ this relation is approximately (see Appendix II):

$$v_{j*} = V_j' u_{j*} \qquad (12)$$

where

V_j = orthogonal matrix whose row-vectors are q_j', r_j', p_j' respectively.

$$u_{j*}' = [\ -\alpha_j^{-1} \sum_{i,k} \xi_{ijk} (p_j' \delta_{ijk}) / \sigma^2,$$

$$-\beta_j^{-1} \sum_{i,k} \eta_{ijk} (p_j' \delta_{ijk}) / \sigma^2,\ 0\ ]$$

The components of v_{j*} in the basis (q_j, r_j, p_j) are the components of u_{j*}. Let $u'_{j*} = (u_{1j*}, u_{2j*}, 0)$. Let u_j be the value of u_{j*} when $E = 0$ in δ_{2jk}, $k=1,..,n_{2j}$. Let $u'_j = (u_{1j}, u_{2j}, 0)$. Then (12) and the methods of Appendix II yield the approximate relations:

$$\text{Var}(u_{1j}) = 1/\alpha_j,\ \text{Var}(u_{2j}) = 1/\beta_j,\ \text{Cov}(u_{1j}, u_{2j}) = 0 \qquad (13)$$

Using (7) in (13) we find

$$\text{Var}(u_{1j}) << \text{Var}(u_{2j}) \qquad (14)$$

The relation $\text{Cov}(u_{1j}, u_{2j}) = 0$ in (13) implies that the direction of greatest variation of v_j is either q_j or r_j and (14) implies that this direction is r_j and that v_j tends strongly to be oriented in the r_j direction. When $E \neq 0$ the expressions for $\text{Var}(u_{1j*})$ and $\text{Var}(u_{2j*})$ will be different from those in (13) and $\text{Cov}(u_{1j*}, u_{2j*})$ will not necessarily be 0. Hovever, a relation of the form

$$\text{Var}(u_{1j*}) << \text{Var}(u_{2j*})$$

will still be valid as long as E is small. This information can be used to compare the magnitudes of the terms in (11).

Let w be a vector or scalar random variable and let rms(w) denote the positive square root of the mean of w'w. We have from (14):

$$\text{rms}(u_{1j}) << \text{rms}(u_{2j}) \qquad (15)$$

We assume that $\text{rms}(u_{1j})/\text{rms}(u_{2j})$ is a reasonable measure of the strength with which v_j tends to be aligned with the

r_j axis. Then (15) implies that v_j tends strongly to be aligned with the r_j axis. We have

$$\text{rms}(e_{ijk}) \simeq \sigma, \quad \text{rms}(u_j) \simeq 1/\sqrt{\beta_j}.$$

As $|s_{ijk} + e_{ijk}| = 1$ and $|s_{ijk}| = 1$ we have $e'_{ijk}s_{ijk} = -e'_{ijk}e_{ijk}/2$. This implies that e_{ijk} is nearly perpendicular to s_{ijk} because $\text{rms}(e_{ijk}) << 1$. As s_{ljk} is close to q_j we find that e_{ljk} is nearly perpendicular to q_j. Therefore the angle between e_{ljk} and p_j varies approximately uniformly between 0 and 2π. Let λ be a scalar that is uniformly distributed between 0 and 2π. The probability density for λ is $\lambda/2\pi$ over this range. We have

$$\int_0^{2\pi} \cos^2\lambda \, d\lambda/2\pi = 1/2$$

Thus $\text{rms}(p'_j e_{ljk}) \simeq \sigma/\sqrt{2}$.

v_j tends strongly to be oriented in the r_j direction. Thus the magnitude of the cosine of the angle between v_j and s_{ljk} tends strongly to be $|\eta_{ljk}|$. This implies

$$\text{rms}(v'_j s_{ljk}) \simeq |\eta_{ijk}|/\sqrt{\beta_j} \qquad (16)$$

The angle between e_{ljk} and v_j is highly likely to be only slightly different from the angle between e_{ljk} and r_j because v_j tends strongly to be oriented in the r_j direction. The angle between e_{ljk} and r_j is approximately uniformly distributed between 0 and 2π. Thus

$$\text{rms}(v'_j e_{ljk}) \simeq \sigma/2\sqrt{\beta_j} \qquad (17)$$

Now, max $|\eta_{ijk}| = 10\sigma$. Thus (16) and (17) imply that terms

of the form $v_j' e_{1jk}$ are not negligible compared to terms of the form $v_j' s_{1jk}$. The term $v_j' e_{1jk}$ is not linear in the e_{ijk}. From this result we infer that terms of the form $v_{j*}' \delta_{1jk}$ are not negligible compared to terms of the form $v_{j*}' s_{1jk}$ in (11). By a similar argument terms of the form $v_j' \Lambda e_{2jk}$ are not negligible compared to terms of the form $v_j' \Lambda s_{2jk}$. From this result we infer that terms of the form $v_{j*}' \delta_{2jk}$ are not negligible compared to terms of the form $v_{j*}' \Lambda s_{2jk}$ in (11). The terms $v_{j*}' \delta_{ijk}$ are non-linear in the elements of ε and the e_{ijk}. Thus (11) is not necessarily well-approximated by the system of equations we obtain by ignoring the non-linear terms. The discussion at the close of Argument 1 is therefore applicable to (11) also.

These arguments suggest that the functional relation between ε and the e_{ijk} has sufficient non-linearity to rule out the use of linear statistical theory to obtain an accurate description of the distribution of ε from the s_{ijk}, Λ and the distributions of e_{ijk}.

CHAPTER V

A Second Measure of Fit

V.1 The Measure of Fit

Λ is the true rotation tensor. The matrix $\hat{B}_j$ was defined in section III.5 . Let B_j denote the matrix whose entries are equal to those of $\hat{B}_j$ when $\hat{s}_{ijk} = s_{ijk}$ and $\hat{\Lambda} = \Lambda$. Let the eigenvalues of B_j be $\alpha_j, \beta_j, \gamma_j = 0$. We assume $\alpha_j > \beta_j > 0$. Let q_j, r_j, p_j be eigenvectors of unit length associated with $\alpha_j, \beta_j, \gamma_j$ respectively. There are two such eigenvectors for each eigenvalue but they differ only in sign. We choose q_j, r_j, p_j to satisfy the relation $q_j \times r_j = p_j$ where 'x' denotes the vector product. Let K_j denote the plane normal to p_j.

The matrices $\hat{B}_{ij}$ and B_{ij} were defined in section III.4 . The eigenvalues of $\hat{B}_{ij}$ are $\hat{\alpha}_{ij}, \hat{\beta}_{ij}, \hat{\gamma}_{ij}$ with associated eigenvectors of unit length $\hat{q}_{ij}, \hat{r}_{ij}, \hat{p}_{ij}$ respectively. The eigenvalues of B_{ij} are $\alpha_{ij}, \beta_{ij}, \gamma_{ij} = 0$ with associated eigenvectors of unit length q_{ij}, r_{ij}, p_{ij} respectively. We choose p_j, p_{1j}, and p_{2j} to satisfy the relation $p_j = p_{1j} = \Lambda p_{2j}$.

Let

$$\hat{C}_{2j} = \Lambda \hat{B}_{2j} \Lambda', \quad C_{2j} = \Lambda B_{2j} \Lambda'$$

The eigenvalues of $\hat{C}_{2j}$ are $\hat{\alpha}_{2j}, \hat{\beta}_{2j}, \hat{\gamma}_{2j}$ with respective associated eigenvectors of unit length $\Lambda \hat{q}_{2j}, \Lambda \hat{r}_{2j}, \Lambda \hat{p}_{2j}$. The eigenvalues of C_{2j} are $\alpha_{2j}, \beta_{2j}, \gamma_{2j} = 0$ with respective associated eigenvectors $\Lambda q_{2j}, \Lambda r_{2j}, \Lambda p_{2j}$.

The statistical distribution of $(\hat{s}_{1jk}, k=1,..,n_{1j})$ induces a statistical distribution of the matrix $\hat{B}_{1j}$. Hence the eigenvector associated with the minimum eigenvalue of $\hat{B}_{1j}$ has a statistical distribution. Our calculated eigenvector $\hat{p}_{1j}$ is a sample from this distribution. Similarly, the statistical distribution of $(\Lambda\hat{s}_{2jk}, k=1,..,n_{2j})$ induces a statistical distribution of $\hat{C}_{2j}$. The calculated eigenvector $\hat{p}_{2j}$ when rotated to $\Lambda\hat{p}_{2j}$ is a sample from the distribution of the eigenvector associated with the minimum eigenvalue of $\hat{C}_{2j}$. When $p_{1j} = \Lambda p_{2j}$ the random vector $\hat{p}_{1j} - \Lambda\hat{p}_{2j}$ is non-zero in general due to the statistical distributions of both $(\hat{s}_{1jk}, k=1,..,n_{1j})$ and $(\Lambda\hat{s}_{2jk}, k=1,..,n_{2j})$. The distribution of $\hat{s}_{ijk}$ is specified by its mean s_{ijk} and the positive scalar σ_{ijk}(see section III.3). When both $0 << \beta_{ij} < \alpha_{ij}$ and $\sigma_{ijk} << 1$, $k=1,..,n_{ij}$ (see discussion in Appendix II) the distribution of $\hat{p}_{ij}$ is concentrated near p_{ij}. In this circumstance the projection of $\hat{p}_{1j} - \Lambda\hat{p}_{2j}$ onto K_j is a useful approximation to $\hat{p}_{1j} - \Lambda\hat{p}_{2j}$. Let w_j be this projection.

Let D_{1j} be a 2 x 3 matrix with rows equal to q_{1j}' and r_{1j}' respectively. Let D_{2j} be a 2 x 3 matrix with rows equal to $(\Lambda q_{2j})'$ and $(\Lambda r_{2j})'$ respectively. $D_{ij}v$ gives the projection of a vector v onto K_j in terms of the components of the projection of v with respect to basis vectors (q_{1j},r_{1j}) or $(\Lambda q_{2j},\Lambda r_{2j})$ as appropriate. Let $w_{1j} = D_{1j}\hat{p}_{1j}$, $w_{2j} = D_{2j}\Lambda\hat{p}_{2j}$.

Let (q_j,r_j) be the orthonormal basis in which the components of w_j will be expressed (we note that any two ortho-

normal vectors in K_j would suffice for this purpose). Though (q_j,r_j), (q_{1j},r_{1j}) and $(\Lambda q_{2j},\Lambda r_{2j})$ are all bases of K_j they are not identical in general. We obtain the components of w_j from the components of w_{1j} and w_{2j} as follows:

Let D_j be a 2 x 3 matrix with rows equal to q_j' and r_j' respectively. $D_j v$ gives the projection of a vector v onto K_j in terms of the components of the projection of v with respect to the basis (q_j,r_j). Let M_{ij} be the 2 x 2 matrix of rotation through an angle ψ_{ij} defined by

$$M_{1j} = \begin{bmatrix} q_j' q_{1j} & q_j' r_{1j} \\ r_j' q_{1j} & r_j' r_{1j} \end{bmatrix} = \begin{bmatrix} \cos\psi_{1j} & \sin\psi_{1j} \\ -\sin\psi_{1j} & \cos\psi_{1j} \end{bmatrix}$$

$$M_{2j} = \begin{bmatrix} q_j' \Lambda q_{2j} & q_j' \Lambda r_{2j} \\ r_j' \Lambda q_{2j} & r_j' \Lambda r_{2j} \end{bmatrix} = \begin{bmatrix} \cos\psi_{2j} & \sin\psi_{2j} \\ -\sin\psi_{2j} & \cos\psi_{2j} \end{bmatrix}$$

Then $D_j = M_{1j}D_{1j} = M_{2j}D_{2j}$ and $w_j = M_{1j}w_{1j} - M_{2j}w_{2j}$.

When both $0 << \beta_{ij} < \alpha_{ij}$ and $\sigma_{ijk} << 1$, $k=1,..,n_{ij}$, the distribution of w_{ij} is approximately bivariate-normal with mean 0 and covariance matrix A_{ij} defined by (see Appendix II):

$$A_{ij} = \begin{bmatrix} 1/\alpha_{ij} & 0 \\ 0 & 1/\beta_{ij} \end{bmatrix}$$

The distribution of w_j is approximately bivariate-normal with mean 0 and covariance matrix A_j defined by

$$A_j = M_{1j}A_{1j}M_{1j}' + M_{2j}A_{2j}M_{2j}'$$

(see Morrison, 1967, Chapter 3). The matrix A_j provides information about the variation in w_j when $\hat{p}_{2j}$ is rotated to $\hat{\Lambda}\hat{p}_{2j}$. To the extent that this approximation is valid the probability density for the set $(w_j, j=1,..,J)$ is proportional to

$$\prod_{1\leq j\leq J} \exp\{-\tfrac{1}{2}w_j' A_j^{-1} w_j\} \qquad (1)$$

Let

$$\Phi = \sum_{1\leq j\leq J} w_j' A_j^{-1} w_j$$

Φ is proportional to the logarithm of (1). Φ depends upon Λ, s_{ijk}, $\hat{s}_{ijk}$ and σ_{ijk} through A_j and w_j. A_j depends only upon Λ, s_{ijk} and σ_{ijk}. To the extent that w_j is a useful approximation to $\hat{p}_{1j} - \hat{\Lambda}\hat{p}_{2j}$ the vector w_j is dependent only upon Λ, $\hat{s}_{ijk}$ and σ_{ijk}. As Λ and A_j are unknown we estimate them by the following procedure:

Let $\hat{\Lambda}$ be the rotation tensor for a trial reconstruction. The points $(t_{ijk}, i=1,2; k=1,..,n_{ij})$ were defined in section III.5 for $\hat{\Lambda}$. Let $\hat{T}_{ij}$ be the weighted covariance matrix (defined as in section III.4) for the points $(t_{ijk}, k=1,..,n_{ij})$ and associated $(\sigma_{ijk}, k=1,..,n_{ij})$. Let $\hat{T}_j$ be the weighted covariance matrix for the points $(t_{ijk}, i=1,2; k=1,..,n_{ij})$ and associated $(\sigma_{ijk}, i=1,2; k=1,..,n_{ij})$. Let $\hat{a}_{ij}, \hat{b}_{ij}, \hat{c}_{ij}$ be the eigenvalues of $\hat{T}_{ij}$. We assume $\hat{a}_{ij} > \hat{b}_{ij} > \hat{c}_{ij}$. We have $\hat{c}_{ij} = 0$ from the definition of $\hat{T}_{ij}$. Similarly let $\hat{a}_j, \hat{b}_j, \hat{c}_j$ be

the eigenvalues of $\hat{T}_j$ where $\hat{a}_j > \hat{b}_j > \hat{c}_j = 0$. Let $\hat{g}_{ij}, \hat{h}_{ij}, \hat{f}_{ij}$ be eigenvectors of unit length associated with $\hat{a}_{ij}, \hat{b}_{ij}, \hat{c}_{ij}$ respectively. There are two eigenvectors of unit length associated with each eigenvalue but they differ only in sign. We choose $\hat{g}_{ij}$ and $\hat{h}_{ij}$ such that $\hat{g}_{ij} \times \hat{h}_{ij} = \hat{f}_{ij}$. Similarly, let $\hat{g}_j, \hat{h}_j, \hat{f}_j$ be eigenvectors of unit length associated with $\hat{a}_j, \hat{b}_j, \hat{c}_j$ respectively, where $\hat{g}_j \times \hat{h}_j = \hat{f}_j$.

Let $\hat{D}_{ij}$ be a 2 x 3 matrix with rows given by, respectively, $\hat{g}_{ij}'$ and $\hat{h}_{ij}'$. Let $\hat{w}_{1j} = \hat{D}_{1j}\hat{p}_{1j}$, $\hat{w}_{2j} = \hat{D}_{2j}\hat{\Lambda}\hat{p}_{2j}$. Let $\hat{D}_j$ be a 2 x 3 matrix with rows given by, respectively, $\hat{g}_j'$ and $\hat{h}_j'$. Let $\hat{M}_{ij}$ be the 2 x 2 matrix of rotation defined by

$$\hat{M}_{ij} = \begin{bmatrix} \hat{g}_j'\hat{g}_{ij} & \hat{g}_j'\hat{h}_{ij} \\ \hat{h}_j'\hat{g}_{ij} & \hat{h}_j'\hat{h}_{ij} \end{bmatrix}$$

Then $\hat{D}_j = \hat{M}_{1j}\hat{D}_{1j} = \hat{M}_{2j}\hat{D}_{2j}$. Let $\hat{w}_j = \hat{M}_{1j}\hat{w}_{1j} - \hat{M}_{2j}\hat{w}_{2j}$. Let $\hat{A}_{ij}$ be defined by

$$\hat{A}_{ij} = \begin{bmatrix} 1/\hat{a}_{ij} & 0 \\ 0 & 1/\hat{b}_{ij} \end{bmatrix}$$

Let $\hat{A}_j = \hat{M}_{1j}\hat{A}_{1j}\hat{M}_{1j}' + \hat{M}_{2j}\hat{A}_{2j}\hat{M}_{2j}'$. Then the second measure of fit (the first was Φ_0) is

$$\Phi_1 = \sum_{1 \le j \le J} \hat{w}_j'\hat{A}_j^{-1}\hat{w}_j$$

We seek that $\hat{\Lambda}$ for which Φ_1 is minimized. Though the method seems reasonable the points t_{ijk} presumably do not produce the exact minimum value of Φ_1 for trial $\hat{\Lambda}$. Thus the estimates of

Λ and s_{ijk} that minimize Φ presumably are not identical to the $\hat{\Lambda}$ and t_{ijk} that minimize Φ_1.

V.2 A Method for Obtaining An Approximate Uncertainty Region for the Rotation Tensor Using Φ_1

Let $\hat{\Lambda}$ be the rotation tensor that minimizes Φ_1. Associated with $\hat{\Lambda}$ and the data $\hat{s}_{1jk}$ and $\hat{\Lambda}\hat{s}_{2jk}$ are matrices $\hat{A}_j$ and $\hat{D}_j$, j=1,..,J (see section V.1). Let

$$\Delta_j = \hat{D}_j\hat{A}_j^{-1}\hat{D}_j$$

The non-negative scalar $(\hat{p}_{1j} - \hat{\Lambda}\hat{p}_{2j})'\Delta_j(\hat{p}_{1j} - \hat{\Lambda}\hat{p}_{2j})$ is the contribution of the j <u>th</u> section to Φ_1.

Let u_{1jk} be a perturbation in $\hat{s}_{1jk}$ such that $|\hat{s}_{1jk} + u_{1jk}| = 1$ and $|u_{1jk}| << 1$. Let u_{2jk} be a perturbation in $\hat{\Lambda}\hat{s}_{2jk}$ due to a perturbation in $\hat{s}_{2jk}$, where $|u_{2jk}| << 1$ and $|\hat{\Lambda}\hat{s}_{2jk} + u_{2jk}| = 1$. Let v_{1j} be the resultant perturbation in $\hat{p}_{1j}$, where $|\hat{p}_{1j} + v_{1j}| = 1$ and $|v_{1j}| << 1$. Let v_{2j} be the be the resultant perturbation in $\hat{\Lambda}\hat{p}_{2j}$ caused by the perturbation in $\hat{p}_{2j}$, where $|\hat{\Lambda}\hat{p}_{2j} + v_{2j}| = 1$ and $|v_{2j}| << 1$. For ease of notation let $\rho_j = \hat{\Lambda}\hat{p}_{2j}$.

Let Λ_* be a rotation tensor in a neighborhood of $\hat{\Lambda}$. We have

$$\Lambda_* \simeq (I + E)\hat{\Lambda}$$

where E is an antisymmetric perturbation matrix with independent elements $\varepsilon_1,\varepsilon_2,\varepsilon_3$ (see Appendix I). Let $\varepsilon' = (\varepsilon_1,\varepsilon_2,\varepsilon_3)$ where $|\varepsilon| << 1$.

We may define matrices $\hat{A}_{ij}(\varepsilon)$, $\hat{M}_{ij}(\varepsilon)$, $\hat{D}_{ij}(\varepsilon)$, $\hat{A}_j(\varepsilon)$ and $\hat{D}_j(\varepsilon)$ for Λ_* in a neighborhood of $\hat{\Lambda}$ given perturbations u_{ijk} and data s_{ijk} in the same way that $\hat{A}_{ij}$, $\hat{M}_{ij}$, $\hat{D}_{ij}$, $\hat{A}_j$ and $\hat{D}_j$ were defined. Let

$$d_j(\varepsilon) = (I + E)(\rho_j + v_{2j}) - (p_{1j} + v_{1j})$$

$$\Delta_j(\varepsilon) = [\hat{D}_j(\varepsilon)]'[\hat{A}_j(\varepsilon)]^{-1}\hat{D}_j(\varepsilon)$$

Then the measure of fit for Λ_* in a neighborhood of $\hat{\Lambda}$ is approximately

$$\Phi_1(\varepsilon) = \sum_{1\le j\le J} [d_j(\varepsilon)]'\Delta_j(\varepsilon)d_j(\varepsilon)$$

$\hat{f}_j$ was defined in section V.1 . When $|\hat{p}_{1j} - \rho_j|$ is small the projection of $\hat{p}_{1j} - \rho_j$ onto the plane normal to $\hat{f}_j$ is a good approximation to $\hat{p}_{1j} - \rho_j$. This implies that $\hat{D}_j(\varepsilon=0)d_j(\varepsilon)$ is a good approximation to $\hat{D}_j(\varepsilon)d_j(\varepsilon)$ when $|\varepsilon| << 1$. We will use $\hat{A}_j$ as an approximation to $\hat{A}_j(\varepsilon)$. Then

$$\Phi_1(\varepsilon) \simeq \sum_{1\le j\le J} [d_j(\varepsilon)]'\Delta_j d_j(\varepsilon) \qquad (1)$$

We seek an $\hat{\varepsilon}$ such that (1) is minimized, where $|\hat{\varepsilon}| << 1$. Let ∂_m denote $\partial/\partial\varepsilon_m$, m=1,2,3. We find $\hat{\varepsilon}$ by substituting (1) in the equations

$$\partial_m\Phi_1 = 0, \quad m=1,2,3.$$

The zero <u>th</u> order equations are

$$\sum_{1\le j\le J} (\rho_j - \hat{p}_{1j})'\Delta_j\partial_m(E\rho_j) = 0, \quad m=1,2,3$$

The first-order equations are

$$\sum_{1\le j\le J}(\rho_j - \hat{p}_{1j})'\Delta_j\partial_m(Ev_{2j}) + \sum_{1\le j\le J}(E\rho_j)'\Delta_j(E\rho_j)$$

$$+ \sum_{1\le j\le J}(v_{2j} - v_{1j})'\Delta_j\partial_m(E\rho_j) = 0,\ m=1,2,3 \qquad (2)$$

Define

$D_{j,m} = \Delta_j\partial_m(E\rho_j)$, with components $D_{j,m}^{(n)}$, n=1,2,3.

$C_j = \Delta_j(\rho_j - \hat{p}_{1j})$, with components $C_j^{(n)}$, n=1,2,3

Let $\rho_j^{(n)}$, n=1,2,3 be the components of ρ_j. Let Q be a 3 x 3 matrix with elements $(Q)_{mn}$ given by

$$(Q)_{m1} = \sum_{1\le j\le J}[\rho_j^{(3)}D_{j,m}^{(2)} - \rho_j^{(2)}D_{j,m}^{(3)}]$$

$$(Q)_{m2} = \sum_{1\le j\le J}[-\rho_j^{(3)}D_{j,m}^{(1)} + \rho_j^{(1)}D_{j,m}^{(3)}]$$

$$(Q)_{m3} = \sum_{1\le j\le J}[\rho_j^{(2)}D_{j,m}^{(1)} - \rho_j^{(1)}D_{j,m}^{(2)}]$$

Let

$$Y_j = \begin{bmatrix} 0 & -C_j^{(3)} & C_j^{(2)} \\ C_j^{(3)} & 0 & -C_j^{(1)} \\ -C_j^{(2)} & C_j^{(1)} & 0 \end{bmatrix}$$

$$Z_j = \begin{bmatrix} D_{j,1}^{(1)} & D_{j,1}^{(2)} & D_{j,1}^{(3)} \\ D_{j,2}^{(1)} & D_{j,2}^{(2)} & D_{j,2}^{(3)} \\ D_{j,3}^{(1)} & D_{j,3}^{(2)} & D_{j,3}^{(3)} \end{bmatrix}$$

Set all $v_{ij} = 0$ except for v_{2k}. Then (2) becomes

$$(Z_k + Y_k)v_{2k} + Q\hat{\varepsilon} = 0$$

Set all $v_{ij} = 0$ except for v_{1k}. Then (2) becomes

$$Z_k v_{1k} - Q\hat{\varepsilon} = 0$$

In a linear approximation the contributions from all v_{ij} are additive. Thus

$$\hat{\varepsilon} \simeq Q^{-1} \sum_{1 \le j \le J} [Z_j v_{1j} - (Z_j + Y_j)v_{2j}] \qquad (3)$$

We would like to use (3) to obtain some information about the set of $\hat{\varepsilon}$ that produce acceptable reconstructions. This will be accomplished as follows:

We will treat the v_{ij} as independent random variables. This implies that we treat $\hat{\varepsilon}$ as a random variable. Let T denote the covariance matrix of $\hat{\varepsilon}$. $\hat{D}_{ij}v_{ij}$ is the projection of v_{ij} onto the plane with basis $(\hat{g}_{ij}, \hat{h}_{ij})$ (see section V.1). When $|v_{ij}| << 1$ $\hat{D}_{ij}v_{ij}$ is a good approximation to v_{ij}. We assume that the covariance matrix of $\hat{D}_{ij}v_{ij}$ is $\hat{A}_{ij}$. Then (3) gives T in terms of $\hat{A}_{ij}$. We obtain this relation as follows:

The vectors $\hat{f}_{ij}$ were defined in section V.1 . Let Π_{ij} be the rotation matrix with rows given by, respectively, $\hat{g}'_{ij}$, $\hat{h}'_{ij}$, $\hat{f}'_{ij}$. We have

$$\Pi_{ij} = \begin{bmatrix} \hat{D}_{ij} \\ \hline \hat{f}'_{ij} \end{bmatrix}$$

We have $|\hat{p}_{1j} + v_{1j}| = 1$, $|\hat{p}_{1j}| = 1$, $|v_{1j}| << 1$ and $\hat{f}_{1j} = \hat{p}_{1j}$.

This implies $|\hat{f}'_{1j}v_{1j}| << |v_{1j}|$. Similarly $\hat{f}_{2j} = \hat{\Lambda}\hat{p}_{2j}$ and $|\hat{f}'_{2j}v_{2j}| << |v_{2j}|$. With these results and $v'_{ij} = \Pi'_{ij}\Pi_{ij}v_{ij}$ we have

$$v'_{ij} \simeq (v'_{ij}\hat{g}_{ij}, v'_{ij}\hat{h}_{ij}, 0)\Pi_{ij} \tag{4}$$

Let

$$\Gamma_{ij} = \begin{bmatrix} \hat{A}_{ij} & 0 \\ & 0 \\ 0\ 0 & 0 \end{bmatrix} \tag{5}$$

From (4) and (5) we have

$$\mathrm{Cov}(v_{ij}) \simeq \Pi'_{ij}\Gamma_{ij}\Pi_{ij} \tag{6}$$

where Cov(.) denotes the covariance matrix of the argument (see methods in Morrison, 1967, Chapter 2). From (6) and (3) we obtain

$$T \simeq Q^{-1}\{\sum_{1\le j\le J} Z_j\Pi'_{1j}\Gamma_{1j}\Pi_{1j}Z'_j + (Z_j + Y_j)\Pi'_{2j}\Gamma_{2j}\Pi_{2j}(Z_j + Y_j)'\}(Q^{-1})'$$

(see methods in Morrison, 1967, Chapter 2).

Let τ_1, τ_2, τ_3 be the eigenvalues of T. We assume $\tau_1 > \tau_2 > \tau_3 > 0$. Let t_1, t_2, t_3 be eigenvectors of unit length associated with τ_1, τ_2, τ_3 respectively. There are two such eigenvectors for each eigenvalue but they differ only in sign. The direction of greatest variation of $\hat{\varepsilon}$ is t_1. If the reconstruction of $\hat{\Lambda}$ is reasonable in all sections than this direction will approximately correspond to the direction of least

increase in $\Phi_1(\varepsilon)$ for $|\varepsilon| = k$, where k is a constant. That is, $\Phi_1(kt_1) < \Phi_1(kt_2) < \Phi_1(kt_3)$, for $|k| << 1$.

Let u denote the pole of rotation for $\hat{\Lambda}$ and let u + t be the pole of rotation that corresponds to $\hat{\varepsilon}$. $\hat{\Lambda}$ can be written $\hat{\Lambda} = R'AR$ where R is a rotation matrix (see section V.3). The projection of u + t into the coordinate frame of the row vectors of R is approximately $(\omega_1,\omega_2,1)$, where $|\omega_1| << 1$ and $|\omega_2| << 1$. Let $\omega' = (\omega_1,\omega_2)$. The methods of section V.3 provide for an approximate relation of the form $\omega = P\hat{\varepsilon}$ where P is a linear transformation. Let M be the covariance matrix of ω. Then M = PTP' (see Morrison, 1967, Chapter 2). Let μ_1,μ_2 be the eigenvalues of M. We assume $\mu_1 > \mu_2 > 0$. Let m_1 and m_2 be eigenvectors of unit length associated with μ_1 and μ_2 respectively. The direction of greatest variation of ω is m_1. Let $\bar{\Phi}_1$ denote the value of Φ_1 for a specified pole of rotation at the angle that minimizes Φ_1 for the pole. If the reconstruction of $\hat{\Lambda}$ is reasonable in all sections then m_1 will approximately correspond to the direction of least increase of $\bar{\Phi}_1$ for $|\omega|$ = constant. Also m_2 will approximately correspond to the direction of greatest increase of $\bar{\Phi}_1$ for $|\omega|$ = constant (and m_1 is normal to m_2 because $\mu_1 \neq \mu_2$). Let c be a positive constant. The relation $\omega'M^{-1}\omega = c$ specifies an ellipse of semi-axes $(c\mu_1)^{1/2}$, $(c\mu_2)^{1/2}$ in ω-space. The set of poles of rotation that correspond to the relation $\omega'M^{-1}\omega \leq c$ can provide an approximate description of an uncertainty region for the pole

of rotation if the following conditions are met:

(i) m_1 and m_2 are in approximate correspondence with the directions of least increase and greatest increase of $\overline{\Phi}_1$ respectively.

(ii) $\sqrt{\mu_1}$ and $\sqrt{\mu_2}$ are approximately proportional to the dimensions of the uncertainty region.

(iii) c is properly chosen.

Conditions (i) and (ii) ought to hold, approximately, if the reconstruction of $\hat{\Lambda}$ is reasonable in all sections. Condition (iii) can be satisfied by examination of a small number of reconstructions.

V.3 Relation Between Λ_* and ε

Let u be the pole of rotation for $\hat{\Lambda}$. The rotation $\hat{\Lambda}$ can be written $\hat{\Lambda} = R'AR$ where R is a rotation matrix with elements ρ_{ij}, $1 \leq i,j \leq 3$, $(Ru)' = (0,0,1)$ and

$$A = \begin{bmatrix} \cos\psi & \sin\psi & 0 \\ -\sin\psi & \cos\psi & 0 \\ 0 & 0 & 1 \end{bmatrix}$$

Here ψ is the angle of rotation for $\hat{\Lambda}$ and pole u (see also discussions in section III.7 and Appendix III). Let Λ_* be a rotation tensor in a neighborhood of $\hat{\Lambda}$. We have

$$\Lambda_* \simeq (I + E)\hat{\Lambda} \qquad (1)$$

Let $u + t$ be the pole for Λ_* where $|u + t| = 1$ and $|t| << 1$. The equation that defines $u + t$ is

$$\Lambda_*(u + t) = u + t, \quad |u + t| = 1, \quad |t| << 1. \qquad (2)$$

The projection of $u + t$ into the coordinate frame of the row vectors of R is

$$R(u + t) \simeq (\omega_1, \omega_2, 1)$$

where $|\omega_1| << 1$ and $|\omega_2| << 1$. With this relation, (1) and the relation $\hat{\Lambda} = R'AR$ we obtain a first-order perturbation equation from (2) (see also discussion of accuracy of approximation in section III.7):

$$A(\omega_1, \omega_2, 0)' + RER'(0,0,1)' \simeq (\omega_1, \omega_2, 0)' \qquad (3)$$

The row vectors of R form a right-handed orthonormal basis. Hence (3) can be simplified to

$$\begin{bmatrix}\omega_1\\ \omega_2\end{bmatrix} \simeq \frac{1}{2}\begin{bmatrix} 1 & -\sin\psi/(\cos\psi - 1)\\ \sin\psi/(\cos\psi - 1) & 1\end{bmatrix}\begin{bmatrix}-\rho_{21}\varepsilon_1 - \rho_{22}\varepsilon_2 - \rho_{23}\varepsilon_3\\ \rho_{11}\varepsilon_1 + \rho_{12}\varepsilon_2 + \rho_{13}\varepsilon_3\end{bmatrix}$$

(4)

The angle of rotation for Λ_* is $\psi + \delta$ where $|\delta| << 1$. We have

$$\text{Trace}[(I + E)\hat{\Lambda}] \simeq 1 + 2\cos(\psi + \delta) \qquad (5)$$

Let λ_{ij}, $1 \leq i,j \leq 3$, be the elements of $\hat{\Lambda}$. From (5) we obtain (see also discussion in section III.7 about accuracy of approximation):

$$\delta \simeq -[\varepsilon_1(\lambda_{32} - \lambda_{23}) + \varepsilon_2(\lambda_{13} - \lambda_{31}) + \varepsilon_3(\lambda_{21} - \lambda_{12})]/2\sin\psi$$

(6)

As ε is calculated after the rotation $\hat{\Lambda}$ has been applied to the relevant dataset, the perturbation pole u + t that is determined by ε and (4) is also rotated by $\hat{\Lambda}$. Thus the original coordinates of u + t are approximately $\hat{\Lambda}'R'(\omega_1,\omega_2,1)'$.

ACKNOWLEDGEMENTS

I am grateful to Roxanne Regan, Peter Briggs, Larry Lawver, Pam Thompson, Tony Irving, Inez Fung, Jim Bishop, John Crowe, Ray Hartman and Jim Barnes for helping to ease the pain. My parents kindly provided an occasional refuge from the storm. The support of John Sclater and Pete Molnar throughout this effort is appreciated. Richard Dudley, Dan McKenzie and Michael Woodroofe made suggestions that improved the presentation of the material. This research has been supported by the National Science Foundation under Grant 74-026360 CE.

REFERENCES

Bullard, E.C., J.E. Everett and A.G. Smith, The Fit of the Continents Around the Atlantic, In: A Symposium on Continental Drift, Edited by P.M.S. Blackett, E.C. Bullard and S.K. Runcorn, Phil. Trans. Roy. Soc. London, A, 1088, 41-51, 1965.

Courant, R. and D. Hilbert, Methods of Mathematical Physics, Vol. I, Interscience Publishers, New York, 1953.

Cramér, Harald, Mathematical Methods of Statistics, Princeton University Press, Princeton, 1974.

Fisher, R.A., Statistical Methods and Scientific Inference, Hafner Publishing Co., New York, 1959.

Goldstein, H., Classical Mechanics, Addison-Wesley Publishing Co., Reading, Massachusetts, U.S.A., 1950.

Hess, H.H., History of the Ocean Basins, In: Petrologic Studies - Buddington Memorial Volume, Geol. Soc. Am., New York, 1962, pp. 599-620.

Hildebrand, F.B., Methods of Applied Mathematics, Prentice-Hall, Inc., Englewood Cliffs, New Jersey, 1965.

Isacks, B., J. Oliver and L.R. Sykes, Seismology and the New Global Tectonics, Jour. Geophys. Research, 73, 5855-5899, 1968.

Kendall, M.G. and A. Stuart, The Advanced Theory of Statistics, Vol. II, Griffin, London, 1973.

Le Pichon, X., J. Francheteau and J. Bonnin, Plate Tectonics, Elsevier Scientific Publishing Co., Amsterdam, 1973.

Mardia, K.V., Statistics of Directional Data, Academic Press, London and New York, 1972.

McKenzie, D.P., D. Davies and P. Molnar, Plate Tectonics of the Red Sea and East Africa, Nature, 226, 243-248, 1970.

McKenzie, D.P., and W.J. Morgan, Evolution of Triple Junctions, Nature, 224, 125-133, 1969.

McKenzie, D.P. and R.L. Parker, The North Pacific: An Example of Tectonics on a Sphere, Nature, 216, 1276-1280, 1967.

McKenzie, D.P. and J.G. Sclater, The Evolution of the Indian Ocean Since the Late Cretaceous, Geophys. J. Roy. Astron. Soc., 24, 437-528, 1971.

Morgan, W.J., Rises, Trenches, Great Faults and Crustal Blocks, Jour. Geophys. Research, 73, 1959-1982, 1968.

Morrison, D.F., Multivariate Statistical Methods, McGraw-Hill, New York, 1967.

Rudin, W., Principles of Mathematical Analysis, Second Edition, McGraw-Hill, New York, 1964.

Taylor, F.B., Bearing of the Tertiary Mountain Belt on the Origin of the Earth's Plan, Bull. Geol. Soc. Am., 21, 179-226, 1910.

Vine, F.J., Spreading of the Ocean Floor: New Evidence, Science, 154, 1405-1415, 1966.

Wegener, A., Die Entstehung der Kontinente und Ozeane, Friedr. Vieweg und Sohn, Braunschweig, 1929 (reprinted as The Origin Of Continents and Oceans by Dover Publications, New York, 1966).

Wilkinson, J.H., The Algebraic Eigenvalue Problem, Clarendon Press, Oxford, 1965.

Wilson, J. Tuzo, A New Class of Faults and Their Bearing on Continental Drift, Nature, 207, 343-347, 1965.

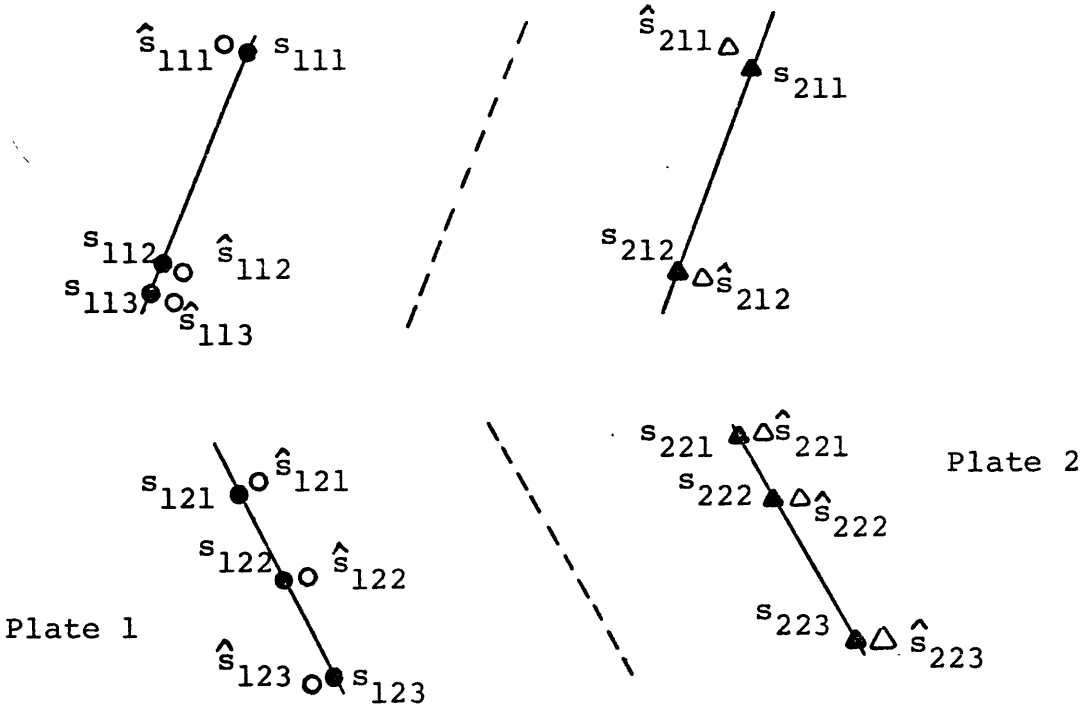
$\hat{s}_{111}$
s_{111}
s_{112}
$\hat{s}_{112}$
s_{113}
$\hat{s}_{113}$
$\hat{s}_{211}$
s_{211}
s_{212}
$\hat{s}_{212}$
s_{121}
$\hat{s}_{121}$
s_{122}
$\hat{s}_{122}$
Plate 1
$\hat{s}_{123}$
s_{123}
s_{221}
$\hat{s}_{221}$
Plate 2
s_{222}
$\hat{s}_{222}$
s_{223}
$\hat{s}_{223}$

(a)

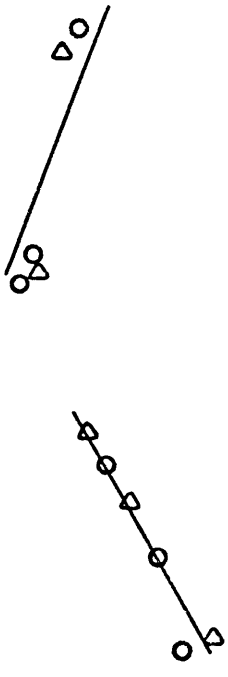

(b)

FIGURE I

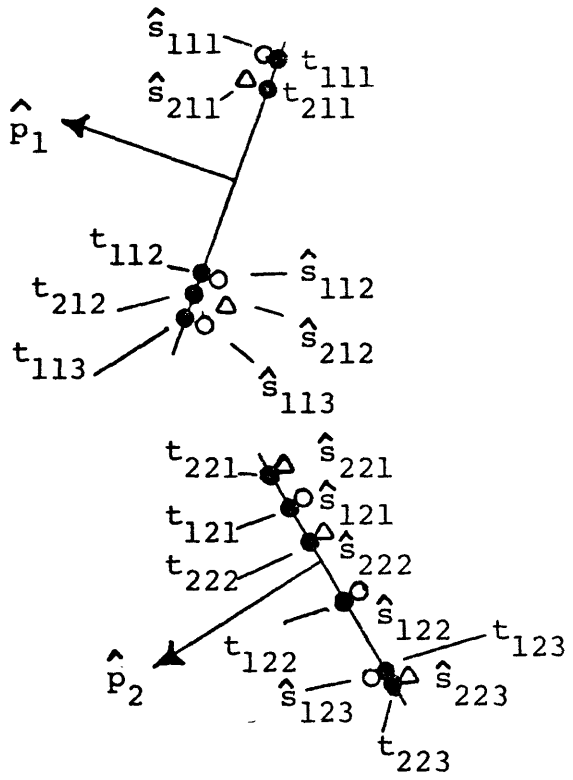

FIGURE II

Data and Projected Points Along Common Great-Circle Arc Segments on a Reconstruction Specified by Rotation Tensor $\hat{\Lambda}$

All points $\hat{s}_{2jk}$ have been rotated from $\hat{s}_{2jk}$ to $\hat{\Lambda}\hat{s}_{2jk}$. $\hat{p}_j$ is the unit vector normal to the jth great-circle. t_{1jk} is the intersection of the meridian through $\hat{p}_j$ and $\hat{s}_{1jk}$ with the great-circle normal to $\hat{p}_j$. t_{2jk} is the intersection of the meridian through $\hat{p}_j$ and $\hat{\Lambda}\hat{s}_{2jk}$ with the great-circle normal to $\hat{p}_j$.

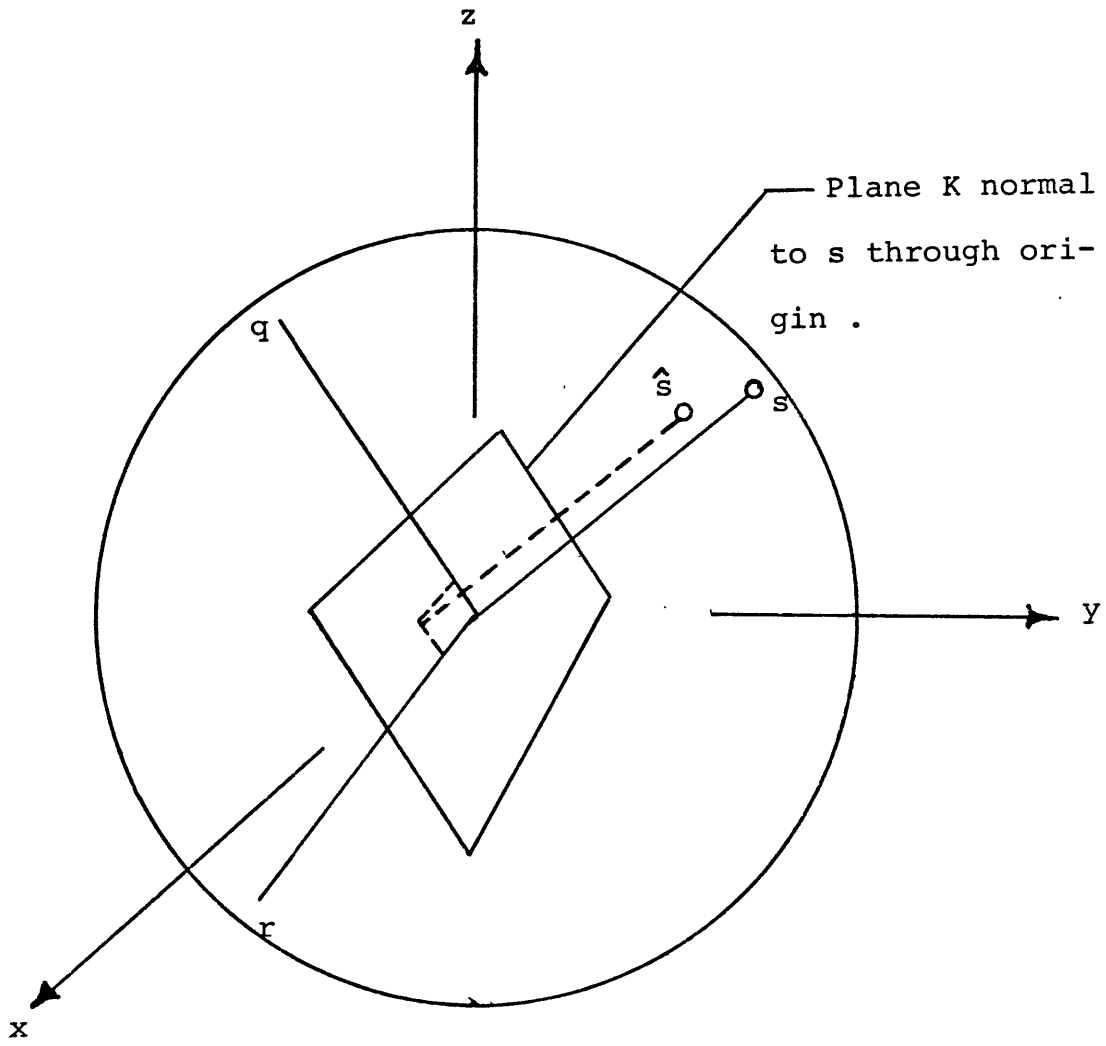

FIGURE III

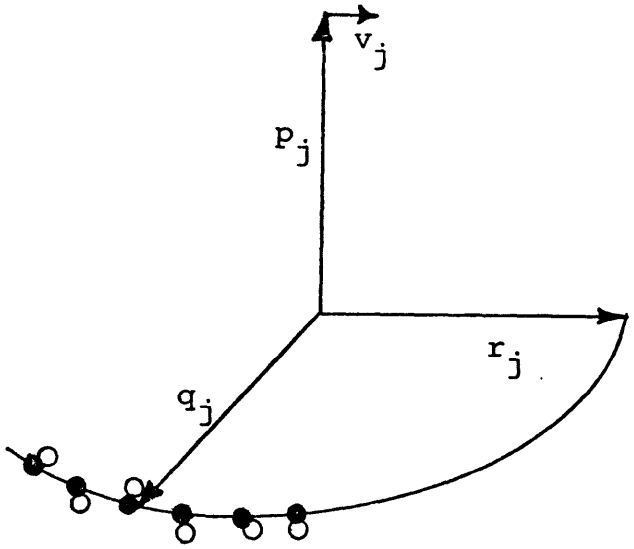

FIGURE IV

Representative Data Set

The filled circles represent the points

$$\{s_{1jk}, k=1,..,n_{1j}; \Lambda s_{2jk}, k=1,..,n_{2j}\}$$

The open circles represent the points

$$\{\hat{s}_{1jk}, k=1,..,n_{1j}; \Lambda \hat{s}_{2jk}, k=1,..,n_{2j}\}$$

q_j, r_j, p_j are the eigenvectors of B_j (see section IV.5). $p_j + v_j$ is an eigenvector of unit length associated with the minimum eigenvalue of $\hat{B}_j$ (see section IV.5).

APPENDIX I

The Existence of Reconstructions That Are Similar to the True Reconstruction

We seek rotation tensors $\hat{\Lambda}$ in a neighborhood of Λ for which the points $\hat{\Lambda}s_{2jk}$ are closest to Λs_{2jk}. For $\hat{\Lambda}$ in a neighborhood of Λ we have

$$\hat{\Lambda} \simeq (I+E)\Lambda \qquad (1)$$

where I is the identity matrix and E is a 3x3 antisymmetric perturbation matrix (Goldstein, 1950, pp 125-127):

$$E = \begin{bmatrix} 0 & \varepsilon_3 & -\varepsilon_2 \\ -\varepsilon_3 & 0 & \varepsilon_1 \\ \varepsilon_2 & -\varepsilon_1 & 0 \end{bmatrix}$$

Let $\varepsilon' = (\varepsilon_1, \varepsilon_2, \varepsilon_3)$. Then $Ew = w \times \varepsilon$ for any vector w where 'x' denotes the vector product.

Let

$$v_{2jk} = \Lambda s_{2jk}$$

$$d_{2jk} = \hat{\Lambda} s_{2jk} - v_{2jk}$$

$$\rho_{2jk} = d'_{2jk} d_{2jk} / \sigma^2_{2jk} = |d_{2jk}|^2 / \sigma^2_{2jk}$$

$$S = \sum_{j,k} \rho_{2jk}$$

Using (1) we obtain

$$\rho_{2jk} \simeq v'_{2jk} E'E v_{2jk} / \sigma^2_{2jk} \qquad (2)$$

We have $|Ev_{2jk}|^2 = |v_{2jk} \times \varepsilon|^2 = \varepsilon'\varepsilon - (\varepsilon' v_{2jk})^2$. Substitution of this relation into (2) yields

$$\rho_{2jk} \simeq [\varepsilon'\varepsilon - (\varepsilon' v_{2jk})^2]/\sigma^2_{2jk} \qquad (3)$$

Let the 3x3 positive semidefinite symmetric matrix B be defined by

$$B = \sum_{j,k} \sigma^{-2}_{2jk} v_{2jk} v'_{2jk}$$

Let

$$K = \sum_{j,k} \sigma^{-2}_{2jk}$$

Then

$$S = K\,\varepsilon'\varepsilon + \varepsilon' B \varepsilon$$

Expression (3) implies that the minimum S = 0 is attained only when $\varepsilon = 0$ unless all v_{2jk} are co-axial, in which case $\varepsilon = cv_{2jk}$ is the solution where c is any real constant, $|c| \ll 1$.

We therefore seek those ε for which S is a minimum subject to the constraint

$$\varepsilon'\varepsilon - c^2 = 0$$

where c is a real constant, $0 < |c| \ll 1$. The vectors ε of magnitude $|c|$ that minimize S are among the solutions of

$$\nabla S - \gamma \nabla(\varepsilon'\varepsilon - c^2) = 0, \quad \varepsilon'\varepsilon = c^2$$

where γ is a scalar and ∇ denotes gradient. This equation is equivalent to $(B+KI)\varepsilon = \gamma\varepsilon$ so that $\varepsilon'(B+KI)\varepsilon = \gamma c^2$; hence the desired ε is an eigenvector associated with the minimum eigenvalue γ of B+KI. As $K\varepsilon'\varepsilon = Kc^2$ we have $\varepsilon' B \varepsilon = \tau c^2$ where $\tau = \gamma - K$, $\tau > 0$. For fixed K, τ is a minimum when γ is

a minimum; hence the desired ε is an eigenvector associated with the minimum eigenvalue τ of B. Let τ_1 be the minimum eigenvalue of B. We assume τ_1 is distinct. Let t_1 be an associated eigenvector of unit length. There are two such eigenvectors but they differ only in sign. The desired solution is

$$\varepsilon = ct_1 \quad .$$

APPENDIX II

Let $s_k'=(x_k,y_k,z_k)$, $1\leq k\leq n$, be points on the unit sphere and let σ_k, $1\leq k\leq n$, be positive scalars. The distance of s_k from the plane normal to the unit vector w is $w's_k$ and this distance weighted by σ_k is $w's_k/\sigma_k$. Define the 3x3 positive semidefinite symmetric matrix B:

$$B = \sum_{1\leq k\leq n} \sigma_k^{-2} \begin{bmatrix} x_k^2 & x_k y_k & x_k z_k \\ y_k z_k & y_k^2 & y_k z_k \\ z_k x_k & z_k y_k & z_k^2 \end{bmatrix}$$

The sum of squares of the weighted distances of s_k, $1\leq k\leq n$, from the plane normal to w is

$$\sum_{1\leq k\leq n} (w's_k/\sigma_k)^2 = w'Bw$$

The unit vectors w that minimize this sum are among the solutions of

$$\nabla w'Bw - \gamma\nabla(w'w-1) = 0,\ w'w=1,$$

where γ is a scalar and ∇ denotes gradient. This equation is equivalent to $Bw = \gamma w$ so that $w'Bw = \gamma$; hence the desired w is an eigenvector associated with the minimum eigenvalue γ of B. Let α,β,γ be the eigenvalues of B. We assume $\alpha>\beta>\gamma\geq 0$. Let u,v,w be the respective associated eigenvectors of unit length. Then the two unit vectors r that minimize r'Br are $r=\pm w$. Let $[e_1,e_2,e_3]$ be the standard basis vectors in R^3 and and let Q be a rotation matrix such that $e_1=Qu$, $e_2=Qv$, $e_3=Qw$. The vector $Qs_k=(\xi_k,\eta_k,\zeta_k)'$ represents the coordinates of s_k in a coordinate system where B is diagonalized. In this

system B is given by

$$B = \begin{bmatrix} \alpha & 0 & 0 \\ 0 & \beta & 0 \\ 0 & 0 & \gamma \end{bmatrix}, \quad \alpha > \beta > \gamma \geq 0. \tag{1}$$

and $Be_3 = e_3$. For the remainder of this appendix we work in this particular coordinate system. Let

$$\Delta = \begin{bmatrix} \delta_{11} & \delta_{12} & \delta_{13} \\ \delta_{21} & \delta_{22} & \delta_{23} \\ \delta_{31} & \delta_{32} & \delta_{33} \end{bmatrix} \text{ where } \Delta' = \Delta.$$

The eigenvalues and eigenvectors of $B+\Delta$ are perturbations of the eigenvalues and eigenvectors of B when Δ is a perturbation of B. Let $\tau_i+\lambda_i$, $i=1,2,3$ be the eigenvalues of $B+\Delta$ where $\tau_1=\alpha$, $\tau_2=\beta$, $\tau_3=\gamma$. Let $(e_i+\nu_i)$, $i=1,2,3$ be the associated eigenvectors, where $(e_i+\nu_i)'(e_i+\nu_i) = 1$, $|\nu_i| << 1$ and $\nu_i' = (\varepsilon_{1i}, \varepsilon_{2i}, \varepsilon_{3i})$. We have

$$\varepsilon_{11} = -(\varepsilon_{21}^2+\varepsilon_{31}^2)/2 - \tfrac{1}{4}[(\varepsilon_{21}^2+\varepsilon_{31}^2)^2] + O[(\varepsilon_{21}^2+\varepsilon_{31}^2)^3]$$
$$\varepsilon_{22} = -(\varepsilon_{12}^2+\varepsilon_{32}^2)/2 - \tfrac{1}{4}[(\varepsilon_{12}^2+\varepsilon_{32}^2)^2] + O[(\varepsilon_{12}^2+\varepsilon_{32}^2)^3]$$
$$\varepsilon_{33} = -(\varepsilon_{13}^2+\varepsilon_{23}^2)/2 - \tfrac{1}{4}[(\varepsilon_{13}^2+\varepsilon_{23}^2)^2] + O[(\varepsilon_{13}^2+\varepsilon_{23}^2)^3]$$

The equation for λ_i, ν_i is

$$(B+\Delta)(e_i+\nu_i) = (\tau_i+\lambda_i)(e_i+\nu_i) \tag{2}$$

The eigenvalues of $B+\Delta$ are the solutions of

$$\det[B+\Delta-(\tau_i+\lambda_i)I] = 0 \tag{3}$$

where I is the identity matrix and det[.] is the determinant function. From (3) we find

$$\lambda_1 = \delta_{11}-\delta_{12}\delta_{21}/(\beta-\alpha) - \delta_{13}\delta_{31}/(\gamma-\alpha)$$
$$\lambda_2 = \delta_{22}-\delta_{12}\delta_{21}/(\alpha-\beta) - \delta_{32}\delta_{23}/(\gamma-\beta) \qquad (4)$$
$$\lambda_3 = \delta_{33}-\delta_{13}\delta_{31}/(\alpha-\gamma) - \delta_{32}\delta_{23}/(\beta-\gamma)$$

through second order in the elements of Δ. To solve for $\nu_i, i=1,2,3$ we demonstrate the approach for ν_3 and then repeat it for ν_1 and ν_2.

If $(\gamma+\delta_{33})(e_3+\nu_3)$ is subtracted from both sides of (2) then the first two rows of the equation are written

$$(\alpha-\gamma)\varepsilon_{13} + \delta_{12}\varepsilon_{23} + \delta_{13} = \delta_{13}\varepsilon_{33} + (\lambda_3-\delta_{11})\varepsilon_{13}$$
$$\delta_{21}\varepsilon_{13} + (\beta-\gamma)\varepsilon_{23} +\delta_{23} = \delta_{23}\varepsilon_{33} + (\lambda_3-\delta_{22})\varepsilon_{23}$$

As $\varepsilon_{33} \simeq -(\varepsilon_{13}^2+\varepsilon_{23}^2)/2$ and $\lambda_3 \simeq \delta_{33}$ the first and second order perturbations are provided by the solution of the system

$$(\alpha-\gamma)\varepsilon_{13} + \delta_{12}\varepsilon_{23} + \delta_{13} = (\delta_{33}-\delta_{11})\varepsilon_{13}$$
$$\delta_{21}\varepsilon_{13} + (\beta-\gamma)\varepsilon_{23}+\delta_{23} = (\delta_{33}-\delta_{22})\varepsilon_{23}$$

Whence we conclude

$$\begin{matrix}\varepsilon_{13} \\ \varepsilon_{23}\end{matrix} = \begin{matrix}-\delta_{13}/(\alpha-\gamma) + \delta_{21}\delta_{23}/(\alpha-\gamma)(\beta-\gamma) + \delta_{13}(\delta_{11}-\delta_{33})/(\alpha-\gamma)^2 \\ -\delta_{23}/(\beta-\gamma) + \delta_{12}\delta_{13}/(\alpha-\gamma)(\beta-\gamma) + \delta_{23}(\delta_{22}-\delta_{33})/(\beta-\gamma)^2\end{matrix}$$

(5)

This is correct through second order in the elements of Δ. With (5) and

$$\varepsilon_{33} \simeq -[\delta_{13}^2/(\alpha-\gamma)^2 + \delta_{23}^2/(\beta-\gamma)^2]/2$$

the perturbed eigenvector $(\varepsilon_{13},\varepsilon_{23},1+\varepsilon_{33})$ is correct through second order in δ_{ij}. With an analogous approach we find

$$\begin{matrix}\varepsilon_{21} \\ \varepsilon_{31}\end{matrix} = \begin{matrix}-\delta_{21}/(\beta-\alpha) + \delta_{32}\delta_{31}/(\beta-\alpha)(\gamma-\alpha) + \delta_{21}(\delta_{22}-\delta_{11})/(\beta-\alpha)^2 \\ -\delta_{31}/(\gamma-\alpha) + \delta_{23}\delta_{21}/(\beta-\alpha)(\gamma-\alpha) + \delta_{31}(\delta_{33}-\delta_{11})/(\gamma-\alpha)^2\end{matrix}$$

and

$$\begin{matrix}\varepsilon_{12} \\ \varepsilon_{32}\end{matrix} = \begin{matrix}-\delta_{12}/(\alpha-\beta) + \delta_{31}\delta_{32}/(\alpha-\beta)(\gamma-\beta) + \delta_{12}(\delta_{11}-\delta_{22})/(\alpha-\beta)^2 \\ -\delta_{32}/(\gamma-\beta) + \delta_{13}\delta_{12}/(\alpha-\beta)(\gamma-\beta) + \delta_{32}(\delta_{33}-\delta_{22})/(\gamma-\beta)^2\end{matrix}$$

These relations and relations (5) and (4) can also be obtained by methods discussed in Wilkinson (1965, Chapter 2, pp. 68-70) or Courant and Hilbert (1953, pp. 42-44).

Let the coordinates of s_k be expressed in the basis u,v,w so that $s_k'=(\xi_k,\eta_k,\zeta_k)$. Assume that the s_k are all in the plane normal to w, so that $\gamma=0$ and $s_k'=(\xi_k,\eta_k,0)$, $k=1,\ldots,n$. From (1) we have

$$\sum_{1\le k\le n} \xi_k^2/\sigma_k^2 = \alpha, \quad \sum_{1\le k\le n} \xi_k\eta_k/\sigma_k^2 = 0, \quad \sum_{1\le k\le n} \eta_k^2/\sigma_k^2 = \beta \qquad (6)$$

Let $\hat{s}_k = s_k+\mu_k$ where $|\hat{s}_k|=1$, $|\mu_k|<<1$ and $\mu_k'=(\mu_{1k},\mu_{2k},\mu_{3k})$ in u,v,w. Let

$$\hat{B} = \sum_{1\le k\le n} \hat{s}_k\hat{s}_k'/\sigma_k^2 = B + \Delta$$

Then

$$\Delta = \sum_{1\le k\le n} (\mu_k s_k'+s_k\mu_k'+\mu_k\mu_k')/\sigma_k^2$$

Let $\hat{\gamma}$ be the smallest eigenvalue of $\hat{B}$. Then by (4) we have

$$\hat{\gamma} = \sum_{1\le k\le n} \mu_{3k}^2/\sigma_k^2 - \Big(\sum_{1\le k\le n} \xi_k \mu_{3k}/\sigma_k\Big)^2/\alpha - \Big(\sum_{1\le k\le n} \eta_k \mu_{3k}/\sigma_k^2\Big)^2/\beta$$

$$+O(|\mu|^3) \quad \text{where } |\mu|^2 = \sum_{1\le k\le n} \mu_k'\mu_k$$

Suppose the μ_{3k} are independent normal random variables with mean 0 and variance σ_k^2. Let $G_k = \mu_{3k}/\sigma_k$. Then G_k are independent standard normal variables. Let $G'=(G_1,\ldots,G_n)$. Then

$$G'G = \sum_{1\le k\le n} \mu_{3k}^2/\sigma_k^2$$

Let

$$v^{(1)} = (v_1, v_2, \ldots, v_n)$$
$$v^{(2)} = (w_1, w_2, \ldots, w_n)$$

where $v_i = \xi_i/\sigma_i\alpha^{1/2}$, $i=1,\ldots,n$

$w_j = \eta_j/\sigma_j\beta^{1/2}$, $j=1,\ldots,n$

Then by (6), $v^{(1)}$ and $v^{(2)}$ are orthogonal unit vectors in R^n, where R^n denotes n-dimensional Euclidean space. We can construct vectors $v^{(3)},\ldots,v^{(n)}$ such that $v^{(1)},\ldots,v^{(n)}$ is an orthonormal basis of R^n by a method such as the Gram-Schmidt orthogonalization procedure (see, e.g., Hildebrand, 1965, pp. 34-36). The quantity G'G is the squared magnitude of G; hence G'G is invariant with respect to an orthogonal transformation of the basis vectors of R^n. Thus

$$G'G = \sum_{1\le k\le n} (G'v^{(k)})^2$$

and $\hat{\gamma} = \sum_{3\leq k\leq n} (G'v^{(k)})^2$.

The scalar $G'v^{(k)}$ is a standard normal random variable and the $G'v^{(k)}$, k=1,...,n are mutually independent because G has a multivariate-normal distribution with mean 0 and covariance matrix I where I is the identity matrix. Therefore $\hat{\gamma}$ is the sum of squares of n-2 independent normal variables, each with mean 0 and variance 1, i.e., a χ^2 variable with n-2 degrees of freedom (see Morrison, 1967, p. 10 for definition of a χ^2 random variable).

We also have

$$(\delta_{13},\delta_{23}) = \sum_{1\leq k\leq n} (\xi_k\mu_{3k},\eta_k\mu_{3k})/\sigma_k^2$$

through first order in perturbation theory. Then, using (5) we find

$$\mathrm{Var}(\varepsilon_{13}) = \alpha^{-2} \sum_{1\leq k\leq n} \xi_k^2/\sigma_k^2 = 1/\alpha$$

$$\mathrm{Var}(\varepsilon_{23}) = \beta^{-2} \sum_{1\leq k\leq n} \eta_k^2/\sigma_k^2 = 1/\beta$$

$$\mathrm{Cov}(\varepsilon_{13},\varepsilon_{23}) = (\alpha\beta)^{-1} \sum_{1\leq k\leq n} \xi_k\eta_k/\sigma_k^2 = 0$$

Hence the covariance matrix of $(\varepsilon_{13},\varepsilon_{23})$ becomes

$$\begin{bmatrix} 1/\alpha & 0 \\ 0 & 1/\beta \end{bmatrix} .$$

APPENDIX III

Let $u' = (0,0,1)$

$$T = \begin{bmatrix} \cos\psi & \sin\psi & 0 \\ -\sin\psi & \cos\psi & 0 \\ 0 & 0 & 1 \end{bmatrix}, \quad -\pi \leq \psi \leq \pi$$

We have $T'T = I$ and $\det(T) = 1$; hence T is a rotation matrix. u is a unit vector. u is an eigenvector of T with eigenvalue $= 1$ because $Tu = u$. The unit vector $-u$ is also an eigenvector of T with eigenvalue $= 1$. ψ is determined up to sign by $\text{Trace}(T) = 1+2\cos\psi$, $-\pi \leq \psi \leq \pi$. The sign of ψ is determined by the sign of $\sin\psi$.

Let Δ be a matrix such that $(T+\Delta)'(T+\Delta) = I$ and $\det(T+\Delta) = 1$. Hence $T+\Delta$ is a rotation matrix. Let δ_{ij}, $1 \leq i,j \leq 3$, be the elements of Δ. Let $u+\nu$ be the pole of rotation and let $\psi+\lambda$ be the angle of rotation for $T+\Delta$. Let $\nu' = (\varepsilon_1,\varepsilon_2,\varepsilon_3)$ and $e' = (\varepsilon_1,\varepsilon_2)$. From $(u+\nu)'(u+\nu) = 1$ we obtain

$$\varepsilon_3 = -\frac{1}{2}\, e'e - \frac{1}{4}(e'e)^2 + O[(e'e)^3]$$

Δ is a perturbation of T when $|\delta_{ij}| \ll 1$ and $|\delta_{ij}| \ll |\psi|$. Then $|\nu| \ll 1$ and $\varepsilon_3 \simeq -e'e/2$. We seek $u+\nu$ in a neighborhood of u for which

$$(T+\Delta)(u+\nu) = u+\nu \qquad (1)$$

Let

$$A = \begin{bmatrix} \cos\psi-1 & \sin\psi \\ -\sin\psi & \cos\psi-1 \end{bmatrix}$$

Using $\varepsilon_3 \simeq -e'e/2$ in the first two rows of (1) we obtain

the relation

$$Ae = -\begin{bmatrix}\delta_{13}\\ \delta_{23}\end{bmatrix} - \begin{bmatrix}\delta_{11} & \delta_{12}\\ \delta_{21} & \delta_{22}\end{bmatrix} e + \frac{1}{2}\, e'e \begin{bmatrix}\delta_{13}\\ \delta_{23}\end{bmatrix} \qquad (2)$$

The terms of (2) involving e'e are of third order in δ_{ij}. The components of e through second order in δ_{ij} are obtained directly from the remaining terms of (2). These components are given by

$$e = -A^{-1}\begin{bmatrix}\delta_{13}\\ \delta_{23}\end{bmatrix} + A^{-1}\begin{bmatrix}\delta_{11} & \delta_{12}\\ \delta_{21} & \delta_{22}\end{bmatrix} A^{-1}\begin{bmatrix}\delta_{13}\\ \delta_{23}\end{bmatrix}$$

where

$$A^{-1} = \frac{-1}{2(\cos\psi - 1)}\begin{bmatrix}\cos\psi - 1 & -\sin\psi\\ \sin\psi & \cos\psi - 1\end{bmatrix}$$

We have $\quad \text{Trace}(T+\Delta) = 1 + 2\cos(\psi+\lambda)$

With $|\lambda| << 1$ we find

$$\cos(\psi+\lambda) = \cos\psi - \lambda\sin\psi - (\lambda^2/2)\cos\psi + O(\lambda^3)$$

With $\text{Trace}(T+\Delta) = 1 + 2\cos\psi + \delta_{11} + \delta_{22} + \delta_{33}$ we obtain

$$-2\lambda\sin\psi - \lambda^2\cos\psi \simeq \delta_{11} + \delta_{22} + \delta_{33} \qquad (3)$$

From (3) we obtain

$$\lambda = -(\delta_{11} + \delta_{22} + \delta_{33})/2\sin\psi - \frac{1}{4}\cot\psi \left[\frac{\delta_{11} + \delta_{22} + \delta_{33}}{\sin\psi}\right]^2$$

through second order in δ_{ij}. When the conditions $|\delta_{ij}| << 1$ and $|\delta_{ij}| << |\psi|$ are not met the relation between either e or λ and δ_{ij} is not well-approximated by a linear relation.

THE STATISTICS OF FINITE ROTATIONS IN PLATE TECTONICS

PART II

An Application to the Evolution of the South Pacific

Preface

The data and reconstructions of Molnar et al. (1975) for the times of anomalies 13 and 18 in the South Pacific are re-examined with the statistical tools of the preceding paper. The use of the statistical tools for this kind of data is carefully explained. Uncertainty regions for the poles of rotation are obtained and compared to the subjective uncertainty regions of Molnar et al. (1975).

A. Introduction

The methods of the preceding paper will be used to re-examine the reconstructions obtained by Molnar et al. (1975) for the times of anomalies 13 and 18 in the South Pacific. The available fracture zone crossings and magnetic anomaly identifications were sparsely distributed. A reconstruction obtained from such data is tightly constrained if the uncertainty of each data point is tightly constrained. The location and width of each of the fracture zones in this dataset is not strongly constrained by the magnetics because the magnetic anomaly identifications are rarely in the vicinity of the fracture zones. Hence the probable location and probable width of a fracture zone must be inferred from the bathymetry.

As the data is sparse, a particular section of the reconstructed plate boundary will often have two points from one side of the present ridge axis but only one point from the other side. Thus criterion Φ_0 (see previous paper, section III.5) is directly applicable to this kind of data. For the sake of comparison of results, criterion Φ_1 (see previous paper, Chapter V) was also used with this data. As Φ_1 requires at least two points from each side of the present ridge axis, a dummy point was chosen to augment the single known datum where necessary when Φ_1 was used. A large standard deviation of error was assigned to the dummy point to ensure that it would have little influence upon the reconstruction. The results of this comparison are discussed in

section B.10 of this paper.

The construction of an uncertainty region for the pole and angle was based upon an examination of the distances of the fixed and rotated points from the estimated common great-circle arcs that defined the reconstructed plate boundary for a large number of poles at the angle that minimized the measure of fit for each of the poles.

B. Procedure

1. Preliminary Work

The available sources of data (e.g., published magnetics and bathymetric profiles, bathymetric chart) were examined to ascertain the quality of the data and to obtain estimates of uncertainty for the points. The poles and angles listed in Table 2 of Molnar et al. (1975) were then used to obtain preliminary reconstructions for the times of anomalies 13 and 18. The overall quality of the reconstructions was judged in the light of the above information. Individual data points that seemed inconsistent with the preliminary reconstructions were identified. Their sources were re-examined to see if the quality of this data has been misjudged. In several cases the re-examination showed that the data was of poorer quality than originally thought. The uncertainties associated with these data were increased. Some of the latter points were simply eliminated because they were too uncertain. The remaining re-examined points, if any, were retained in the data sets for the reconstructions. The information gained from re-

examination of the inconsistent points was then used to re-evaluate the quality of the points that originally had seemed consistent with the preliminary reconstruction.

2. Selection of Position of Block Boundary from Magnetic Anomalies and Assignment of Uncertainty

The positions of block boundaries are those of Molnar et al (1975). The place along a given anomaly profile that represents the block boundary of interest is uncertain, and the shape of the anomaly is often quite variable from profile to profile. The factors that affected the estimation of uncertainties are the following:

a. The closeness with which the actual anomaly follows the shape of an anomaly derived from theoretical block models.

b. The clarity of neighboring anomalies along the profile.

c. The presence of a seamount or fracture zone in the vicinity of the anomaly.

A region of uncertainty (along the profile) was assigned to a magnetic anomaly point. The standard deviation of error for this point was set equal to one-half of the width of this region. The weight assigned to the deviation of an actual data point from its hypothetical location was determined by this relation over the range of uncertainty.

3. Selection of Position of Previously Active Transform Fault and Estimation of Uncertainty

The positions of previously active transform faults are

those of Molnar et al. (1975). The place along the bathymetric profile that represents the previously active transform fault is uncertain but the fossil transform fault is constrained to lie within the fracture zone. The width of a fracture zone at a crossing was estimated from the bathymetric profile (or bathymetric chart if the profile was unavailable). It was occasionally difficult to see the limits of a fracture zone in a profile; in this event a large width was assigned. The standard deviation of error was set equal to one-fourth of the assigned width.

4. Systematic Uncertainties Among Fracture Zone Crossings

If a pole of relative motion between two plates remains fixed with respect to the pair of plates for a long period then transform faults will follow small-circles around the pole (see previous paper, Chapter I). The fossil transform faults that are created during this period will also follow small-circles (whether or not the fracture zones associated with the fossil transform faults have a similar shape depends upon the history of relative motion since that period). Thus the difference between the shape of a fossil transform fault and that of a great-circle arc over some length of arc may be caused by the curvature of a small-circle arc.

The maximum value of any such difference for a given length of arc was evaluated with the method of Appendix I. For the data of the present study the maximum length of any one section of fossil transform fault data was approximately

150 km (some fossil transform fault data along each of the Tharp and Heezen fracture zones between offset lineations was separated into two sections; see C and D of this paper for details). We refer to Appendix I. Let d represent the distance (in radians) along a small-circle arc subtended by angle 2w. Then $d=2w \sin\rho$ where ρ= colatitude of the small-circle with respect to the pole. For the data of this study we used $\rho \simeq 30^{\circ}$. Then $w \simeq d$. If d=150 km (in radians) then $\delta \simeq 0.75$ km (in radians) where δ represents the maximum difference between a small-circle arc and a great-circle arc over a distance of 150 km when the small-circle arc is approximately 30° away from the pole. For the data of this study δ is negligible compared to the 20-35 km width of the fracture zone. Thus any difference in shape between a small-circle arc and a great-circle arc for the sections of data in this study is negligible compared to the width of the relevant fracture zones. Furthermore, this also implies that any significant curvature of the fracture zones between offset lineations for the sections of data of this study is not caused by small-circle curvature.

It was occasionally necessary to increase the estimated width of a fracture zone at a crossing to compensate for significant curvature and/or local irregularities among sparsely distributed fracture zone crossings from opposite sides of the ridge axis. This increased the width of the region in which the fossil transform fault was constrained to lie. On

a major fracture zone, along a section of little overall curvature, the increase in width was usually taken to be less than 10% of the linear distance between two crossings. In other areas the increase in width was more subjectively chosen. The standard deviation of error for this crossing was set equal to one-fourth of the increased total width.

5. Correlated Errors

The statistical methodology assumes that uncertainties among the data are mutually independent. This is unlikely to be true for transform fault assignations (at fracture zone crossings) or magnetic anomaly identifications along closely-spaced track lines, for the tectonic histories of adjacent places are highly correlated. For example, there are two crossings of the (transform fault within the) Tharp fracture zone near 140° W. There is an Eltanin 19 crossing at (-52.42, -140.17) and an Eltanin 17 crossing at (-52.55,-139.75). The distance between these crossings is only 32 km. If both crossings were utilized by the statistical methodology in obtaining a reconstruction then the section which contained these points would carry a disproportionately large weight. This problem was eliminated by using the information in both crossings to constrain the Eltanin 19 crossing. The Eltanin 17 crossing was not included in the data set. The bathymetric signatures of the two crossings were similar (Figures 1 & 5, Molnar et al, 1975). The width of uncertainty for the chosen crossing was determined from the Eltanin 19 profile (Figure 5, Molnar et al, 1975) because the Eltanin 17 profile was not immediately available. Neither cruise had satellite navigation. Since the bathymetric chart (Figure 1, Molnar et al, 1975) indicated that the two profiles were consistent in location it seemed reasonable to reduce the navigational uncertainty for the Eltanin 19 crossing.

A similar problem existed elsewhere on the Tharp fracture zone. The Eltanin 23 crossings at (-57.85,-115.32) and (-57.58,-116.0) were 50 km apart. The position of the transform fault was assigned to be midway between the two. The widths associated with the crossings were averaged and the result assigned to be the uncertainty of the midpoint. Since the crossings were made sequentially on Eltanin 23, which had satellite navigation, the navigational error was taken to be the error usually assigned to a single crossing on a satellite-navigated cruise.

6. Navigational Errors

A navigational error with a standard deviation of 1 km was assigned to data which had been gathered on cruises with satellite navigation. Other data were assigned a navigational error with a standard deviation of 9 km. This figure is derived from a discussion by Pitman et al (1968, p 2071).

7. Total Error

Let s_p= standard deviation of error due to uncertainty in the selection of the previous plate boundary from the magnetic anomaly profile or bathymetric profile. For a fracture zone crossing s_p includes any systematic uncertainties. Let s_n= standard deviation of navigational error and let s_t= standard deviation of (total) error due to these sources. Then s_t is computed from the relation $s_t^2 = s_p^2 + s_n^2$.

8. Further Comments on Treatment of the Data

The weight assigned to the deviation of a data point from its hypothetical location is determined by the standard deviation of the statistical error that is assigned to the hypothetical location. If this standard deviation is sufficiently large (compared to the size of the subjective uncertainty region for the point) then the effective range of the Gaussian error will exceed the limits of the subjective uncertainty region. This limitation is unavoidable within the Gaussian framework. It is not a significant limitation for estimation of the best-fit reconstruction if there is a best-fit reconstruction that is consistent with all of the data.

If this limitation exists for the data in a sparse data set (and, as a practical matter, it often will) then method (1) of section III.6 of the previous paper must be used to construct an uncertainty region for the pole of rotation and angle of rotation. When the data are numerous, when there are many bends in the reconstructed plate boundary, and when all or nearly all of the data are strongly constrained to lie within their associated regions of uncertainty then methods (2) or (3) of section III.6 of the previous paper may be used to construct an uncertainty region for the pole and angle.

9. Use of the Computer Program

The poles and angles in Table 2 of Molnar et al. (1975) were used as initial estimates of the reconstruction parameters. The measure of fit was computed for each preliminary reconstruction. A section-by-section decomposition of the measure of fit was obtained. The measure for each section was examined in the light of the reconstruction for the section: fixed points, rotated points, assigned standard deviations of error and estimated common great-circle arc.

A number of poles were chosen in the vicinity of the preliminary pole. The angle of rotation that minimized the measure of fit was obtained for each of these poles and for the preliminary pole by the procedure outlined in section II.4 of the previous paper. The half-range of search for the angle was 1° of rotation. The coarse-scale increment and fine-scale increment for the search (a,b respectively in the notation of section II.4 of the previous paper) were 0.1° and 0.01° respectively. A decomposition of the measure of fit at the computed angle was studied. The distances of fixed and rotated points from the estimated common great-circle arc for each section were examined in the light of the assigned standard deviations of error. Several angles near the computed angle were specified for each of the poles and the associated reconstructions were examined in the same way as the other reconstructions were examined. The results shed light upon whether the angle that minimized the measure of fit (for a given pole) produced a good reconstruction. Moreover, the

effect of a change in pole and angle on the fit of each section of data could be observed.

Next, the program was permitted to search for the pole and angle that minimized the measure of fit. The search routine was given the pole and angle of the preliminary reconstruction as initial estimates. The angle that minimized the measure of fit for the initial pole was found. This task was repeated for eight poles of rotation that lay on a rectangle centered at the initial pole (Figure 1). The latitude increment $\Delta\theta$ and longitude increment $\Delta\phi$ were chosen to make the rectangle nearly square. The initial rectangle was roughly 25 km on each side. The pole for which the measure of fit was a minimum was selected as the new starting point. If no pole on the rectangle was better than the initial estimate then the latitude increment and longitude increment were decreased by a multiplicative factor (=0.5 for this study). The search was continued until the latitude increment and longitude increment became smaller than minimum values which were given to the program. The final rectangle was approximately 2 km on each side.

B.10 Comparison of Criterion Φ_0 with Criterion Φ_1

There were three important results from this comparison. First, for the data of this study the angle that minimized Φ_0 for a given pole was virtually identical to the angle that minimized Φ_1 for the pole. Second, for the data of this study the best-fit pole and angle obtained with Φ_0 were virtually identical to the best-fit pole and angle obtained with Φ_1. By virtually identical we mean that any difference between a quantity computed using Φ_0 and the same quantity computed with Φ_1 was smaller than the search increment or search grid used in this study. Third, the computation associated with Φ_1 was far in excess of the computation associated with Φ_0. Because of these results the use of Φ_0 is preferable to the use of Φ_1.

C. Data and Reconstruction for Anomaly 13 Time

1. Introduction

Figure 2 shows the location of the data. Appendix 2 shows data and estimated uncertainties that were used to obtain the anomaly 13 reconstruction. It was always difficult to translate a qualitative judgement of the magnetic anomaly signature into a quantitative estimate of uncertainty. As a consequence, the poorer signatures usually received large standard deviations of error (see discussion in section B.8 of this paper). The treatment of fracture zone crossings followed section B.3 of this paper.

The data for each of the Tharp and Heezen fracture zones was separated into two groups because the systematic curvature of each fracture zone between its offset lineations was significant compared to the width of the fracture zone. This was detected by careful inspection of the data as it was nearly impossible to detect this problem by eye. For example, the Heezen crossing at (-58.49,-107.23) is 18 km from the great-circle through Heezen crossings (-59.08,-104.88) and (-59.95,-101.75). The width of the Heezen fracture zone in this region is probably less than 35 km. It is very likely that the 18 km difference reflects curvature of the fracture zone rather than navigational errors in the crossings because the crossings were taken from cruises that had satellite navigation. The lineation between the Tharp and Udintsev fracture zones was also separated into two parts because of the likelihood of systematic curvature.

As sections 7 and 8 on the Antarctic plate share a fossil transform point and its associated uncertainties (see Appendix 2), there will be some correlation between the measures of fit for these sections. This correlation will not significantly affect the reconstruction because there is much other data. Regardless of this difficulty, section 8 will carry no weight in the reconstruction because more serious problems exist in the data for this section of the reconstruction. These problems are discussed in detail in the next section.

2. Analysis

Molnar et al.'s (1975) reconstruction has a pole at (74.7,-57.0) and a rotation angle of 27.9 . The measure of fit for this reconstruction is shown in Table 1. The distances of the fixed and rotated points from the estimated common great-circles for this reconstruction are given in Table 1 (distances are given in units of the assigned standard deviation of error). All sections fit well except section 8.

The Heezen crossing at (-51.45,-140.10) on the Pacific plate is rotated to (-58.20,-109.21) by Molnar et al.'s (1975) reconstruction. This is roughly 35 km from the Heezen crossing at (-57.89,-109.35) on the Antarctic plate. The distances of the fixed and rotated point from the estimated common great-circle for this section are 6.5 km and 19.7 km respectively (Table 1). The standard deviation of error as-

signed to these points were 8.6 km and 12.7 km respectively (Appendix 2). The measure of fit for this section (see Table 1) is poor because the distances of these points from the estimated common great-circle are large relative to the standard deviations of error assigned to the points. The extent of the Heezen fracture zone along each of the two tracks was not well-determined because the bathymetric profiles (see Appendix 2 for reference) were hard to interpret. Hence the standard deviations of error assigned to the two crossings may be inaccurate. The crossing at (-51.45,-140.10) was obtained from an Eltanin 19 track. This cruise did not have satellite navigation. Thus it is possible that there was a large navigational error at this crossing. It is also possible that there was some systematic alteration of the Heezen fracture zone near the crossing at (-57.89,-109.35) because there is a major change in trend of this fracture zone in the vicinity of 110°W (see Molnar et al., 1975, Figure 2). These considerations indicated that the poor fit of section 8 was probably not due to a significant error in Molnar et al.'s (1975) reconstruction; rather it was a reflection of the quality of the data.

Further light was shed upon the influence of this data on the reconstruction when the computer program was directed to find both the angle that minimized the measure of fit (i.e., best-fit angle) for the preliminary pole and the most-acceptable (i.e., best-fit) pole and angle. The former was 28.0 and the latter were (74.638,-58.25) , 27.79. The measure

of fit for each of these reconstructions is given in Table 1. The distances of the fixed and rotated points from the estimated common great-circles for these reconstructions are also given in Table 1. It is apparent from the results in Table 1 that the contribution of section 8 to the measure of fit has a substantial influence on the reconstruction. For example, the measure of fit for the best-fit pole and angle is 3.09 and the contribution of section 8 to this measure is 1.41 . Thus 45% of the measure of fit at the best-fit pole and angle is due to this section alone. This influence was judged excessive in proportion to the amount and quality of the data for this section. As a consequence, the measure of fit was not weighted by the data for section 8 in further analysis.

The best-fit angle for the preliminary pole became 27.96 and the best-fit pole and angle became (74.827,-56.865) and 28.01 . The best-fit pole is plotted in Figure 3a. The reconstruction is shown in Figure 4a. The measure of fit for each of these results is given in Table 1. The contribution of section 8 to the measure of fit (see Table 1) was evaluated after these results had been obtained. The distances of the fixed and rotated points from the estimated common great-circles for these reconstructions are also given in Table 1.

An uncertainty region that follows part (1), section III.6 of the previous paper was constructed for the pole of rotation. This was accomplished by inspection of the distances

of fixed and rotated points from the estimated common great-circles for numerous poles at the angle that minimized the measure of fit for each of the poles. Over 250 poles of rotation were examined. Section 8 was not used to weight the reconstruction but it was used to prevent crossing of the Heezen fracture zone in the vicinity of 110° W. The boundary of this region is delineated by the diamond-shaped points in Fig. 3a . The poles and associated angles for these points are given in Table 2. The distances of the fixed and rotated points from the estimated common great-circles are given in Appendix 3 for some reconstructions whose poles lie along the long axis of the uncertainty region. Some of these reconstructions are shown in Figures 4b-4g. The deviations of the fixed and rotated points from the estimated common great-circles are also given for some reconstructions whose poles lie along longitude -57.0 in Appendix 3. Two of these reconstructions are shown in Figures 4h and 4i.

As the pole is moved away from the best-fit pole along the long axis of the region, the fit of some of the magnetic anomaly points at the angle that minimizes the measure of fit for the pole becomes increasingly worse (see Appendix 3). As the pole reaches either (70.6,-73.0) or (77.1,-38.0), the distances of some of the magnetic anomaly points from their estimated common great-circles becomes approximately 1 standard deviation. The standard deviation of error for a magnetic anomaly point was set equal to one-half of the width of the uncertainty region for the point (see B.2). The remaining mag-

netic anomaly points in these sections are less than one standard deviation from the estimated common great-circles for the reconstructions at these two poles; hence there is some freedom to move the common great-circles closer to those points which are more than one standard deviation away. The amount of freedom depends upon both the standard deviations of error that were assigned to the points and the configuration of the points. Thus there are reconstructions for poles along the long axis up to and including (70.6,-73.0) and (77.1,-38.0) that are consistent with the uncertainties assigned to the magnetic anomaly points. As the pole moves beyond (77.1,-38.0) to (77.3,-34.0), the distances of some of the magnetic anomaly points from the estimated common great-circles become a bit larger than one standard deviation. It is barely possible to remove this excess by slight changes in the positions of the common great-circles (compare results in Appendix 3 and Figure 4d). Thus the pole at (77.3,-34.0) marks a limit of acceptable poles along the long axis of the region based on the misfit of magnetic anomaly points alone.

With the exception of the fracture zone V point (-56.97,-104.60) in the reconstruction whose pole is at (70.6,-73.0), all of the fossil transform points for the reconstructions whose poles lie along the long axis are within two standard deviations of the estimated common great-circles (The standard deviation of error for a fossil transform fault was set equal to 1/4 of the width of the fracture

zone - see B.3). The point that is an exception is 2.08 standard deviations from the common great-circle. The extra 0.08 standard deviations is easily eliminated by moving the estimated common great-circle slightly closer to this point and slightly further from the two rotated points. This is possible because the estimated common great-circle is quite close to the two rotated points (see Appendix 3). Hence all of the fossil transform points for the reconstructions whose poles lie along the long axis up to and including (70.6,-73.0) and (77.3,-34.0) (at the angle that minimizes the measure of fit for each of the poles) are within 2 standard deviations of common great-circles. Thus each of these reconstructions is also consistent with the fracture zone information. As the pole moves beyond (70.6,-73.0) to (70.25,-74.0) and then (69.35,-76.0), the distance of one of the magnetic anomaly points from its common great-circle becomes quite a bit larger than one standard deviation. The distances of some fossil transform points from their common great-circles are larger than 2 standard deviations for the reconstruction whose pole is (69.35,-76.0). The distance of the fracture zone V point (-56.97,-104.60) from the estimated common great-circle is 2.48 standard deviations for this reconstruction. This distance cannot be reduced to less than 2 standard deviations without causing the distance of one of the other fracture zone V points to exceed 2 standard deviations. Thus there is no acceptable reconstruction for the

pole at (69.35,-76.0).

As the pole is moved away from the best-fit pole along longitude -57.0, the fit of some of the fossil transform points at the angle that minimizes the measure of fit for the pole becomes rapidly worse. The fit of the magnetic anomaly points does not change very much (see Figures 4h and 4i for comparison). The reconstruction whose pole is (75.4,-57.0) is unacceptable because one of the fossil transform points in section 9 is too far from the estimated common great-circle (see Appendix 3 and Figure 4h). The point is 2.5 standard deviations away. The excess distance (0.5 standard deviations) is 3 km. This excess distance is too large to be eliminated by changing the position of the common great-circle because the rotated point nearby permits at most 2 km of shift. The reconstruction whose pole is (75.3,-57.0) is acceptable because the excess distance of the point in section 9 has been reduced to an amount that can be eliminated by slightly changing the position of the common great-circle without forcing the other points in the section beyond their limits of uncertainty.

The reconstruction whose pole is (74.2,-57.0) is unacceptable because there is a fossil transform point in section 8 that is too far from the common great-circle (see Appendix 3 and Figure 4i). The excess distance is too large to be eliminated by changing the position of the common great-circle because the fixed point nearby would be forced beyond its limit of uncertainty. There is also a fossil

transform point in section 9 that is more than 2 standard deviations away from the estimated common great-circle for the section. However, the excess distance can be eliminated by a slight change in the position of the common great-circle without forcing the nearby rotated point beyond its limit of uncertainty.

If the pole is moved to (74.3,-57.0) then the excess distance of the fossil transform point in section 8 that is beyond its limit of uncertainty is reduced to 0.5 standard deviations. This excess represents 6 km. The distance of the nearby fixed fossil transform point from the common great-circle in 6 km less than its maximum permitted distance. Thus the position of the common great-circle can be altered to allow each of these fossil transform points to be 2 standard deviations from a common great-circle. The reconstruction for this pole is therefore at the limit of acceptability.

In Appendix 3 and in Table 2 the angle shown for a given pole is that angle which minimized the measure of fit. If there is an angle of rotation that yields a good reconstruction for a given pole then this criterion will find it. However, this criterion can be questioned when there are not any good reconstructions for a given pole. Each of the poles that were chosen to delineate the boundary of the uncertainty region was selected because the reconstruction specified by the angle that minimized the measure of fit for the pole was not

good. Hence it is possible that a slightly different angle of rotation for any one of these poles would produce a better reconstruction for the pole. This possibility was investigated for a number of poles by examination of the measure of fit and associated reconstruction for each of several angles in the neighborhood of the angle that minimized the measure of fit for each pole. The reconstructions for some of these poles may have been slightly improved at some of the other angles in the neighborhood of the angle that minimized the measure of fit for each pole. The amount of improvement depends upon the extent to which the better reconstructions of a set of poor reconstructions can be judged. Certainly there was no significant improvement in any reconstruction.

Molnar et al. (1975) did not explain how their subjective uncertainty region was obtained or how it was to be interpreted. The poles (75.5,-53.0) and (73.85,-62.0) are just outside Molnar et al.'s (1975) subjective uncertainty region along the long axis of the region defined by the diamond-shaped points in Fig. 3a . The reconstructions for these poles are shown in Figures 4b and 4e. The angle for each pole is the angle that minimized the measure of fit for the pole. The best-fit reconstruction of this study is shown in Figure 4a. The distances of the fixed and rotated points from the estimated common great-circles for these reconstructions and the best-fit reconstruction of Molnar et al. (1975) are given in, respectively, Appendix 3 and Table 1. A close examination of

this information yields two conclusions. First, the differences between the reconstruction of Molnar et al. (1975) and the best-fit reconstruction of this study are negligible. Second, the differences between either of the two reconstructions whose poles lie just outside Molnar et al.'s (1975) subjective uncertainty region and the best-fit reconstruction of this study are very small compared to the standard deviations of error assigned to the data points.

Ellipses of variation for the pole of rotation were constructed according to Chapter V of the previous paper. These ellipses are shown in Fig. 3a . The results that produced these ellipses are given in Appendix 4. The orientation of the ellipses is in reasonable agreement with the orientation of the uncertainty region of this study.

D. Data and Reconstruction for Anomaly 18 Time

1. Introduction

Figure 2 shows the location of the data. Appendix 5 shows data and assigned uncertainties used to obtain the anomaly 18 reconstruction. The fracture zone V crossings on the Antarctic plate at (-58.00,-99.00) and (-57.92,-99.57), which were shown by Molnar et al. (1975), were not used in the reconstruction because their quality was believed to be poor. There are several reasons for this judgement. The location and trend of fracture zone V implied by these two points is grossly inconsistent with both the location inferred from fracture zone V on the Pacific plate (which was determined from magnetics data on a satellite-navigated cruise) and the location and trend of each of the Heezen, Tharp and Udintsev fracture zones on the Antarctic plate. There are no usable magnetics data within 100 km of these fracture zone V crossings. The bathymetric chart of Molnar et al. (1975, Figure 1) shows that there is no distinctive bathymetric signature at either of these two locations. There is a feature several hundred km to the east which looks like a seamount. The 2400 fm and 2600 fm contours for this feature have been extended several hundred km further east to meet an Eltanin 21 track and an unidentified track. The two fracture zone V crossings appear to line up with these contours. The extension of these contours is a questionable interpretation. The quality of these two crossings was judged to be poor for these reasons.

The data for each of the Heezen and Tharp fracture zones

was separated into two groups because of the likelihood of systematic curvature of each fracture zone between the respective offset lineations (see discussion in section C.2 of this paper).

2. Analysis

The pole and angle of Molnar et al.'s reconstruction were (75.3,-48.5) and 33.0 . The measure of fit for this reconstruction and the contributions of sections 5 - 8 to the measure of fit are given in Table 3. The distances of the fixed and rotated points from the estimated common great-circles for this reconstruction are also given in Table 3. The magnetics data fits quite well. The fit of the Heezen data and some of the Tharp data do not look good. The program computed the angle that minimized the measure of fit for this pole. This angle was 33.23 . The measure of fit for this reconstruction and the contributions of sections 5 - 8 to the measure of fit are given in Table 3. The distances of the fixed and rotated points from the estimated common great-circles for this reconstruction are also given in Table 3. There is a slightly worse fit of the magnetics and a slightly better fit of the fossil transform points within the fracture zones for this angle compared to the fit for 33.0 . The angle for this pole that minimized the measure of fit of the magnetics alone was computed to be 33.08 . The measure of fit for this reconstruction and the contributions

of sections 5 - 8 to the measure of fit are presented in Table 3. The fit of the magnetics data is slightly better at 33.08 than at either 33.0 or 33.23 . In view of this result, the difference between the reconstructions of 33.0 and 33.23 seems due mainly to differences in the weighting of the fossil transform points.

The pole and angle that minimized the measure of fit were (75.08l,-51.25) and 32.56 . This pole is plotted in Fig. 3b . The reconstruction is shown in Figure 5a. The measure of fit and the contributions of sections 5 - 8 to the measure of fit are presented in Table 3. The distances of the fixed and rotated points from the estimated common great-circles are also given in Table 3. There is a slight overall improvement of the fit of the magnetic anomaly points compared to the preliminary reconstruction. There is a moderate worsening of the fit of the Tharp data which is offset by a large improvement in the fit of the Heezen data. Neither section 6 nor section 7 seems to fit well. Each of sections 5 - 8 contains data from cruises that were not navigated by satellite; hence it is possible that the navigational errors in some of these data are larger than estimated. Some other possible sources of misfit are systematic alteration of the fossil transform fault and misreading of the bathymetric profiles.

An uncertainty region for the pole of rotation was constructed in accordance with part (1), section III.6 of

the previous paper. This was accomplished by inspection of the distances of the fixed and rotated points from the estimated common great-circles for numerous poles at the angle that minimized the measure of fit for each of the poles. More than 100 poles of rotation were examined. The boundary of this region is delineated by the open circles with central dots in Fig. 3b . The poles and associated angles for these poles are given in Appendix 6 along with the distances of the fixed and rotated points from the estimated common great-circles for each of the reconstructions.

The angle shown for each pole in Appendix 6 is that angle which minimized the measure of fit for the pole. This choice of angle could be questioned for poles on the boundary of the uncertainty region for the anomaly 13 reconstruction because there were not any good reconstructions for those poles. As none of the anomaly 18 reconstructions are particularly good with respect to the fossil transform data, this choice of angle can be questioned for all poles that were examined in the construction of the present uncertainty region. As in the anomaly 13 analysis, the reconstructions for a number of poles were investigated by examination of the measure of fit and reconstructed data points for each of several angles in the neighborhood of the angle that minimized the measure of fit for each pole. For some of the poles there was a slight improvement in the poorly-fit sections at the expense of the other sections; hence the reconstructions

for these poles may have been slightly improved at some of the other angles. However, as in the anomaly 13 analysis, there was no significant improvement in the fit of any of the poorly-fit sections.

Let $\bar{\Phi}_0'$ be the measure of fit for a given pole at the angle that minimizes the measure of fit for the pole. For each pole in a neighborhood of the best-fit pole we have a value of $\bar{\Phi}_0$. This defines a surface of $\bar{\Phi}_0$ for poles in a neighborhood of the best-fit pole. The results in Table 4 (compare to Figure 3) indicate that this surface has the shape of a trough. The long axis of the trough represents the direction in which $\bar{\Phi}_0$ increases most slowly as the pole is moved away from the best-fit pole. Now, $\bar{\Phi}_0$ equals the sum of contributions from all sections. Thus it is possible for the contribution to $\bar{\Phi}_0$ from one section to increase rapidly but $\bar{\Phi}_0$ to increase only moderately as the pole is moved away from the best-fit pole if the increase in the contribution of the one section is offset by a decrease in the total contribution of the remaining sections. The shape of the uncertainty region is determined by the requirement that no data point exceed its maximum error with respect to a common great-circle arc. Thus a reconstruction for which the measure of fit is only moderately greater than the measure of fit for the best-fit reconstruction can have an unacceptable fit of the data in one section. This happened in the construction of the uncertainty region for the anomaly 18 reconstruction.

The reason that it happened is that the poor fit of the fossil transform data in sections 5 - 8 makes it difficult to find reconstructions that are consistent with either the fossil transform data or the magnetic anomaly data or both. That the range of acceptable anomaly 18 reconstructions is far smaller than the range of acceptable anomaly 13 reconstructions is due to this reason rather than greater precision in the data for the anomaly 18 reconstruction as compared to the data for the anomaly 13 reconstruction.

Ellipses of variation for the pole of rotation were constructed according to Chapter V of the previous paper. These ellipses are shown in Fig. 3b . The results that produced these ellipses are given in Appendix 7. The orientation of the ellipses is not in reasonable agreement with the orientation of the uncertainty region of this study. This is because the long axis of each ellipse is closely aligned with the long axis of the trough discussed above.

ACKNOWLEDGEMENTS

Pete Molnar kindly provided the author with the coordinates of magnetic anomalies and fossil transform faults identified by Molnar et al. (1975). Several discussions between the two helped the author to evaluate some data that appeared to be of questionable quality. A discussion with Hans Schouten helped the author to improve the presentation of the material. This research has been supported by the National Science Foundation under Grant 74-026360 CE.

REFERENCES

Molnar, P., T. Atwater, J. Mammerickx and S. M. Smith, Magnetic Anomalies, Bathymetry and the Tectonic Evolution of the South Pacific since the Late Cretaceous, Geophys. J. R. astr. Soc., 40, 383-420, 1975.

Pitman, W. C., III, E. M. Herron and J. R. Heirtzler, Magnetic Anomalies in the Pacific and Sea Floor Spreading, Jour. Geophys. Res., 73, 2069-2085, 1968.

APPENDIX I

The Difference Between a Small-Circle Arc and a Great-Circle Arc

Consider the figure in this Appendix. Let

ρ=colatitude of small-circle with respect to pole at N (equal to arc-length of meridian from N to small-circle). We assume $0<\rho<\pi$.

w=half-angle subtended by small-circle segment AB (there are two such half-angles but we want the smaller of the two).

I=point of intersection of meridian bisecting small-circle segment AB with great-circle through points A and B.

From the Law of Cosines for spherical triangle NBA we have

$$\cos(\widehat{AB}) = \cos(\widehat{NA})\cos(\widehat{NB}) + \sin(\widehat{NA})\sin(\widehat{NB})\cos(ANB)$$

From spherical triangles NBA and NBI, respectively, we obtain the relations

$$\frac{\sin(NBA)}{\sin(\widehat{NA})} = \frac{\sin(ANB)}{\sin(\widehat{AB})}$$

$$\frac{\sin(\widehat{NI})}{\sin(NBI)} = \frac{\sin(\widehat{BI})}{\sin(BNI)}$$

With the relations $\widehat{NA}=\widehat{NB}=\rho$, ANB=2w, $\widehat{BI}=\widehat{AB}/2$, BNI=w, and NBI=NBA for these spherical triangles, the three relations

given above equal, respectively:

$$\cos(\widehat{AB}) = \cos^2\rho + \sin^2\rho\cos(2w) \qquad (1)$$

$$\sin(NBA) = \sin\rho\sin(2w)/\sin(\widehat{AB}) \qquad (2)$$

$$\sin(\widehat{NI}) = \sin(NBA)\sin(\widehat{AB}/2)/\sin(w) \qquad (3)$$

From (2) and (3) we have:

$$\sin(\widehat{NI}) = \sin\rho\sin(\widehat{AB}/2)\sin(2w)/[\sin(\widehat{AB})\sin(w)] \qquad (4)$$

We also have:

$$\sin(\widehat{AB}/2)/\sin(\widehat{AB}) = [2\cos(\widehat{AB}/2)]^{-1}$$

$$\sin(2w)/\sin(w) = 2\cos(w)$$

Thus (4) becomes

$$\sin(\widehat{NI}) = \sin\rho\cos(w)/\cos(\widehat{AB}/2) \qquad (5)$$

Using $\cos(\widehat{AB}/2) = [(1+\cos(\widehat{AB}))/2]^{1/2}$ with (1) in (5) we obtain:

$$\sin(\widehat{NI}) = \sin\rho\cos(w)[(1+\cos^2\rho+\sin^2\rho\cos(2w))/2]^{-1/2} \qquad (6)$$

Let $O(e)$ denote a quantity d such that $|d| \leq C|e|$ for all e sufficiently small and some finite constant C. Let $\widehat{NI}=\rho-\delta$. We have $\delta=0$ when $\rho=\pi/2$. Assume $|\delta|<<1$, $|w|<<1$. Then

$$\sin(\widehat{NI}) = \sin\rho-\delta\cos\rho-(\delta^2/2)\sin\rho+O(\delta^3)$$

$$\cos(w) = 1-(w^2/2)+(w^4/4!)+O(w^6)$$

$$\cos(2w) = 1-2w^2+(2w^4/3)+O(w^6)$$

and (6) becomes

$$\delta\cos\rho+(\delta^2/2)\sin\rho+O(\delta^3) = (w^2/2)\sin\rho\cos^2\rho - w^4[(1/4!)\sin\rho-(5/12)\sin^3\rho+(3/8)\sin^5\rho] + O(w^6)$$

(7)

For $|w|<<|\cos\rho|$, $|\delta\sin\rho|<<|\cos\rho|$ we obtain from (7):

$$\delta \simeq \frac{w^2}{4}\sin(2\rho)$$

For given w, $|\delta|$ is a maximum when $\rho=45^\circ$, 135°. If δ,w are measured in degrees then the above relation is equivalent to

$$\delta \simeq (0.436 \times 10^{-2})w^2\sin(2\rho)$$

For $\rho \simeq \pi/2$ we set $\rho=\alpha+\pi/2$ where $|\alpha|<<1$. Then

$$\cos\rho = -\alpha + \alpha^3/3! + O(\alpha^5)$$

$$\sin\rho = 1 - \alpha^2/2 + \alpha^4/4! + O(\alpha^6)$$

and we obtain from (7) the relation

$$-\delta\alpha + \delta^2/2 \simeq w^2\alpha^2/2$$

From this relation we find

$$\delta \simeq -\alpha w^2/2$$

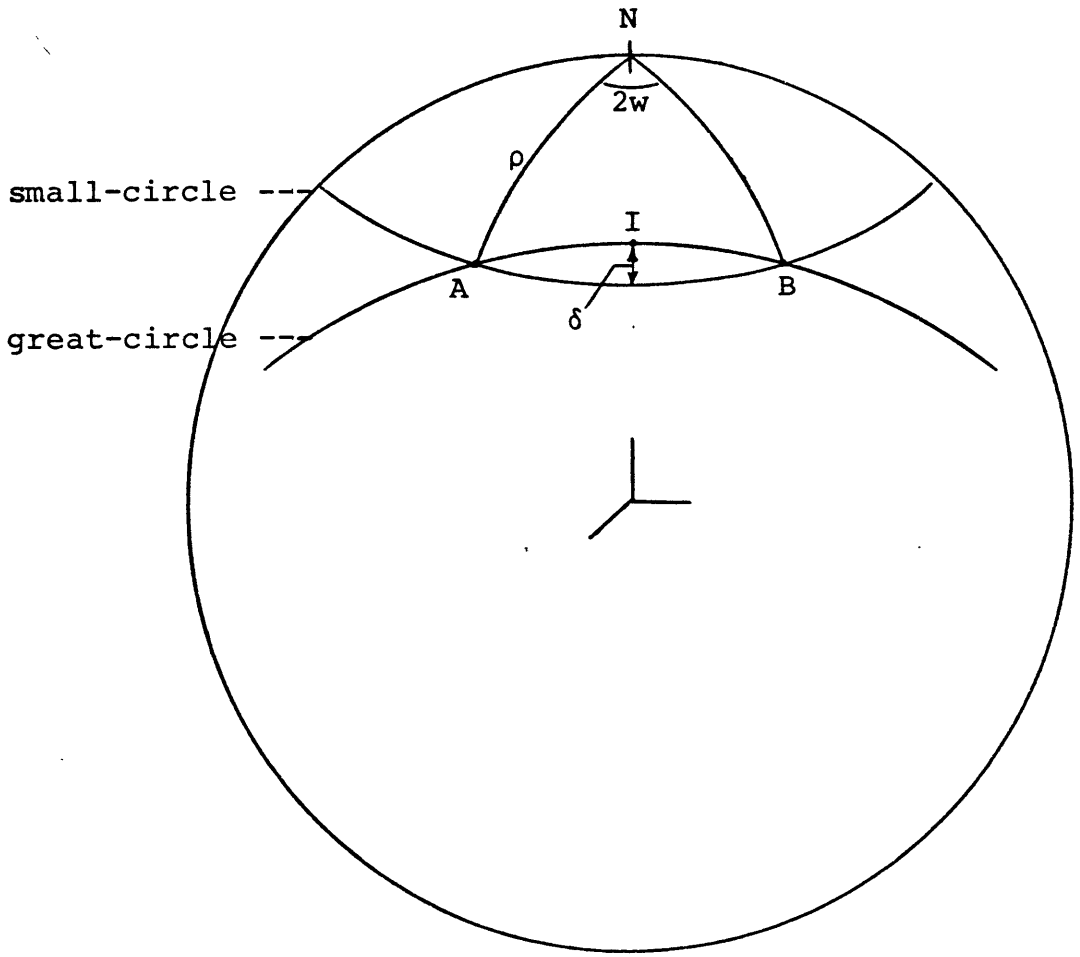

Figure for Appendix I

APPENDIX 2

Usable data: Anomaly 13 reconstruction

Section	Feature
1	Lineation between fracture zones IV and V
2,3	Lineation between fracture zones Tharp and Udintsev: sections 1,2
4	Lineation between fracture zones Udintsev and VIII
5	Fracture zone V
6	Udintsev fracture zone
7,8	Heezen fracture zone: sections 1,2
9,10	Tharp fracture zone: sections 1,2

Tracks are Eltanin (EL), Vema (V), Conrad (CON), Hudson (HUD). Sources (in parentheses) that were used to obtain estimates of uncertainty refer to profile number, figure number or bathymetric chart from Molnar et al (1975) unless otherwise noted. References to other sources are given by Molnar et al (1975). Section 8 carried no weight in the reconstruction (see discussion in text, part (C)). Dummy points were used for criterion Φ_1 (see section A of this paper).

Appendix 2 (continued)

East of Rise (fixed plate)

Section	Coordinates	s. d. error (km) loc	bias	nav	tot	Track (Source)
1	-55.59,-100.38	20.		1.	20.	CON 12-12 (41)
	-56.39,-100.97	15.		1.	15.	HUD '70
2	-57.61,-119.37	30.		1.	30.	EL 23 (42)
	-58.84,-121.16	15.		1.	15.	HUD '70
3	-59.28,-121.98	15.		9.	17.5	V16-7
	-60.18,-123.74	15.		1.	15.	EL 20 (44)
4	-59.95,-130.56	12.5		1.	12.5	EL 20 (45)
	-59.25,-130.00				50.	Dummy
5	-56.97,-104.60	15.		1.	15.	EL 20 [1]
	-56.63,-107.00				75.	Dummy
6	-60.24,-125.60	3.	0.	1.	3.2	EL 20 (44,45)
	-59.76,-127.50	3.	0.	1.	3.2	EL 25 (chart)
7	-59.08,-104.88	8.	0.	1.	8.1	EL 20 (chart)
	-58.49,-107.23	10.5	0.	1.	10.5	EL 23 (chart)
8	-57.89,-109.35	7.5	1.	1.	8.6	EL 43 (19)
	-58.49,-107.23	10.5	0.	1.	10.5	EL 23 (chart)
9	-59.01,-110.17				99.9	Dummy
	-57.71,-115.66	6.	1.	1.	7.1	See note 2 below
10	-59.01,-110.17	7.5	1.5	9.	12.7	EL 19 (Figure 5)
	-57.85,-115.32				99.9	Dummy

Appendix 2 (continued)

West of Rise (rotated plate)

Section	Coordinates	s. d. error (km) loc	bias	nav	tot	Track (Source)
1	-51.19,-133.64	20.		1.	20.	CON 12-12 (33)
	-49.70,-132.50				75.	Dummy
2	-51.67,-150.00	15.		1.	15.	HUD '70
	-50.39,-148.40				75.	Dummy
3	-51.90,-150.59	15.		1.	15.	EL 23 (34)
	-52.57,-151.89	15.		1.	15.	EL 33 (35)
4	-53.23,-159.05	12.5		9.	15.4	EL 19 (36)
	-54.37,-160.64	12.5		1.	12.5	EL 25 (37)
5	-50.10,-137.00	4.	0.	1.	4.1	See note 3 below
	-50.95,-134.70	6.	0.	1.	6.1	CON 12-12 (33)
6	-53.77,-151.82	5.5	4.	1.	9.6	EL 33 (35)
	-52.10,-156.00				99.9	Dummy
7	-52.48,-137.00	9.	0.5	9.	13.1	EL 17 (chart)
	-51.45,-140.10				99.9	Dummy
8	-51.45,-140.10	9.	0.	9.	12.7	EL 19 (Figure 5)
	-52.48,-137.00				99.9	Dummy
9	-50.30,-146.85	6.	0.	9.	10.8	EL 17 (chart)
	-50.90,-145.00	6.	0.	1.	6.1	EL 20 (Figure 5)
10	-52.42,-140.17	4.5	0.	6.	7.5	EL 19 (Figure 5); See note 4 below
	-51.70,-142.83	5.	0.	9.	10.3	EL 17 (chart)

Appendix 2 (continued)

notes:

1 Constrained by magnetics (HUD '70) in south. Bathymetric chart and inference from trend of fracture zone on Pacific plate to establish limit in north (HUD '70,EL 20).

2 Defined from EL 23 crossings at (-57.85,-115.32) , (-57.58,-116.00) to avoid correlated errors (see text, section B.5). Widths at these crossings are, respectively, 28 km and 20 km. Source: bathymetric chart of Molnar et al (1975).

3 Inference from positions of anomaly 18 and anomaly 20 in south. EL 19 track at 140° W to limit trend in north.

4 Navigational error reduced because EL 17 crossing nearby (-52.55,-139.75) indicated that both EL 19 and EL 17 tracks were consistent in location (see text, section B.5).

This Appendix shows distances of fixed and rotated points from the common great-circles for some anomaly 13 reconstructions. Each reconstruction is specified by the latitude and longitude of the pole and the associated angle. The four lines following the pole and angle show the distances of the points for the 10 sections of data. Sections 1-5 are the first two lines, sections 6-10 are the remaining two lines. Section number increases to right. Lines 1 and 3 are fixed points, lines 2 and 4 are rotated points. Order of points is same as in Appendix 2. Dummy points are not included. Sign (+ or -) indicates on which side of the great-circle the point lies. The distance of a point is given relative to the standard deviation of error assigned to the point. Each distance is given in units of 0.01 standard deviations. Thus 113 = 1.13 standard deviations.

Poles Along Axis of Uncertainty Region

69.35,-76.00 (24.02)

-060	129	010	001	014	000	000		248	
-076		-001		-011	000	019	-009	-018	-080
-153	090	061	084	-020	009	-037		206	
185		-207		023		014	021	-105	-022

70.25,-74.00 (24.50)

-048	108	009	-004	013	002	002		228	
-066		004		-009	-004	016	-008	-020	-069
-131	077	063	070	-020	008	-020		194	
159		-191		024		013	007	-096	-025

70.60,-73.00 (24.71)

-043	097	008	-007	011	003	003		208	
-059		007		-007	-004	014	-007	-020	-061
-130	077	059	060	-028	008	-029		177	
158		-172		035		014	014	-086	-024

72.05,-69.00 (25.61)

-025	061	005	-015	011	008	008		168	
-037		015		-004	-013	005	-004	-021	-042
-092	055	053	037	-031	004	002		153	
113		-134		043		008	-008	-071	-027

72.95,-66.00 (26.24)

-015	038	002	-018	014	014	014		138	
-023		019		-003	-023	-005	-001	-020	-031
-067	040	044	024	-036	001	021		135	
082		-102		053		002	-021	-060	-026

73.40,-64.00 (26.63)

-008	022	000	-024	010	014	016		102	
-012		025		000	-022	-009	000	-017	-021
-066	039	030	012	-048	-003	006		104	
081		-065		075		005	-010	-045	-021

73.85,-62.00 (27.02)

-002	010	-002	-026	011	016	021		076	
-005		028		001	-027	-016	002	-014	-014
-057		019	005	-055	-007	007		085	
070		-038		090		004	-009	-036	-018

74.25,-60.00 (27.41)

005	-004	-005	-031	009	017	024		049	
003		033		003	-028	-022	003	-011	-008
-050	030	006	-002	-062	-012	004		063	
061		-009		106		004	-007	-026	-014

75.20,-55.00 (28.39)

020	-030	-012	-035	013	023	037		010	
016		040		006	-041	-041	007	-005	000
-010	007	-018	-007	-064	-023	040		040	
012		035		122		-015	-028	-016	-010

75.50,-53.00 (28.77)

026	-040	-015	-037	013	025	042		-010	
020		043		008	-045	-049	008	-001	003
000	001	-030	-008	-067	-029	046		025	
-001		057		134		-020	-029	-010	-007

75.90,-50.00 (29.35)

036	-055	-022	-043	010	026	049		-038	
025		052		012	-047	-058	009	004	006
017	-008	-050	-008	-070	-040	055		004	
-021		087		151		-028	-032	-002	-001

76.40,-46.00 (30.13)

049	-071	-032	-047	011	028	062		-057	
031		060		016	-054	-074	010	009	007
051	-027	-068	-003	-065	-051	091		-005	
-064		111		156		-056	-048	002	001

76.80,-42.00 (30.94)

063	-089	-047	-055	003	029	073		-073	
035		076		022	-053	-085	008	014	006
083	-046	-088	005	-058	-064	121		-015	
-103		132		161		-087	-056	005	004

77.10,-38.00 (31.76)

077	-104	-066	-063	-008	029	085		-093	
036		093		028	-050	-095	005	021	004
110	-062	-112	017	-051	-080	139		-030	
-135		156		171		-116	-056	009	011

77.30,-34.00 (32.62)

-093	119	-091	-074	-026	029	092		-118	
-035		116		033	-040	-098	000	031	000
128	-074	-143	036	-043	-104	142		-054	
-155		181		187		-136	-046	014	023

Poles Along Longitude -57.00

75.40,-57.00 (28.14)

008	-010	-001	-005	056	030	049		162	
006		006		001	-078	-057	008	-030	-027
091	-051	055	019	009	006	250		200	
-114		-112		-018		-094	-164	-080	-053

75.30,-57.00 (28.12)

009	-013	-004	-010	047	029	044		138	
008		013		001	-070	-051	008	-026	-022
070	-039	044	014	-004	002	210		172	
-088		-089		006		-080	-137	-069	-046

75.20,-57.00 (28.09)

010	-014	-005	-014	040	028	042		113	
008		018		001	-064	-048	008	-022	-018
049	-027	033	009	-018	-002	169		145	
-061		-065		030		-064	-111	-058	-039

74.40,-57.00 (27.89)

019	-026	-004	-057	-025	003	022		-086	
013		057		019	-001	-017	002	013	014
-119	071	-063	-018	-117	-045	-152		-072	
146		119		225		074	089	026	025

74.30,-57.00 (27.86)

020	-027	-001	-061	-031	-002	020		-111	
013		059		022	006	-015	002	018	017
-140	083	-075	-020	-129	-052	-192		-099	
171		142		250		093	113	036	033

74.20,-57.00 (27.85)

022	-030	001	-070	-042	-010	017		-135	
014		065		029	017	-009	000	023	020
-161	095	-088	-020	-138	-061	-230		-126	
196		162		275		115	134	046	042

Appendix 4

Ellipse of Variation of Pole of Rotation: Anomaly 13 Reconstruction

Let T be the covariance matrix of the independent elements $(\varepsilon_1,\varepsilon_2,\varepsilon_3)$ of the infinitesimal rotation that describes the perturbations in the best-fit pole and angle (see Chapter V of the previous paper) with criterion Φ_1. Let t_{ij}, $1\leq i,j\leq 3$, be the elements of T. The distinct elements of T were:

$$t_{11} = 0.1069460292D\text{-}03,\ t_{12} = 0.2217938544D\text{-}03$$
$$t_{22} = 0.5213991841D\text{-}03,\ t_{13} = 0.4442915940D\text{-}03$$
$$t_{23} = 0.1021764362D\text{-}02,\ t_{33} = 0.2078700759D\text{-}02$$

Here the symbol 'D' indicates that the decimal number to the left of 'D' is to be multiplied by 10 (ten) raised to the power of the number to the right of 'D'.

In the notation of section V.2 of the previous paper, a perturbation in the pole is represented by ω. The covariance matrix of ω is M. The eigenvalues of M are μ_1 and μ_2. The associated eigenvectors of unit length are m_1 and m_2. An ellipse of variation for the pole is of the form $\omega' M^{-1}\omega = c$, where c is a positive constant. Two ellipses were defined. One ellipse had c = 4.6, the other had c = 6.0. Each ellipse is specified by the four poles of rotation that lie at the ends of the axes of the ellipse.

The four poles of rotation associated with c = 4.6 were:

Appendix 4 (continued)

(74.138,-55.02), (75.499,-58.877), (77.816,-23.946)
and (68.917,-75.458)

The four poles of rotation associated with c = 6.0 were:

(74.041,-54.776), (75.592,-59.173), (77.852,-18.592)
and (67.992,-77.219)

APPENDIX 5

Usable data: Anomaly 18 reconstruction

Section	Feature
1	Lineation between fracture zones Menard and IV
2	Lineation between fracture zones Tharp and Udintsev
3	Lineation between fracture zones Udintsev and VIII
4	Lineation between fracture zones IX and X
5,6	Heezen fracture zone: sections 1,2
7,8	Tharp fracture zone: sections 1,2

Tracks are Eltanin (EL),Vema (V),Conrad (CON),SouthTow (SOTOW), Monsoon (MON). Sources are same format as in Appendix 2.

East of Rise (fixed plate)

Section	Coordinates	s. d. error (km) loc	bias	nav	tot	Track (Source)
1	-55.52,-98.60	20.		1.	20.	CON 12-12 (41)
	-54.00,-97.25				99.9	Dummy
2	-59.28,-118.68	15.		9.	17.5	V16-7
	-60.50,-120.90	15.		1.	15.	EL 20 (44)
3	-60.05,-127.82	15.		1.	15.	EL 20 (45)
	-61.02,-129.10				99.9	Dummy
4	-66.04,-140.84	15.		1.	15.	EL 42 (47)
	-67.00,-143.00				99.9	Dummy
5	-59.95,-101.75	6.	1.5	1.	7.6	EL 23 (chart)
	-59.08,-104.88	8.	0.5	1.	8.6	EL 23 (chart)
6	-58.49,-107.23	10.5	0.	1.	10.5	EL 23 (chart)
	-57.89,-109.35	7.5	0.	1.	7.6	EL 43 (19)
7	-59.94,-107.95	6.	0.	1.	6.1	EL 23 (chart)
	-59.01,-110.17	7.5	1.	9.	12.4	EL 19 (Figure 5)

Appendix 5 (continued)

8	-57.71,-115.66	6.0	4.0	1.	10.	See note 2, App. 2
	-58.25,-113.00				99.9	Dummy

West of Rise (rotated plate)

Section	Coordinates	s. d. error (km)				Track (Source)
		loc	bias	nav	tot	
1	-46.52,-133.28	10.		1.	10.	SOTOW 2 (31)
	-47.33,-133.92	12.5		9.	15.4	EL 19 (32)
2	-51.52,-152.15	30.		1.	30.	EL 23 (34)
	-51.58,-152.29	15.		1.	15.	EL 33 (35)
	-50.10,-150.38				99.9	Dummy
3	-52.64,-160.28	20.		9.	21.9	EL 19 (36)
	-53.90,-161.86	14.		1.	14.	EL 25 (37)
4	-58.01,-168.34	15.		1.	15.	EL 43 (38)
	-58.84,-172.95	40.		9.	41.	MON 6 (39)
	-59.08,-175.01	20.		1.	20.	EL 33
5	-52.48,-137.00	9.	0.	9.	12.7	EL 17 (chart)
	-51.45,-140.10	9.	0.	9.	12.7	EL 19 (Figure 5)
6	-50.44,-143.00	5.	3.5	9.	12.4	EL 17 (chart)
	-51.45,-140.10				99.9	Dummy
7	-51.70,-142.83	5.	0.	9.	10.3	EL 17 (chart)
	-50.90,-145.00	6.	0.	1.	6.1	EL 20 (Figure 5)
8	-48.42,-151.00	5.	0.	9.	10.3	EL 17 (chart)
	-50.30,-146.85	6.	0.	9.	10.8	EL 17 (chart)

Appendix 6

This Appendix shows distances of fixed and rotated points from the common great-circles for some anomaly 18 reconstructions. The poles shown were at the limit of acceptability. The format is similar to that of Appendix 3. Sections 1-4 are the first two lines. sections 5-8 are the remaining two lines.

75.40,-51.25 (32.48)

```
 019         062   026    029          029
 007 -030  -023 -065   -078  019   -035  005 -011
 070 -018  -022 -021    131 -010    175
-097  006    061        -266  032   -076 -107
```

74.70,-51.25 (32.62)

```
-038        -048 -046    004         -110
-012  049    041  067   -015  004    100  021 -009
-062 -091  -145 -044    039 -195   -036
 049  189    242        -053  088    019  023
```

75.80,-48.50 (33.07)

```
 002         067   024    035          097
 000 -003  -024 -068   -088  020   -098 -004 -016
 052 -022  -022 -017    131  003    212
-071  017    055        -266  025   -095 -129
```

75.10,-48.50 (33.27)

```
-069        -056 -047    005         -053
-020  089    045  073   -016  004    043  015 -008
-093 -088  -154 -033    031 -188   -003
 073  211    236        -044  088    002  005
```

75.90,-47.00 (33.43)

```
-018         048   017    032          111
-008  026   -015 -049   -082  018   -112 -006 -016
 024 -037  -037 -022    124 -014    204
-034  049    080        -237  024   -095 -119
```

75.20,-47.00 (33.65)

```
-097        -074 -061    002         -041
-027  124    056  096   -009  002    031  013 -008
-133 -088  -181 -024    002 -213   -015
 100  252    252        -005  106    009  011
```

75.55,-45.00 (34.09)

```
-105        -065 -044    007         024
-031  138    047  077   -020  005   -032  006 -009
-129 -080  -161 -021    023 -176    045
 098  235    225        -037  085   -025 -019
```

75.90,-44.00 (34.23)

-084		-024	-013	018		100		
-027	113	021	024	-048	011	-103	-004	-014
-080	-069	-109	-026	074	-101	134		
066	169	170		-118	045	-072	-067	

75.10,-53.00 (32.09)

030		058	027	026		-016		
012	-047	-022	-063	-072	018	007	011	-008
078	-017	-024	-026	128	-025	144		
-110	004	071		-261	038	-062	-089	

74.60,-53.00 (32.19)

-005		-023	-023	009		-115		
-003	006	024	033	-026	007	104	022	-008
-007	-075	-103	-049	075	-148	-001		
-003	126	202		-118	067	001	004	

74.80,-55.00 (31.63)

045		066	033	026		-053		
021	-074	-028	-072	-072	019	042	015	-006
098	-005	-018	-025	130	-024	130		
-142	-014	062		-273	043	-054	-083	

74.50,-55.00 (31.68)

030		016	007	015		-111		
011	-046	-001	-018	-045	012	099	021	-006
054	-046	-056	-047	108	-092	047		
-075	052	142		-195	053	-021	-026	

74.30,-57.00 (31.17)

054		050	029	021		-118		
025	-090	-021	-058	-060	017	106	022	-006
094	-017	-029	-040	122	-062	069		
-137	005	099		-243	053	-029	-043	

APPENDIX 7

Ellipse of Variation of Pole of Rotation: Anomaly 18 Reconstruction

The notation follows that in Appendix 4. The distinct elements of T were:

t_{11} = 0.2223989906D-04, t_{12} = 0.3721979597D-04

t_{22} = 0.1021334760D-03, t_{13} = 0.1000441201D-03

t_{23} = 0.2408426093D-03, t_{33} = 0.6180925248D-03

The four poles of rotation associated with c = 4.6 were:

(74.643,-50.104), (75.513,-52.463), (76.675,-39.618),

and (73.018,-60.405).

The four poles of rotation associated with c = 6.0 were:

(74.581,-49.949), (75.573,-52.638), (76.850,-37.792),

and (72.703,-61.507).

Table 1

This Table shows distances of fixed and rotated points from the common great-circles for some anomaly 13 reconstructions. Each reconstruction is specified by the latitude and longitude of the pole and the associated angle. The four lines following the pole and angle show the distances of the points for the 10 sections of data. Sections 1-5 are the first two lines, sections 6-10 are the remaining two lines. Section number increases to right. Lines 1 and 3 are fixed points, lines 2 and 4 are rotated points. Order of points is same as in Appendix 2. Dummy points are not included. Sign (+ or -) indicates on which side of the great-circle the point lies. The distance of a point is given relative to the standard deviation of error assigned to the point. Each distance is given in units of 0.01 standard deviations. Thus 113 = 1.13 standard deviations.

74.70,-57.00 (27.90)

011	-014	-004	-027	016	024	035		-016	
008		028		002	-040	-040	009	000	004
-057	034	-027	-013	-087	-023	-036		009	
071		056		155		018	019	-004	000

74.70,-57.00 (28.00)

019	-027	-011	-049	-009	012	024		-009	
014		053		012	-016	-020	003	-001	003
-056	034	-025	-009	-079	-029	-031		009	
069		049		149		019	015	-004	000

74.638,-58.25 (27.79)

012	-016	-009	-036	006	018	026		044	
009		040		006	-029	-024	003	-010	-006
-030	018	002	-003	-057	-015	030		063	
036		-002		103		-008	-022	-025	-015

74.70,-57.00 (27.96)

016	-022	-008	-040	001	017	029		-012	
012		043		008	-026	-028	005	-001	003
-057	034	-026	-011	-082	-026	-033		009	
070		052		152		019	017	-004	000

74.827,-56.865 (28.01)

015	-021	-008	-034	010	021	032		012	
011		038		005	-035	-033	006	-005	-001
-034	021	-014	-007	-070	-021	009		036	
042		030		127		001	-009	-015	-008

Table 1 (continued)

Shown below are the measure of fit (Φ_0) and the contribution of section 8 to the measure of fit for the five reconstructions in this Table.

Pole Lat - Long	Angle	Φ_0	Contribution of section 8 to Φ_0
74.70,-57.0	27.90	5.52	3.21
74.70,-57.0	28.00	5.14	2.93
74.638,-58.25	27.79	3.09	1.41
74.70,-57.0	27.96	5.24	3.05
74.827,-56.865	28.01	3.57	2.15

Table 2

Given below are the poles of rotation that are represented by the diamond-shaped points in Figure 2. The angle shown for a given pole is the angle that minimized the measure of fit (Φ_0) for the pole.

Pole Lat - Long	Angle	Pole Lat - Long	Angle
75.30,-57.0	28.12	77.05,-38.0	31.75
74.30,-57.0	27.86	77.20,-36.0	32.18
75.55,-55.0	28.49	77.15,-36.0	32.17
74.65,-55.0	28.26	77.30,-34.0	32.62
75.80,-53.0	28.85	74.70,-60.0	27.53
75.00,-53.0	28.67	73.80,-60.0	27.29
76.15,-50.0	29.41	74.30,-62.0	27.15
75.50,-50.0	29.28	73.45,-62.0	26.90
76.55,-46.0	30.17	73.85,-64.0	26.75
76.15,-46.0	30.09	73.00,-64.0	26.51
76.75,-44.0	30.58	73.25,-66.0	26.32
76.40,-44.0	30.49	72.55,-66.0	26.12
76.90,-42.0	30.96	72.25,-69.0	25.66
76.65,-42.0	30.91	71.80,-69.0	25.54
77.00,-40.0	31.35	71.05,-72.0	24.96
76.85,-40.0	31.32	70.90,-72.0	24.91
77.15,-38.0	31.78	70.60,-73.0	24.71

Table 3

This Table shows distances of fixed and rotated points from the common great-circles for some anomaly 18 reconstructions. The format is similar to that of Table 1. Sections 1-4 are the first two lines, sections 5-8 are the remaining two lines.

75.30,-48.50 (33.00)

-018		017	009	022		016		
-006	023	-001	-020	-064	017	-025	007	-008
-052	-090	-106	-056	060	-152	039		
053	166	215		-089	067	-019	-020	

75.30,-48.50 (33.23)

-048		-029	-022	011		-014		
-016	064	026	035	-033	008	004	010	-008
-047	-075	-111	-036	071	-129	061		
037	153	189		-112	059	-032	-030	

75.30,-48.50 (33.08)

-029		001	-002	019		006		
-009	038	008	-001	-053	014	-015	008	-008
-051	-084	-108	-049	064	-144	047		
048	162	206		-097	065	-023	-023	

75.081,-51.25 (32.56)

-005		003	-002	016		-039		
-003	008	007	-003	-045	012	028	013	-007
015	-057	-071	-039	101	-089	081		
-026	085	148		-175	047	-039	-044	

- - - - -

Given below are the measure of fit (Φ_0) and the contributions of each of sections 5 - 8 to the Φ_0 measure of fit for the four reconstructions in this Table.

Pole Lat - Long	Angle	Φ_0	Contribution of section no. 5	6	7	8
75.30,-48.50	33.00	15.07	4.12	6.06	3.91	0.23
75.30,-48.50	33.23	13.69	3.26	4.94	3.77	0.56
75.30,-48.50	33.08	14.26	3.82	5.65	3.85	0.33
75.081,-51.25	32.56	10.60	1.14	2.84	5.10	1.00

Table 4

Given below is the measure of fit (Φ_0) for each of the reconstructions in Appendix 6. The poles of these reconstructions delineate the uncertainty region in Figure 3.

Pole Lat - Long	Angle	Φ_0
75.40,-51.25	32.48	17.63
74.70,-51.25	32.62	22.15
75.80,-48.50	33.07	21.04
75.10,-48.50	33.27	22.38
75.90,-47.00	33.43	19.04
75.20,-47.00	33.65	30.29
75.55,-45.00	34.09	25.55
75.90,-44.00	34.23	19.07
75.10,-53.00	32.09	16.23
74.60,-53.00	32.19	14.95
74.80,-55.00	31.63	18.56
74.50,-55.00	31.68	13.19
74.30,-57.00	31.17	17.45

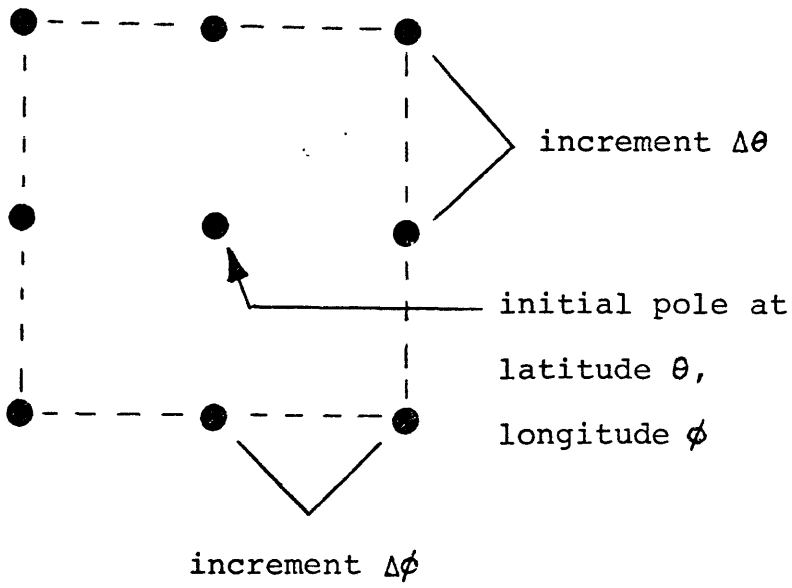
increment Δθ
initial pole at
latitude θ,
longitude φ
increment Δφ

FIGURE 1

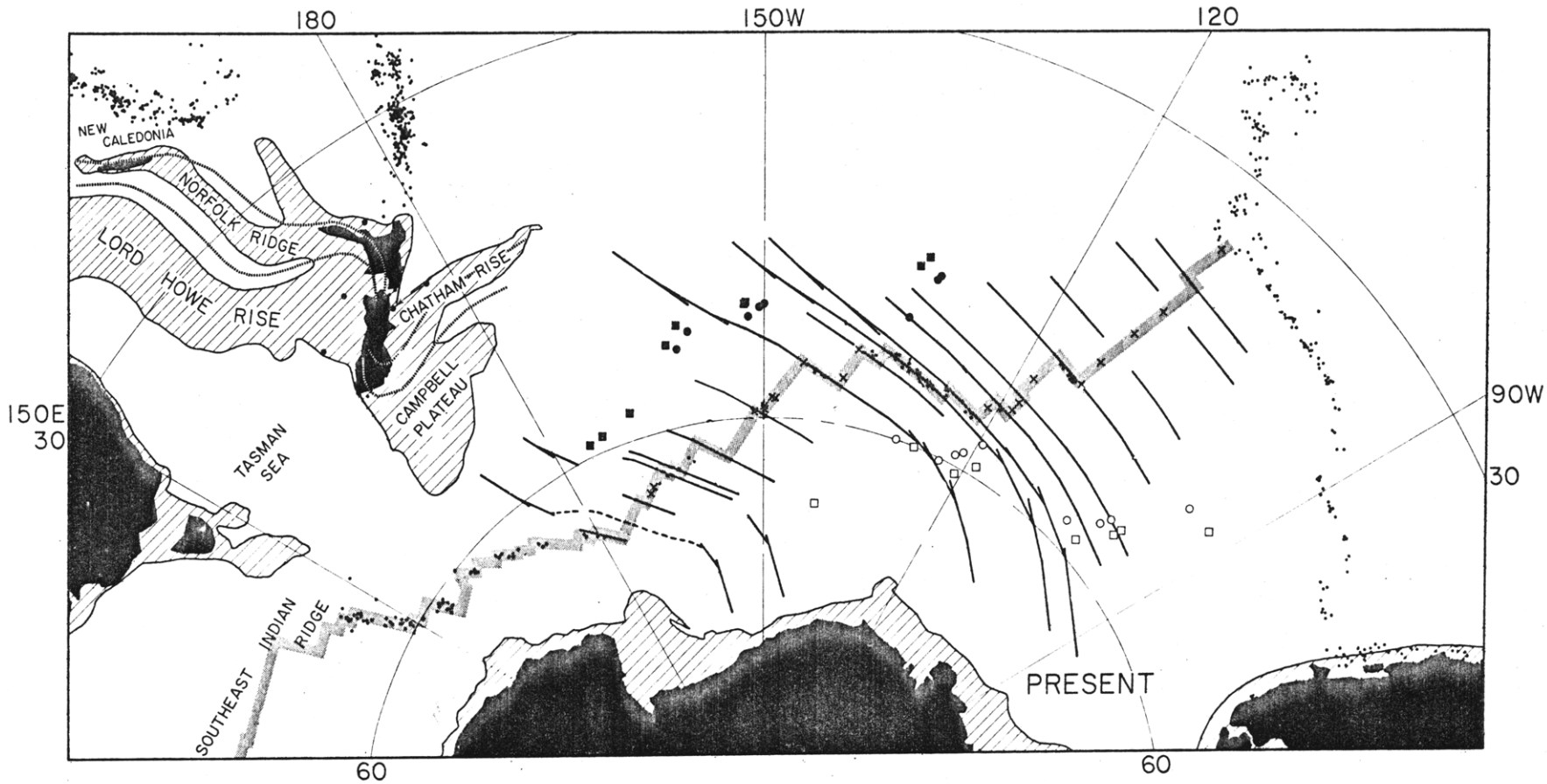

Figure 2: Present configuration of continental fragments, plate boundaries, fracture zones and magnetic anomalies 13 and 18 in South Pacific. Different symbols show position of anomalies 13 (circle) and 18 (square). Black dots show earthquake epicenters, x's are central anomalies. Earthquakes and grey-lines show presently active plate boundaries. Fracture zones are shown by heavy lines (figure after Molnar et al., 1975).

Figure 3a

POLES OF ROTATION - ANOMALY 13 RECONSTRUCTION

● BEST FIT POLE, MOLNAR ET AL (1975)
▲ BEST FIT POLE, THIS STUDY
— SUBJECTIVE UNCERTAINTY REGION, MOLNAR ET AL (1975)
♦ POLES USED TO DEFINE UNCERTAINTY REGION, THIS STUDY
■ POLES TO DEFINE ELLIPSE OF VARIATION, c=4.6
● POLES TO DEFINE ELLIPSE OF VARIATION, c=6.0

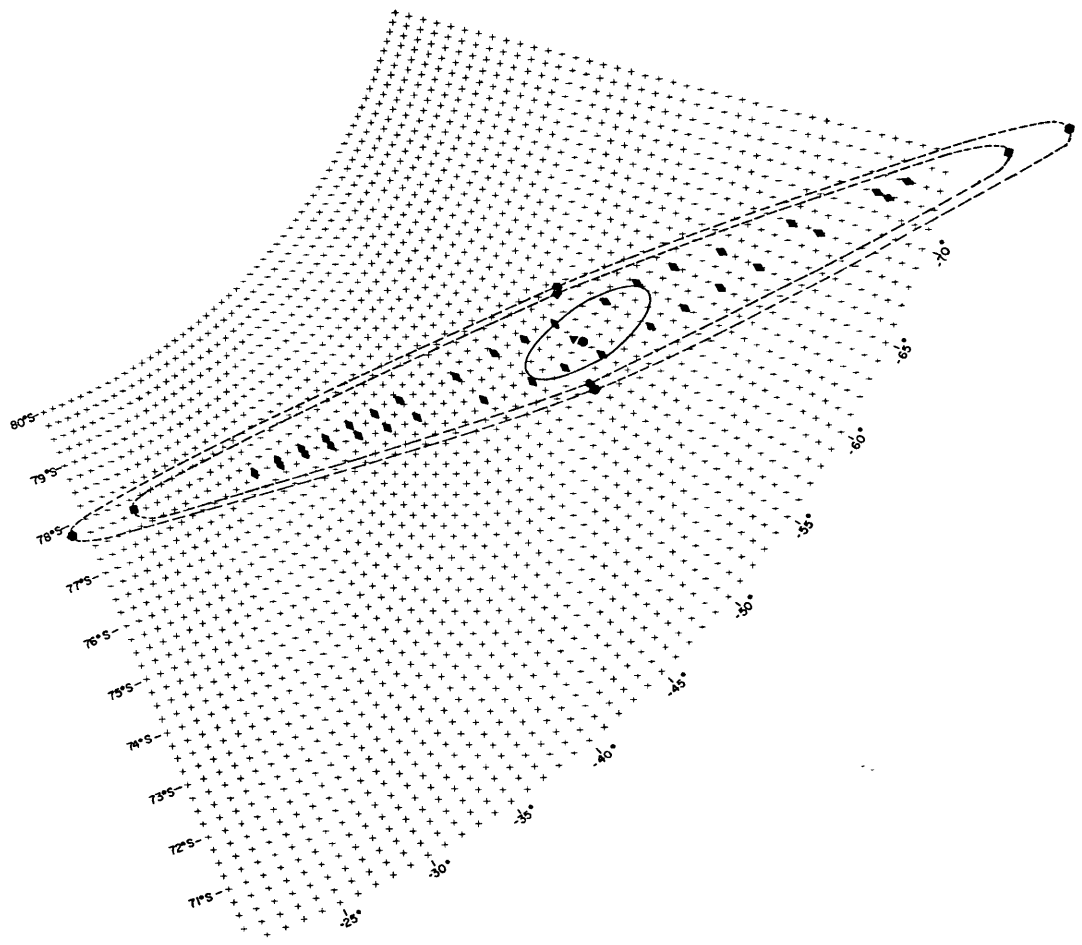

Figure 3b

POLES OF ROTATION- ANOMALY 18 RECONSTRUCTION

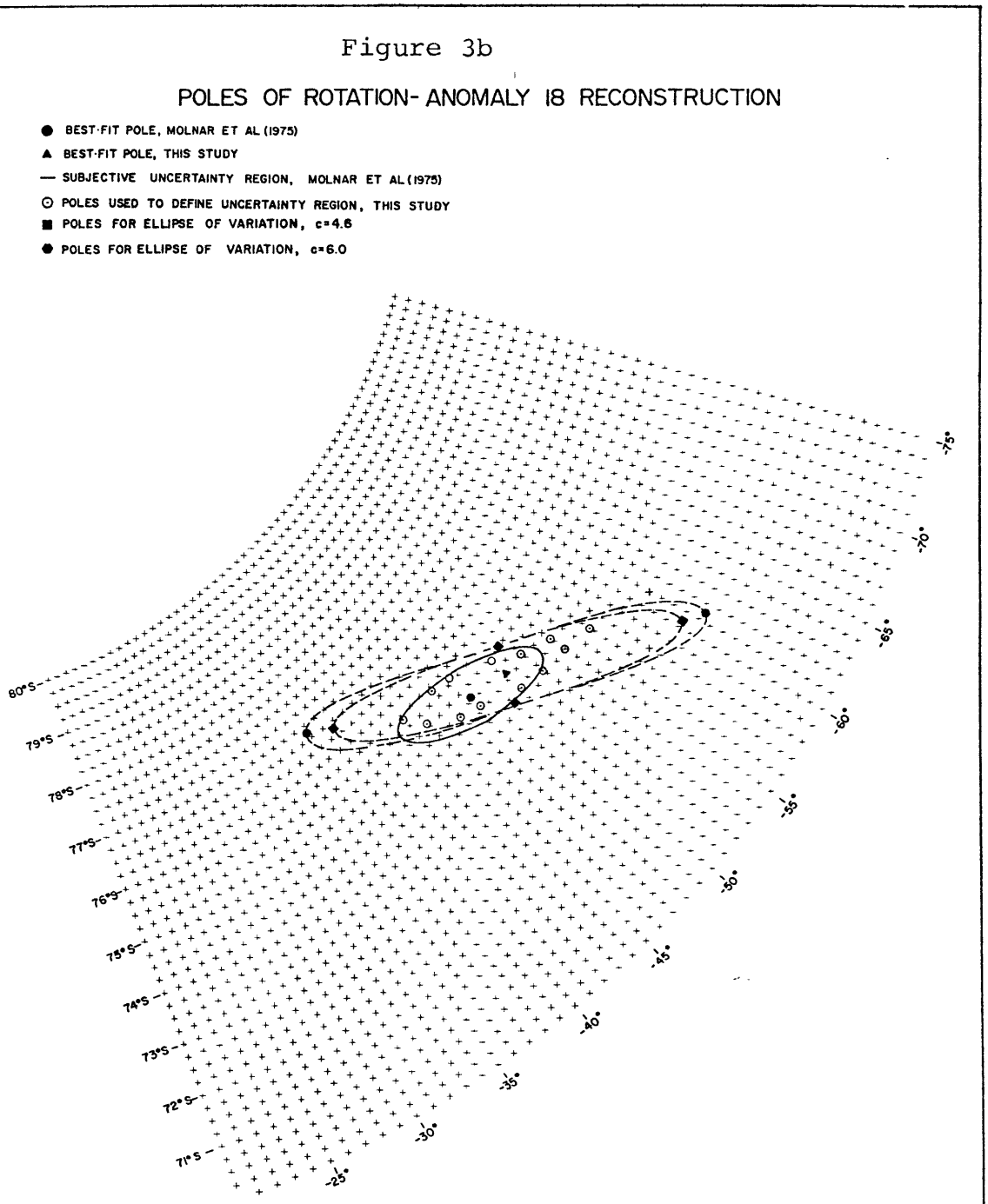

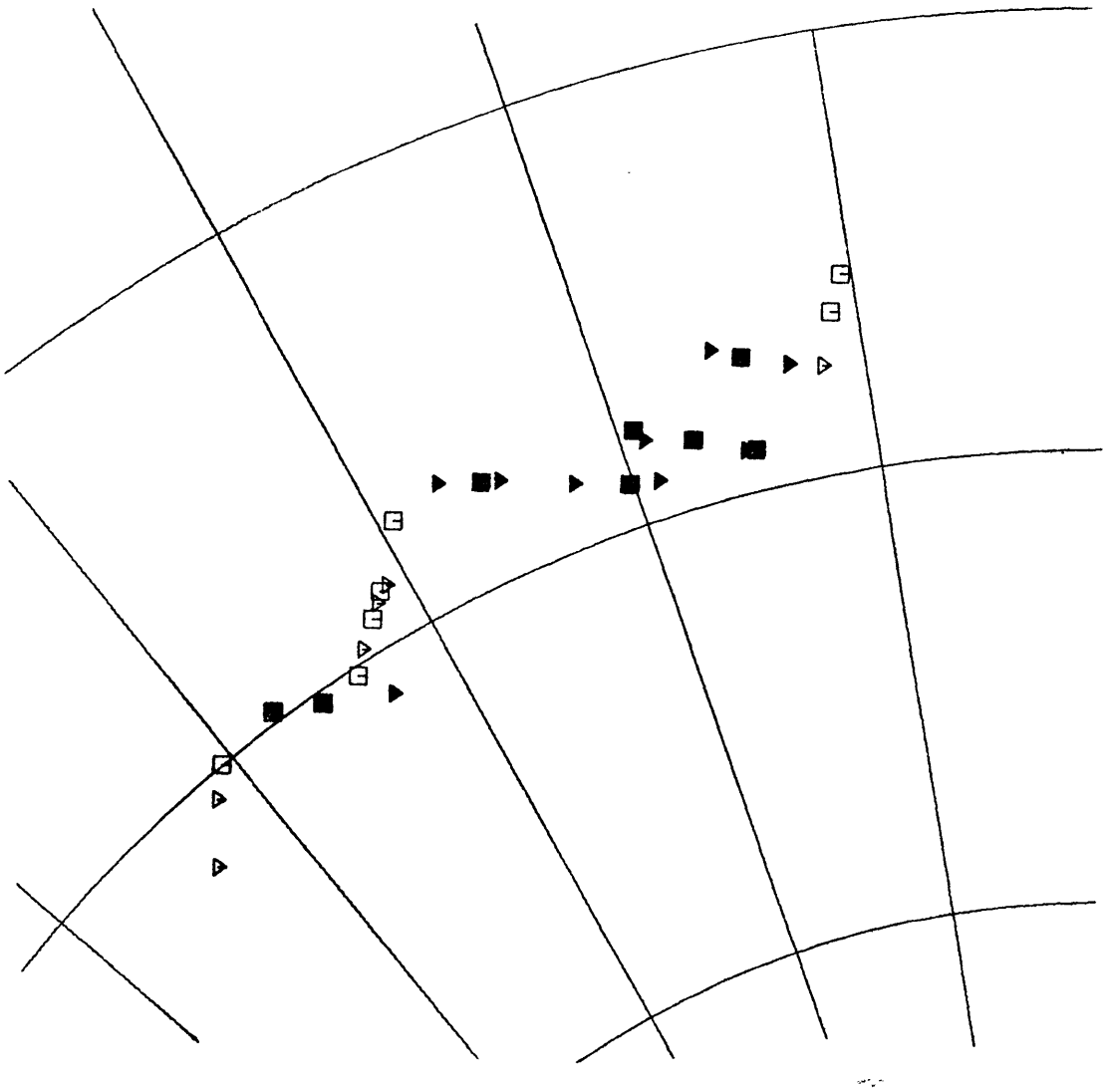

Figure 4a

Anomaly 13 Reconstruction: 74.827,-56.865 (28.01)

Squares are fixed points, triangles are rotated points. Filled symbols are fossil transform fault identifications, open symbols are magnetic anomaly identifications.

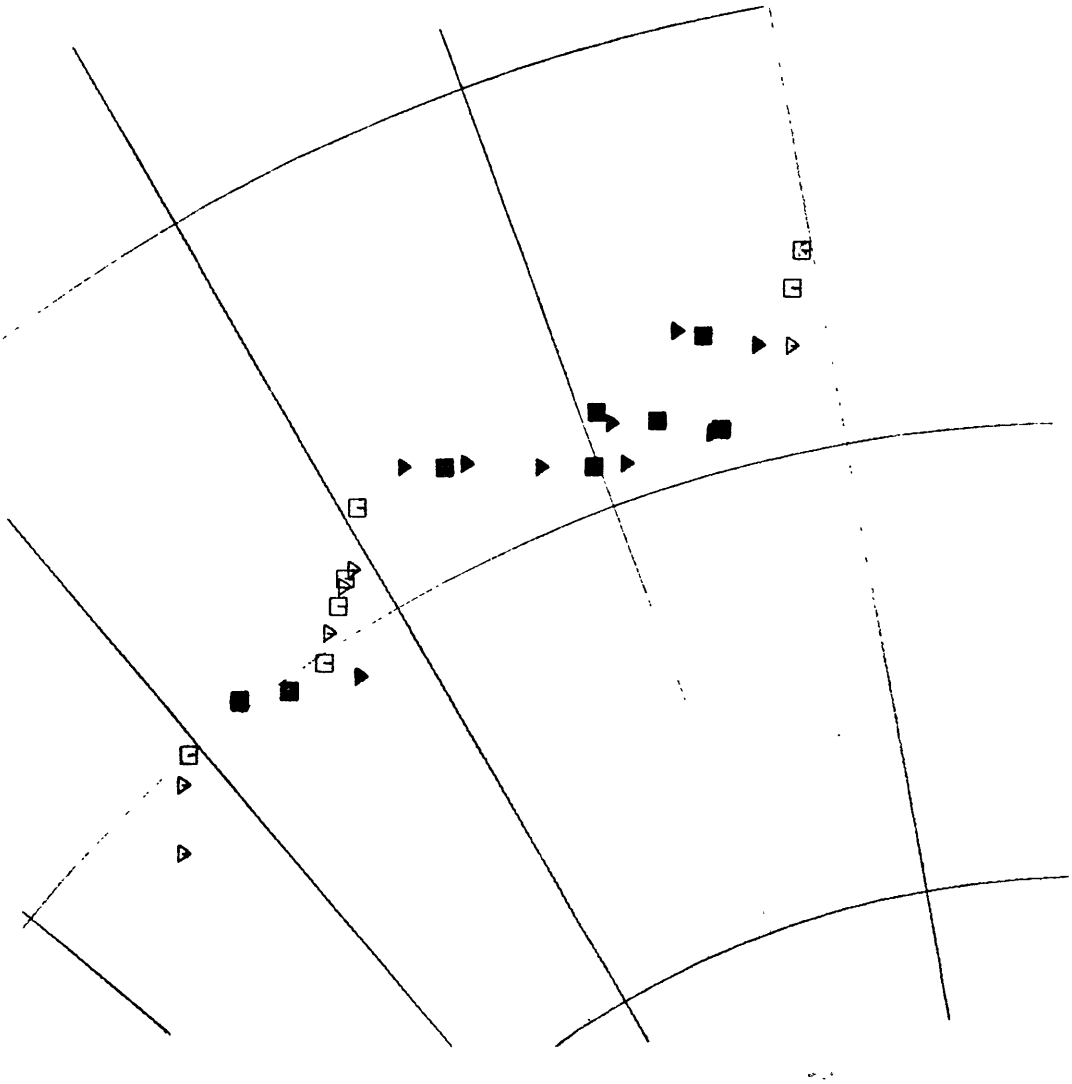

Figure 4b

Anomaly 13 Reconstruction: 75.50,-53.00 (28.77)

Symbols and conventions same as Figure 4a.

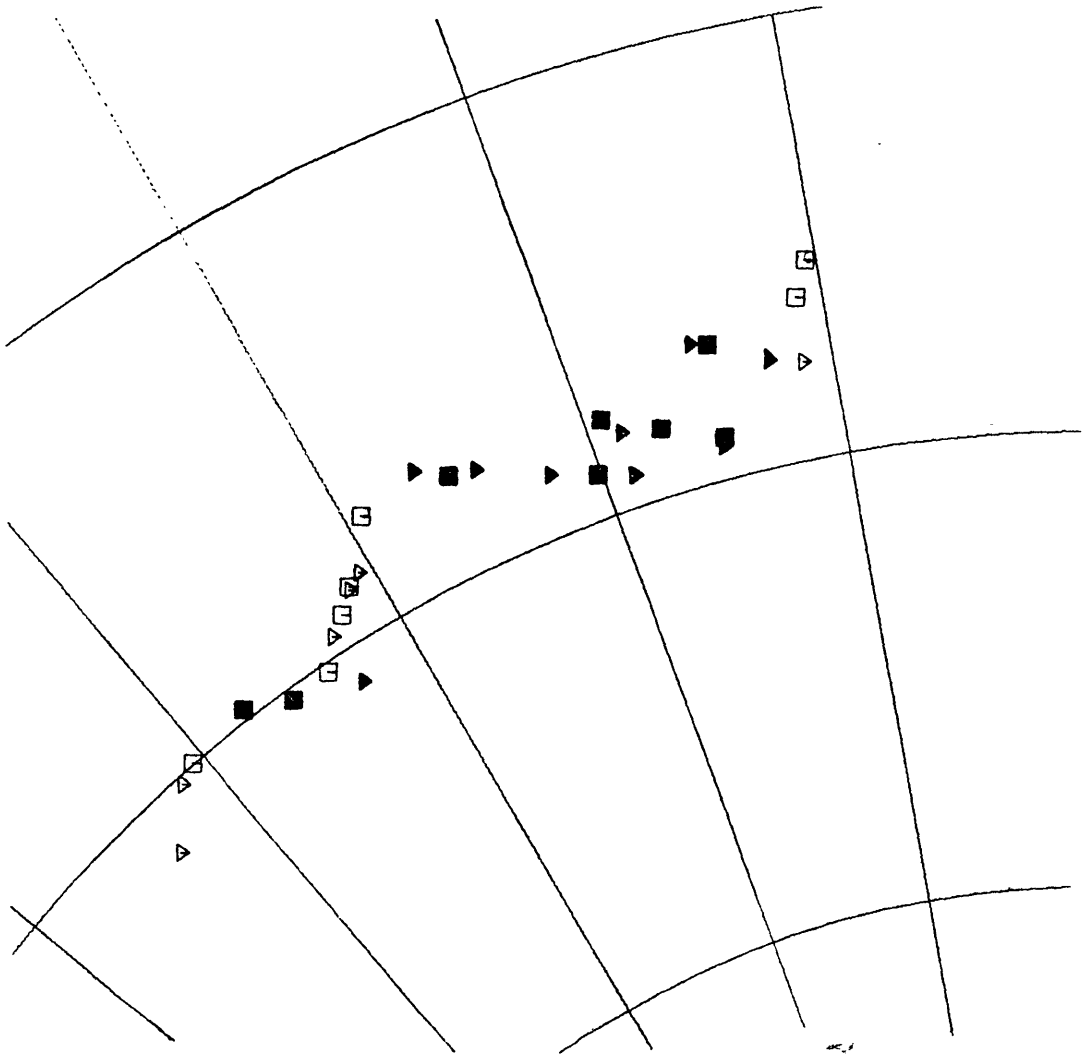

Figure 4c

Anomaly 13 Reconstruction: 76.40, -46.00 (30.13)

Symbols and conventions same as Figure 4a.

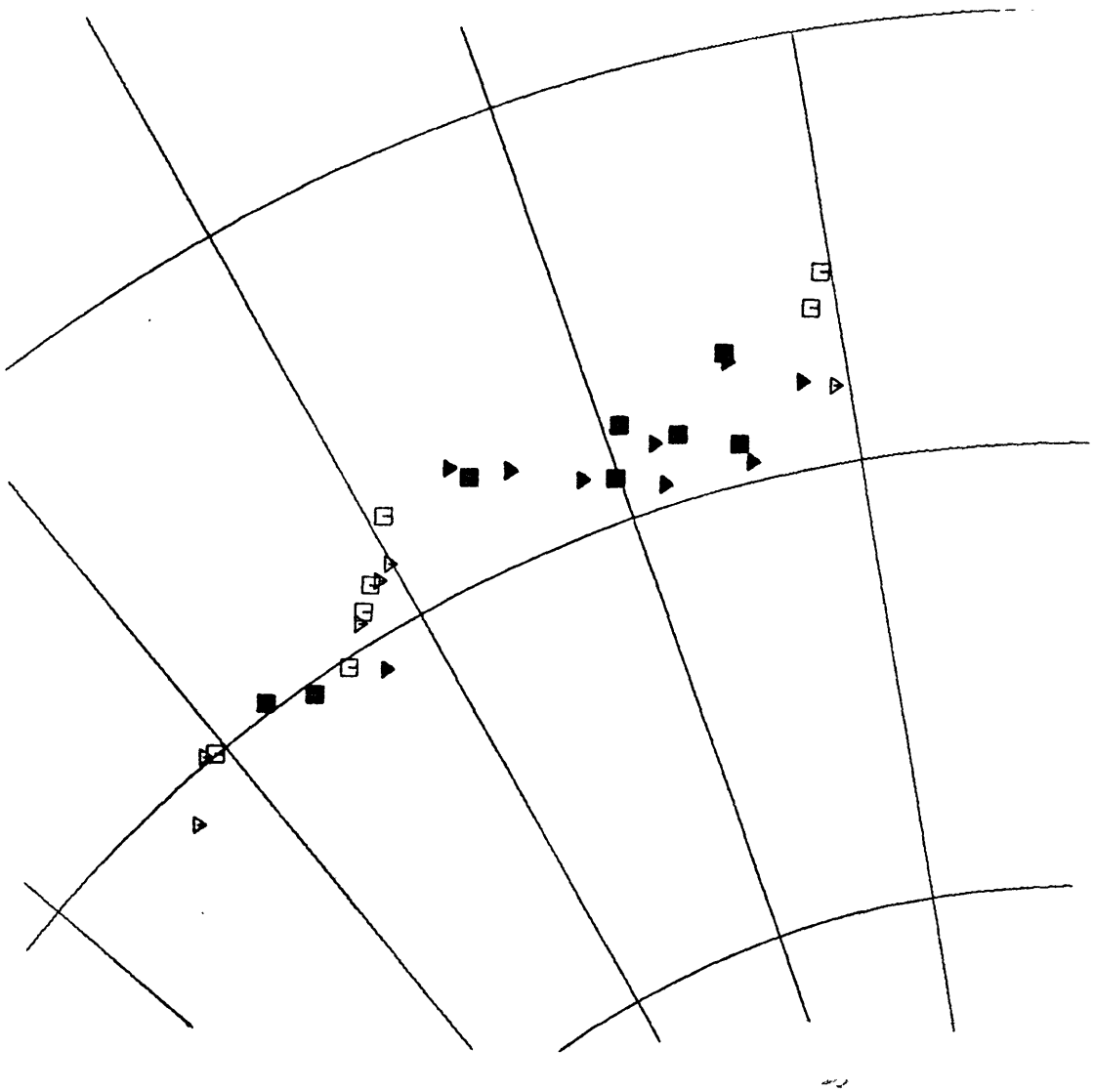

Figure 4d

Anomaly 13 Reconstruction: 77.30,-34.00 (32.62)

Symbols and conventions same as Figure 4a.

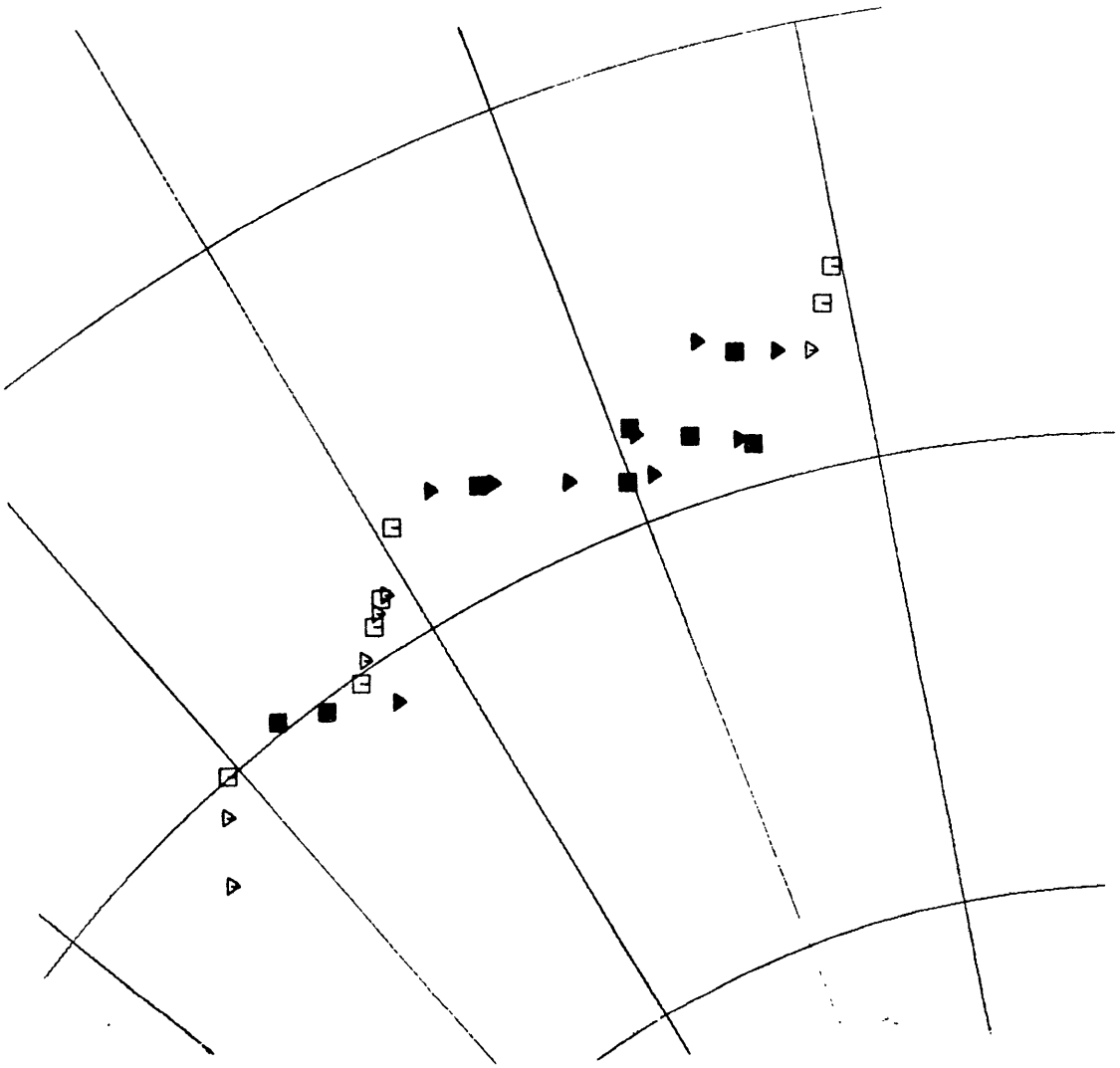

Figure 4e

Anomaly 13 Reconstruction: 73.85,-62.00 (27.02)

Symbols and conventions same as Figure 4a.

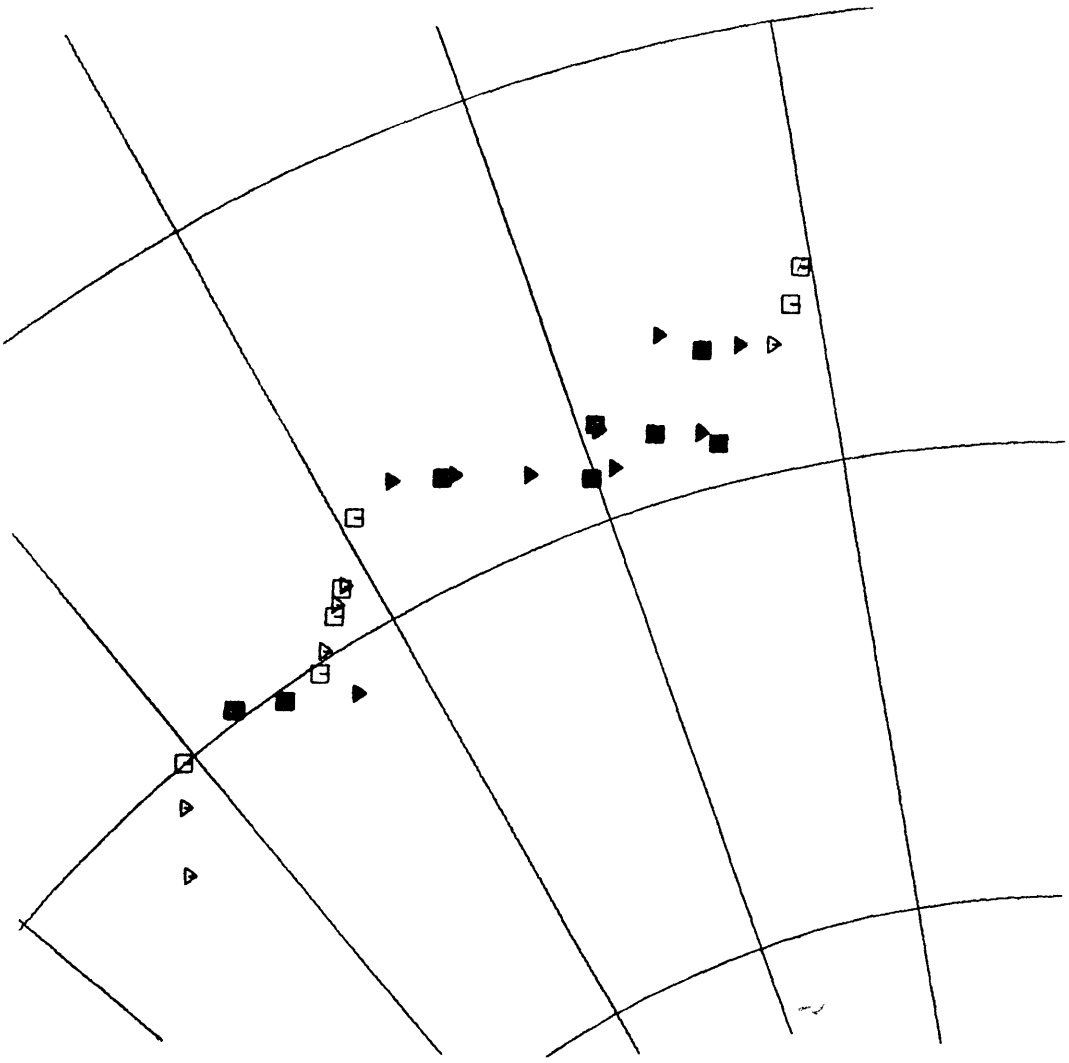

Figure 4f

Anomaly 13 Reconstruction: 72.95,-66.00 (26.24)

Symbols and conventions same as Figure 4a.

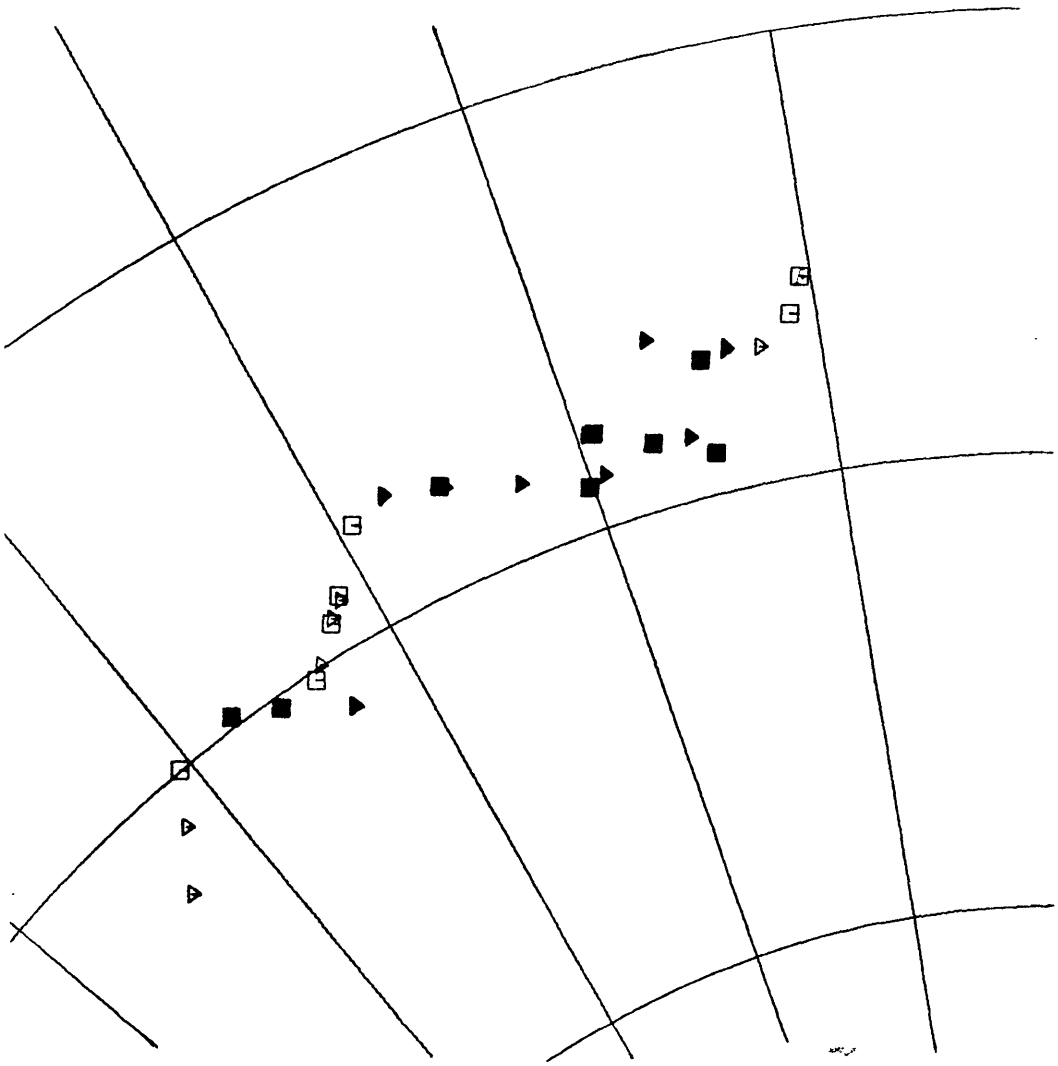

Figure 4g

Anomaly 13 Reconstruction: 70.60,-73.00 (24.71)

Symbols and conventions same as Figure 4a.

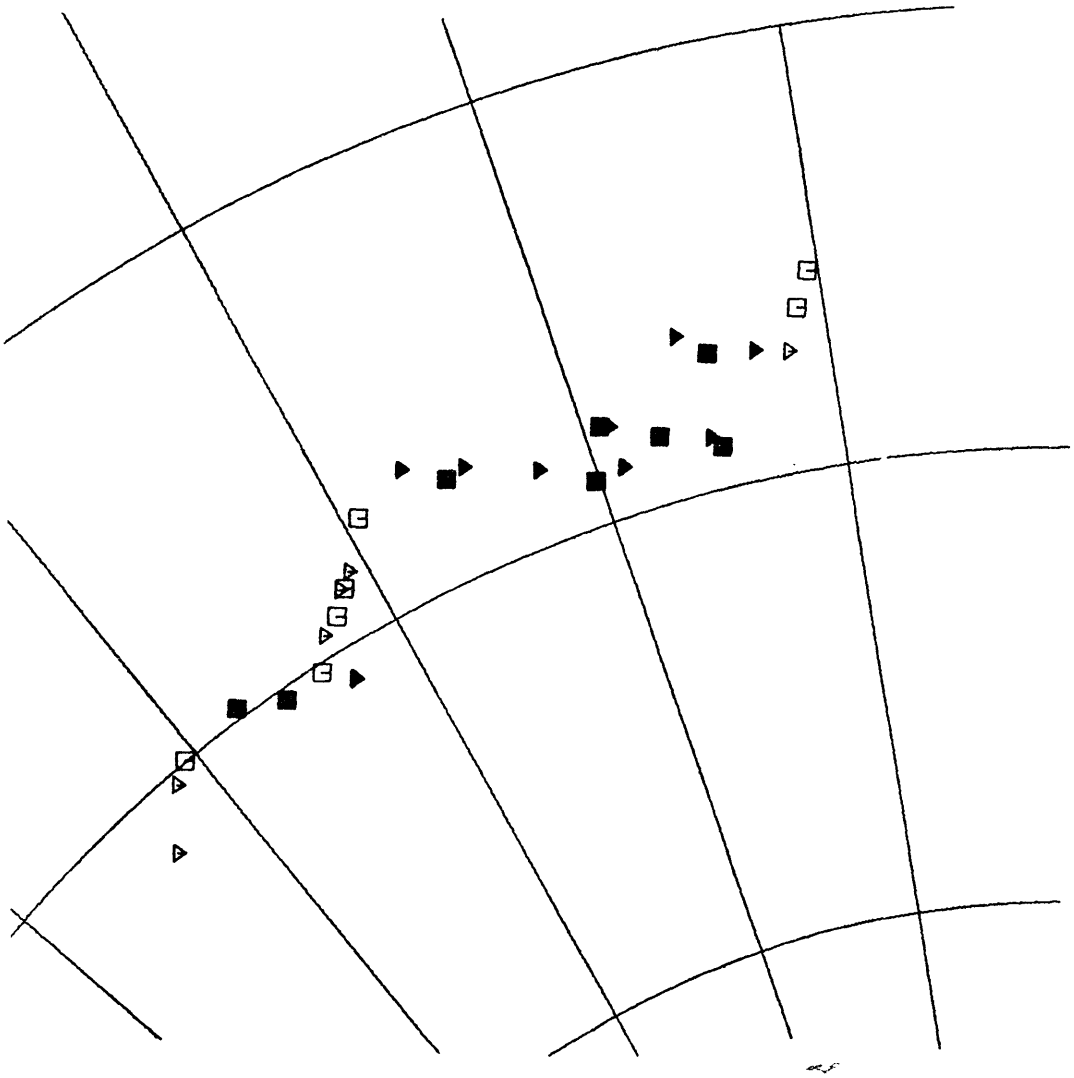

Figure 4h

Anomaly 13 Reconstruction: 75.40,-57.00 (28.14)

Symbols and conventions same as Figure 4a.

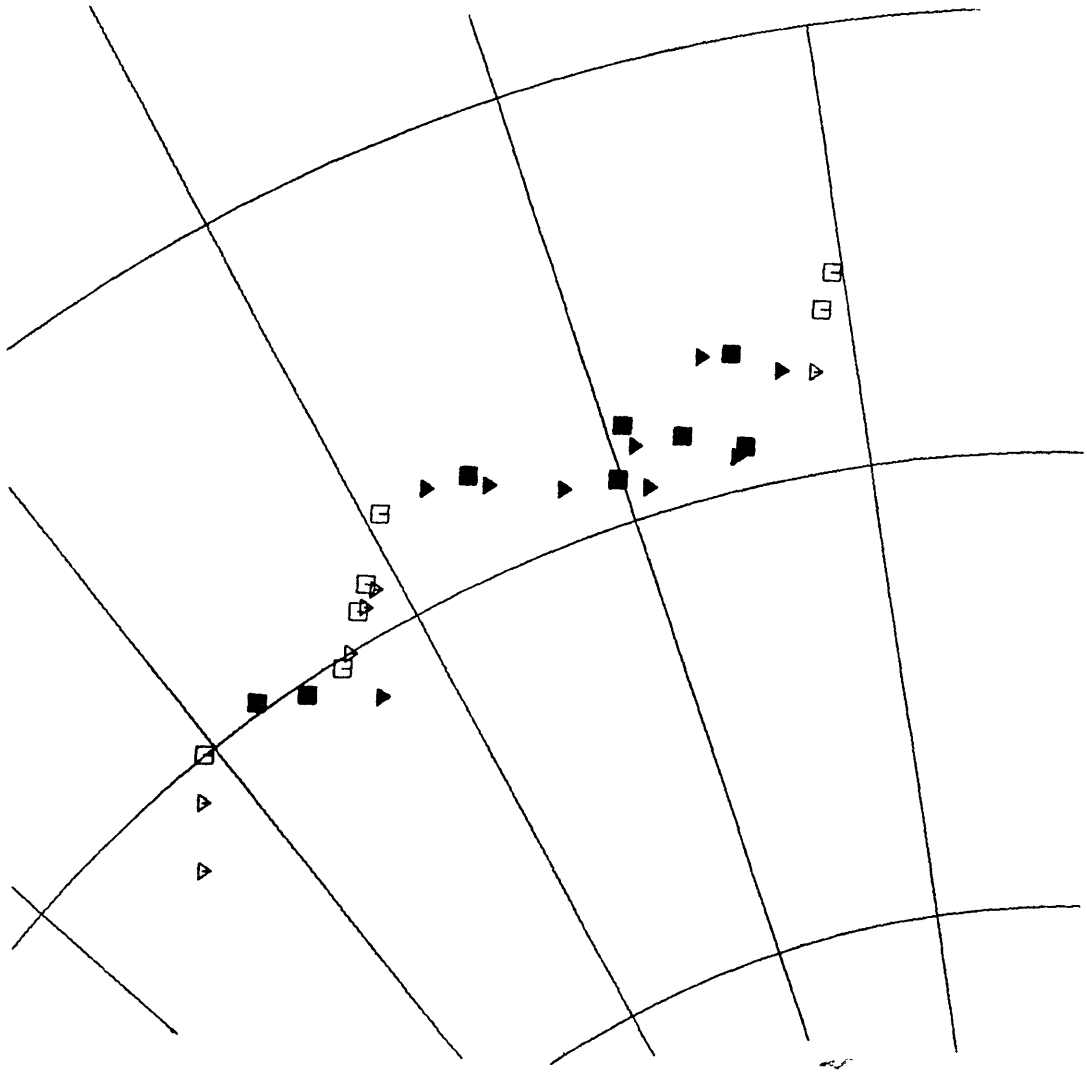

Figure 4i

Anomaly 13 Reconstruction: 74.20,-57.00 (27.85)

Symbols and conventions same as Figure 4a.

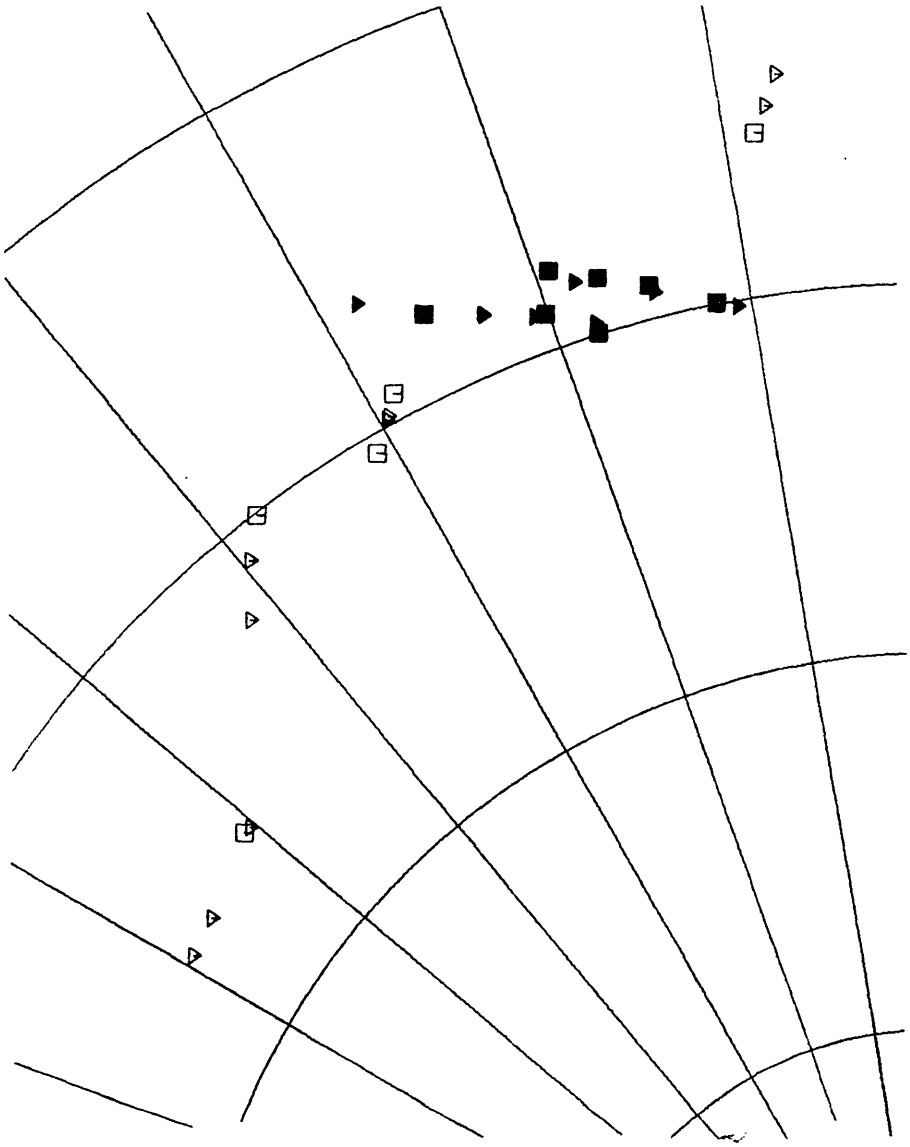

Figure 5a

Anomaly 18 Reconstruction: 75.081,-51.25 (32.56)

Symbols and conventions same as Figure 4a.

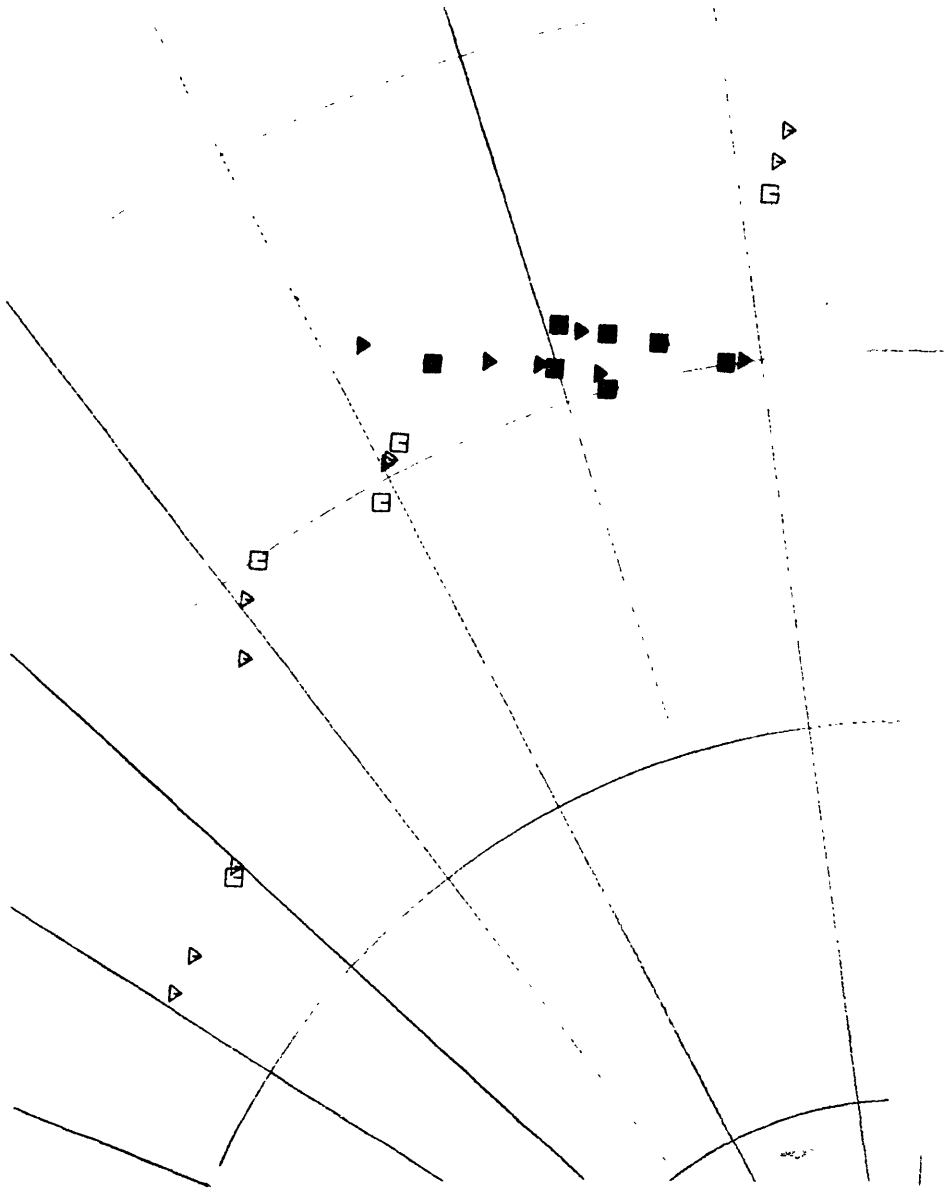

Figure 5b

Anomaly 18 Reconstruction: 75.40,-51.25 (32.48)

Symbols and conventions same as Figure 4a.

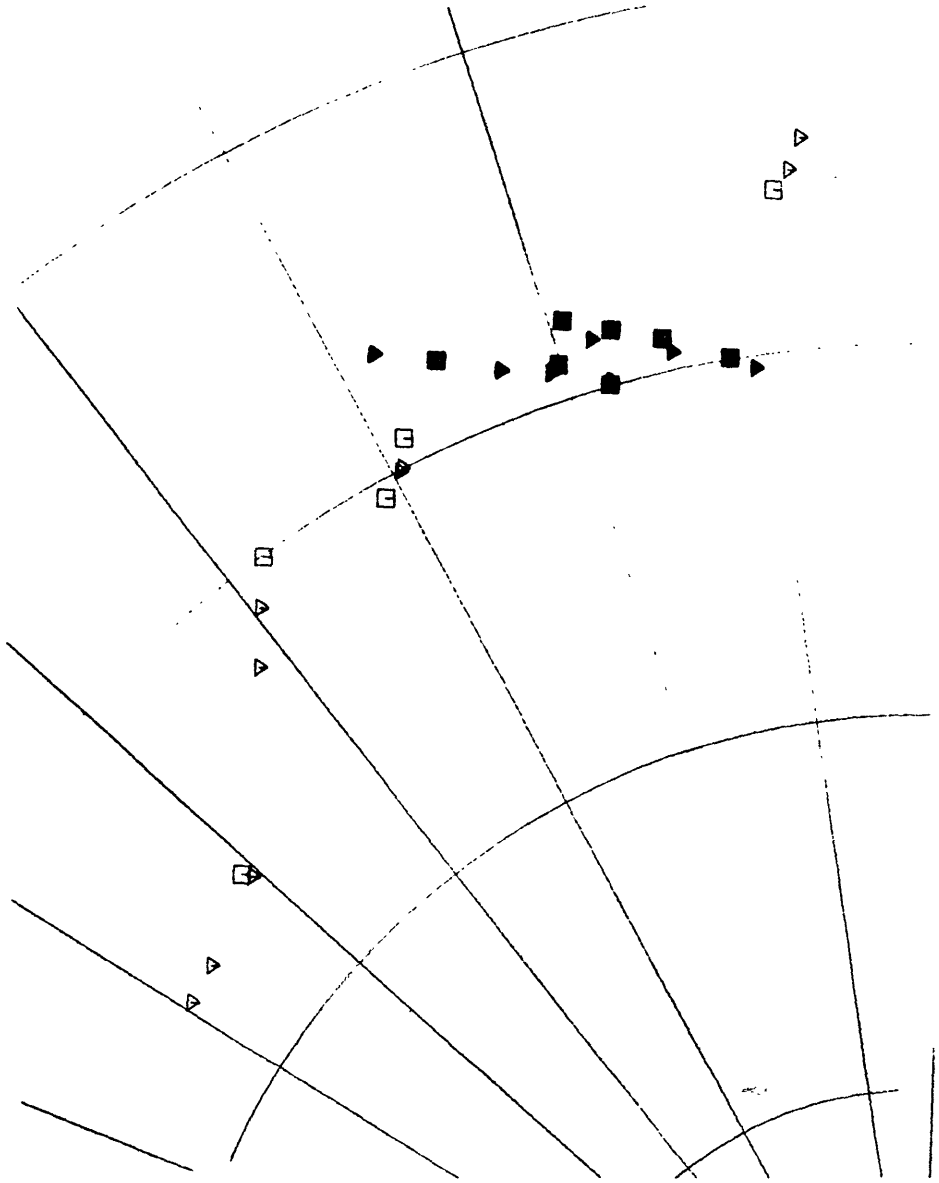

Figure 5c

Anomaly 18 Reconstruction: 74.70,-51.25 (32.62)

Symbols and conventions same as Figure 4a.

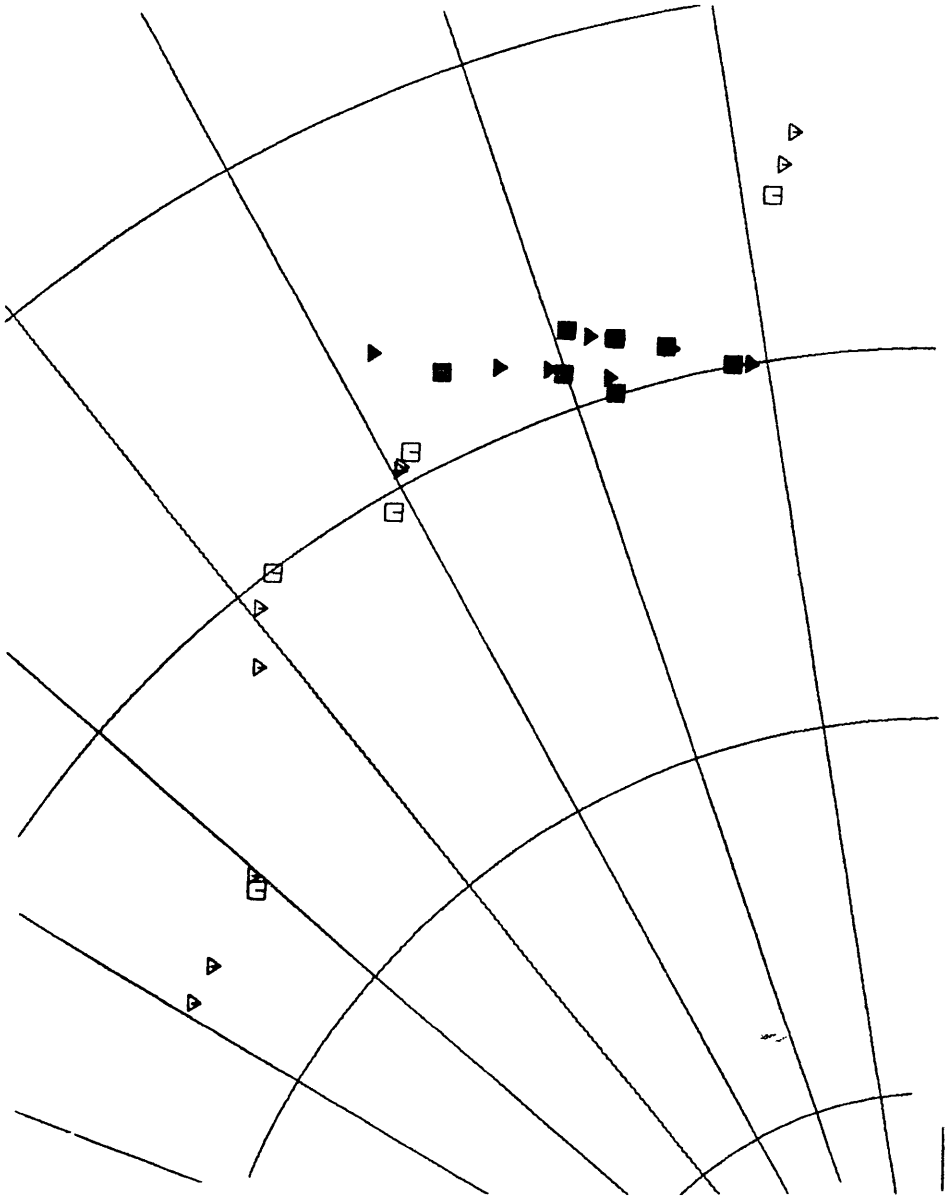

Figure 5d

Anomaly 18 Reconstruction: 75.80,-48.50 (33.07)

Symbols and conventions same as Figure 4a.

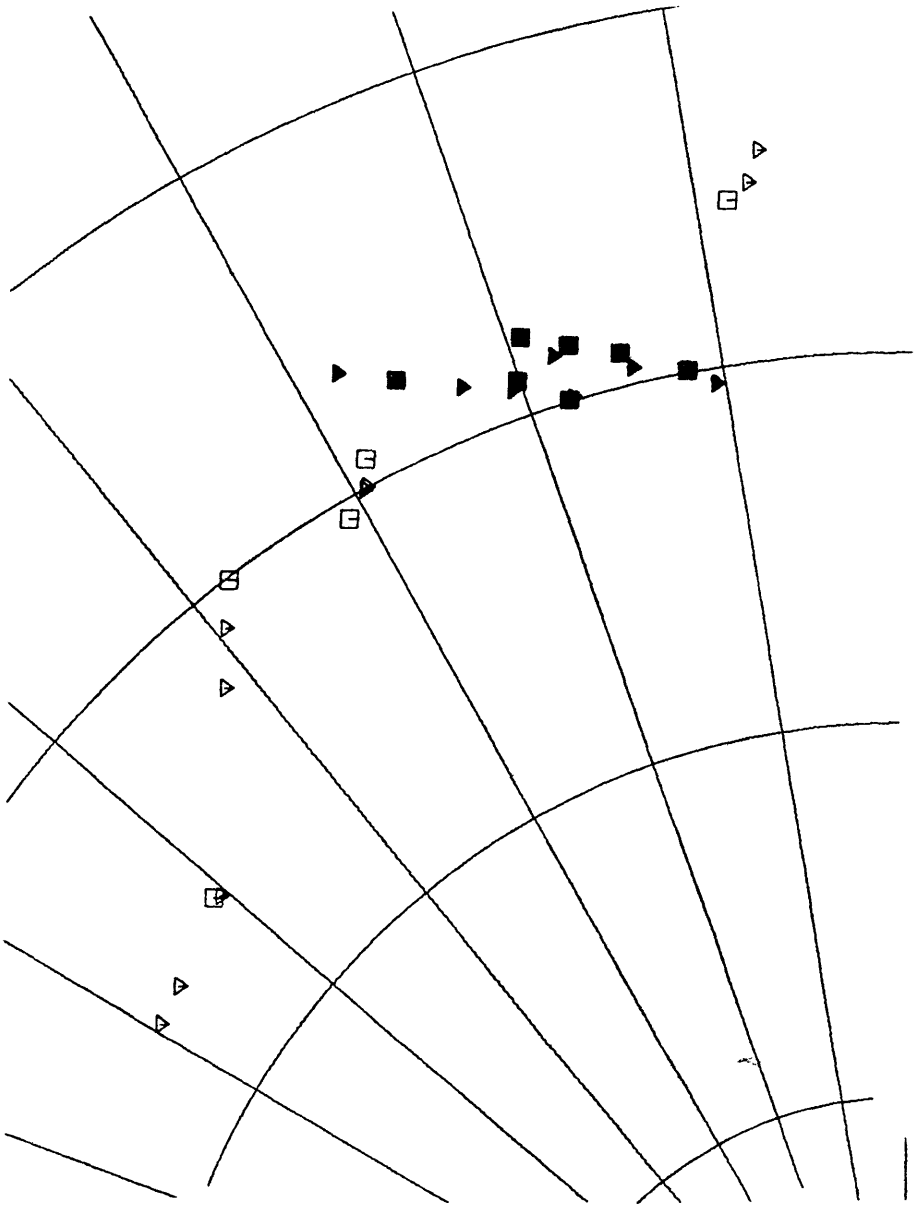

Figure 5e

Anomaly 18 Reconstruction: 75.10,-48.50 (33.27)

Symbols and conventions same as Figure 4a.

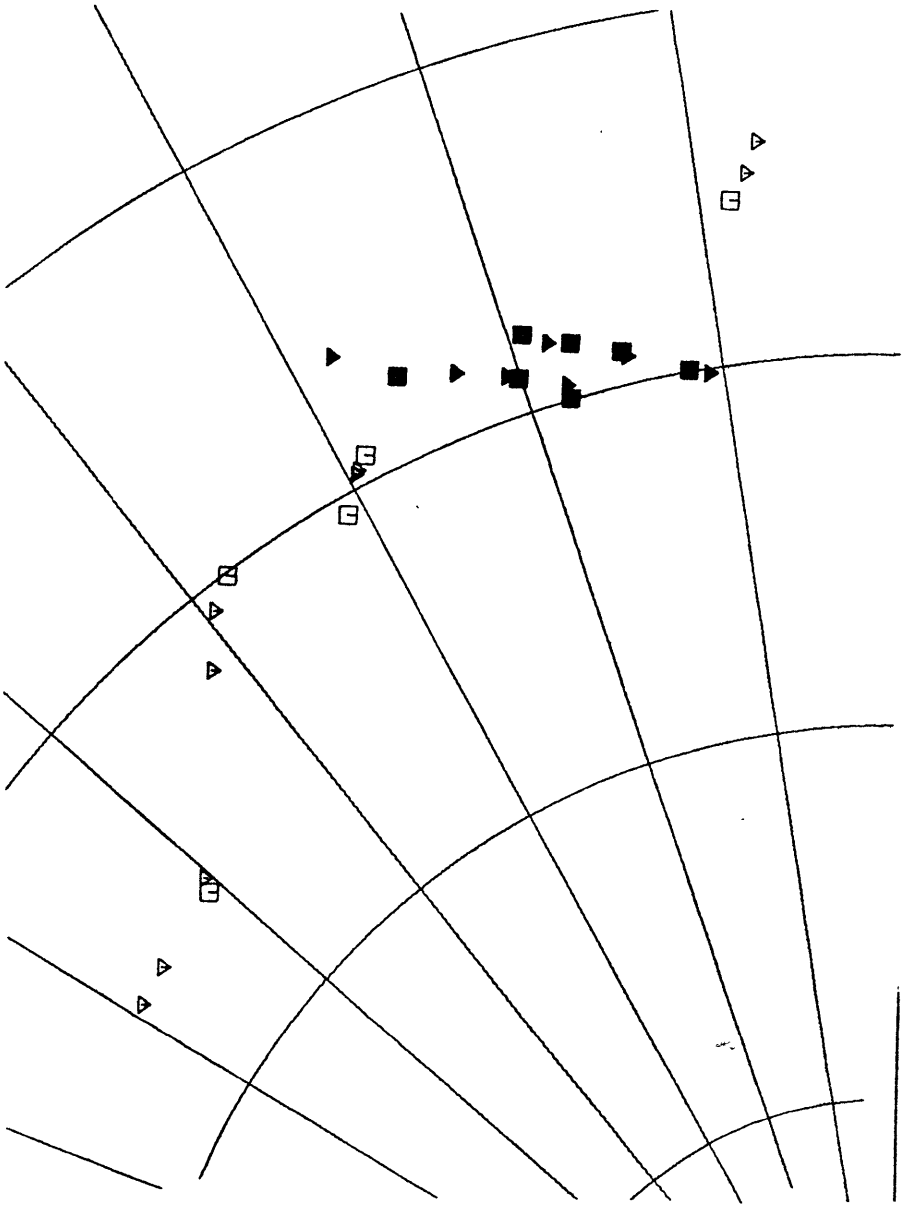

Figure 5f

Anomaly 18 Reconstruction: 75.90,-47.00 (33.43)

Symbols and conventions same as Figure 4a.

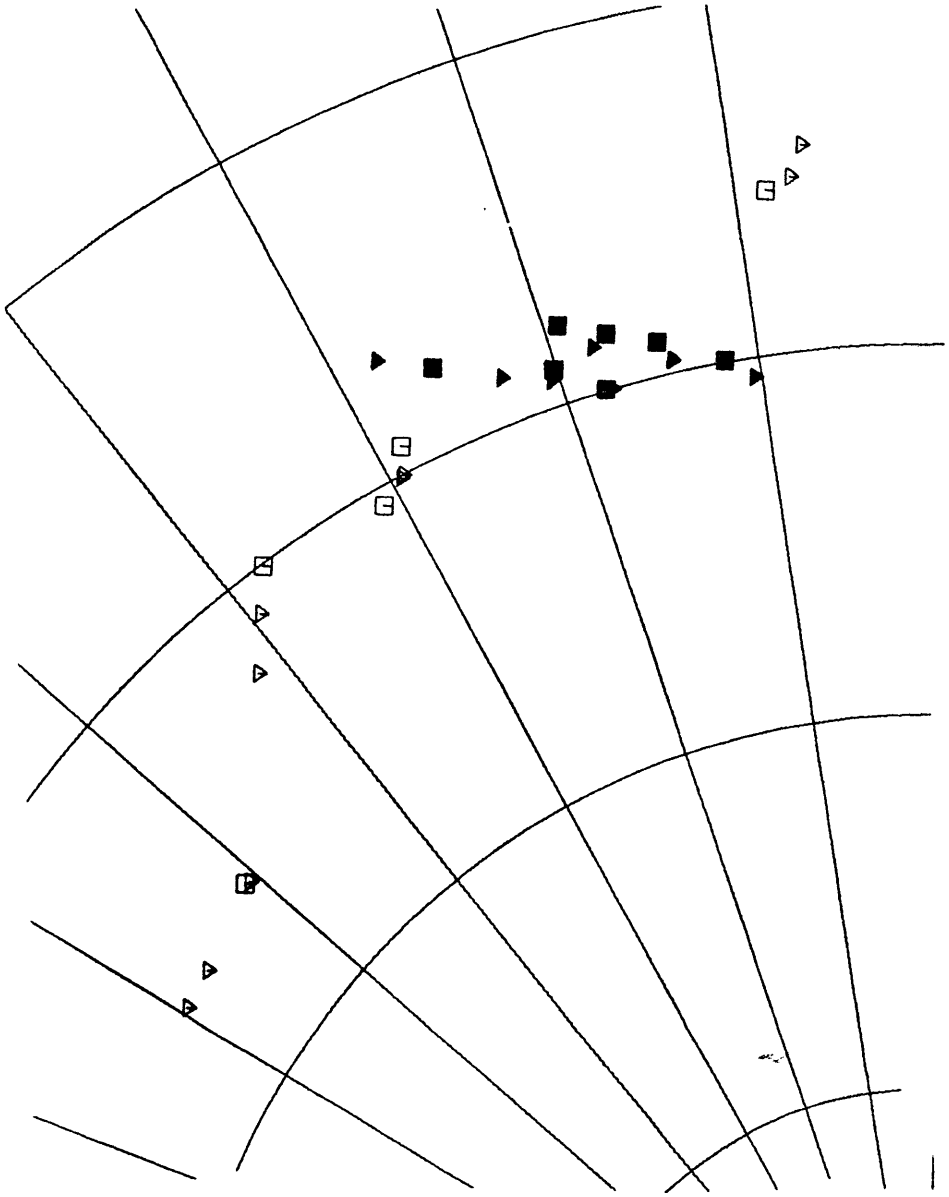

Figure 5g

Anomaly 18 Reconstruction: 75.20,-47.00 (33.65)

Symbols and conventions same as Figure 4a.

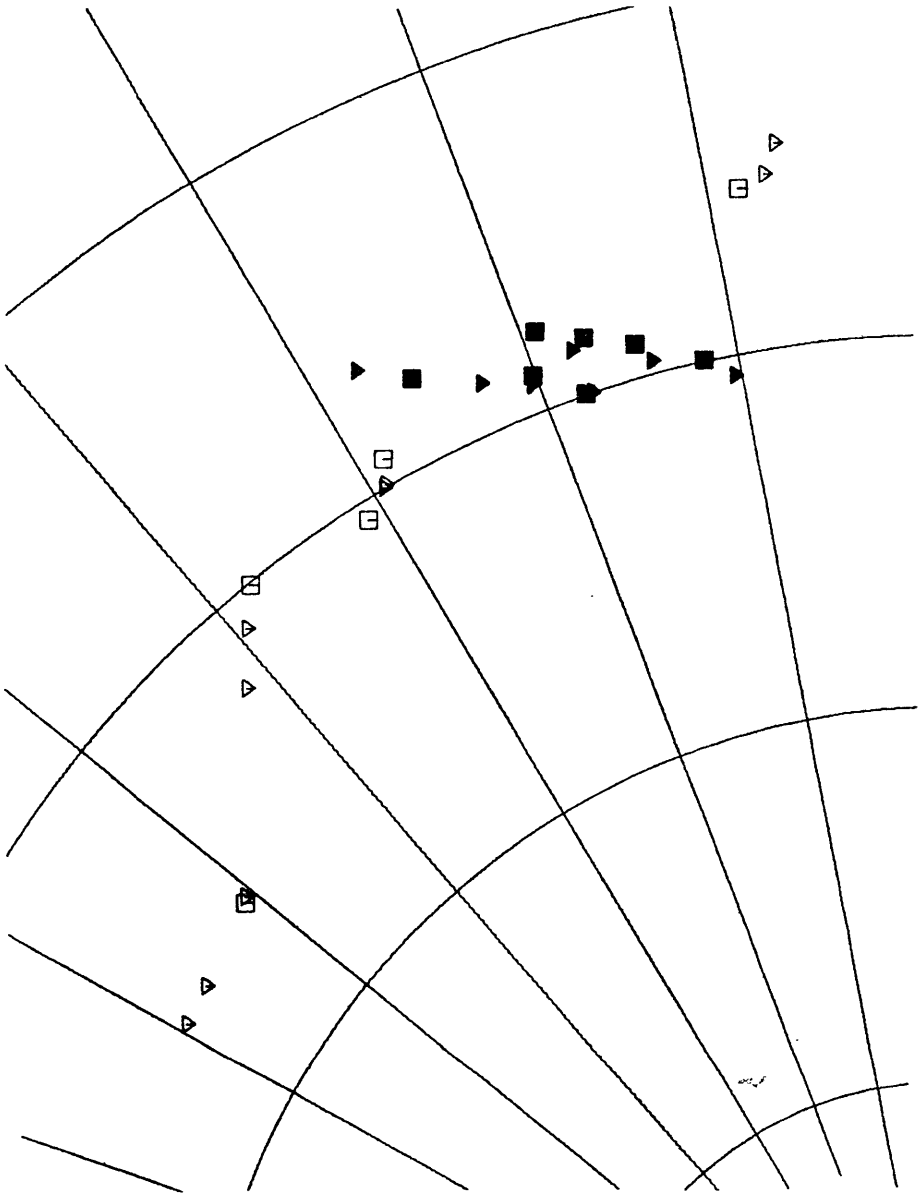

Figure 5h

Anomaly 18 Reconstruction: 75.55,-45.00 (34.09)

Symbols and conventions same as Figure 4a.

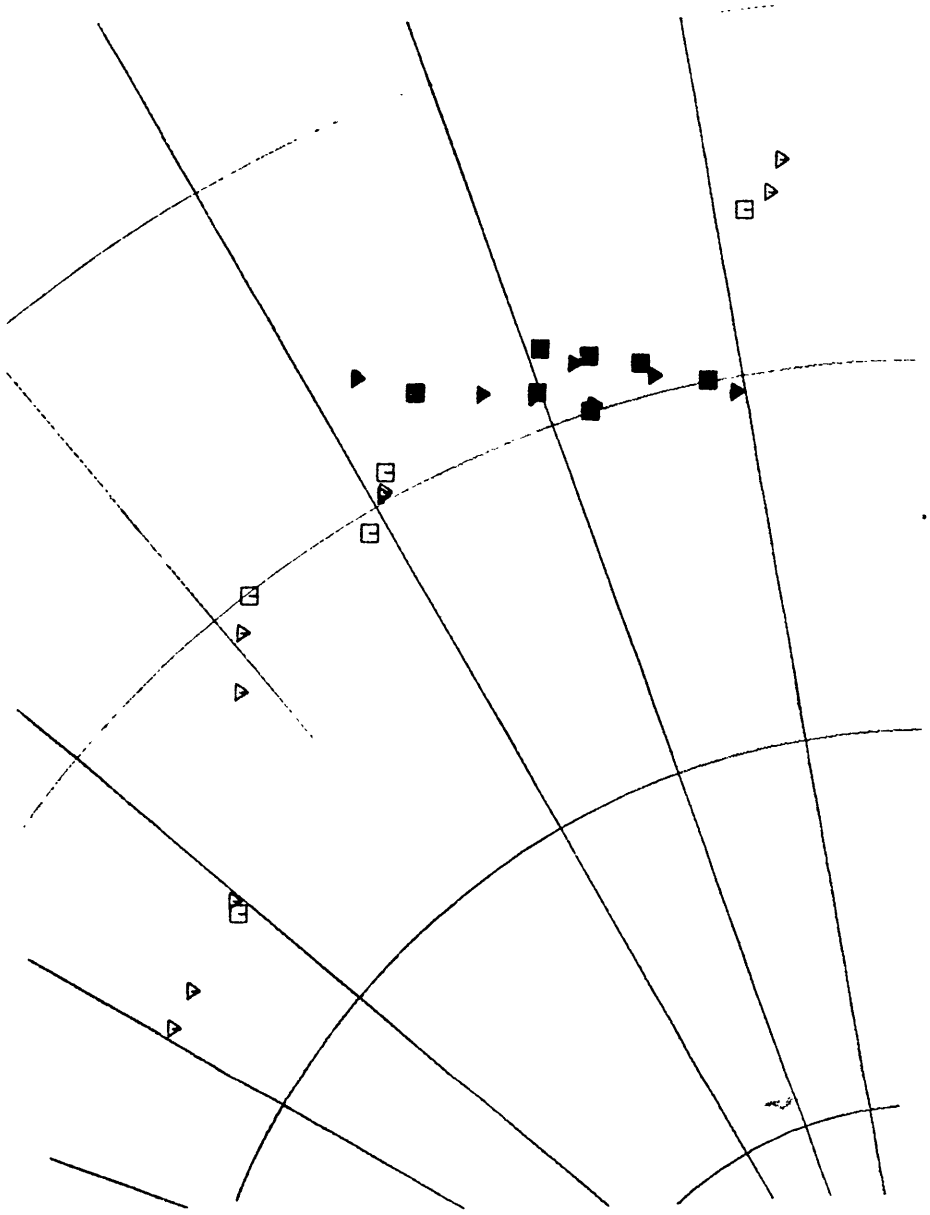

Figure 5i

Anomaly 18 Reconstruction: 75.90,-44.00 (34.23)

Symbols and conventions same as Figure 4a.

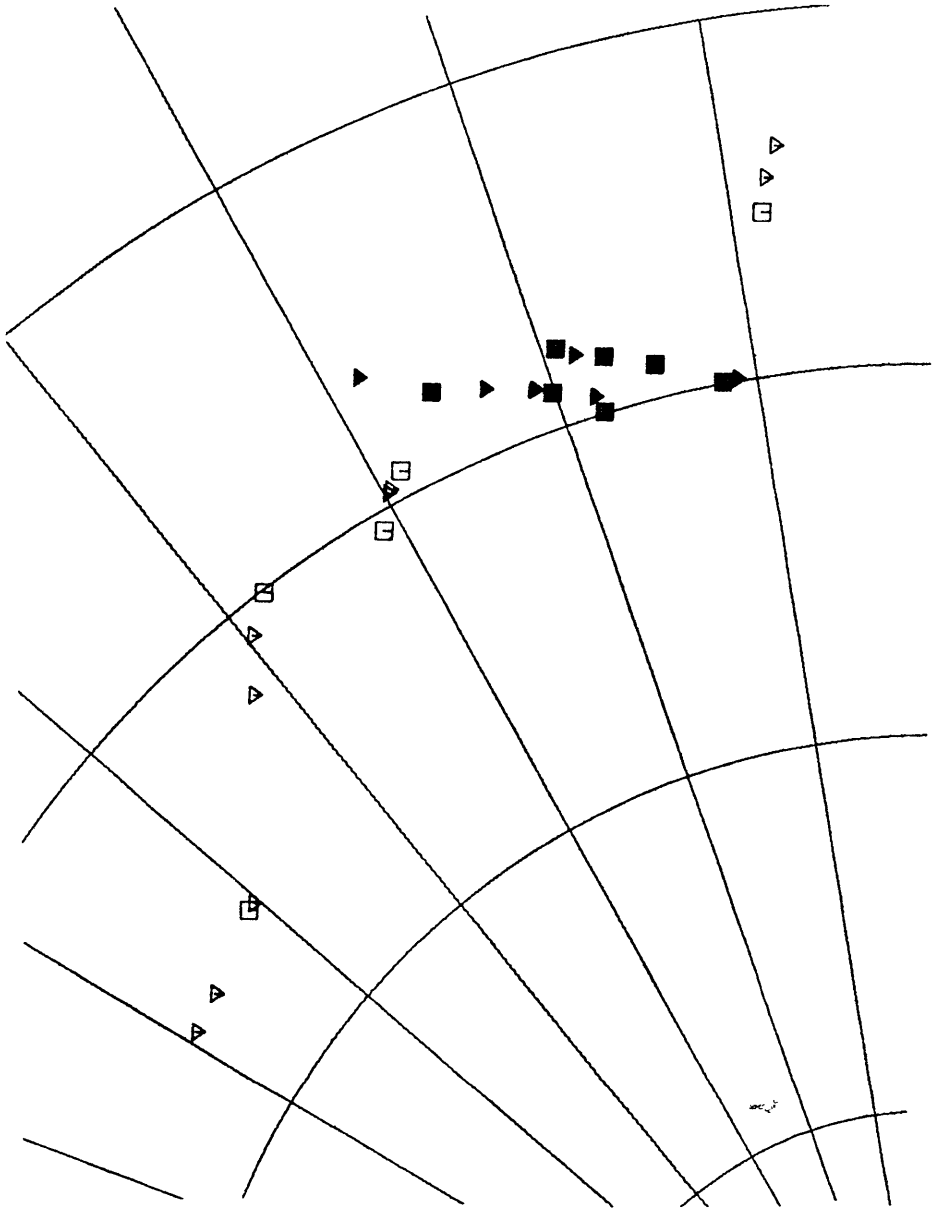

Figure 5j

Anomaly 18 Reconstruction: 75.10,-53.00 (32.09)

Symbols and conventions same as Figure 4a.

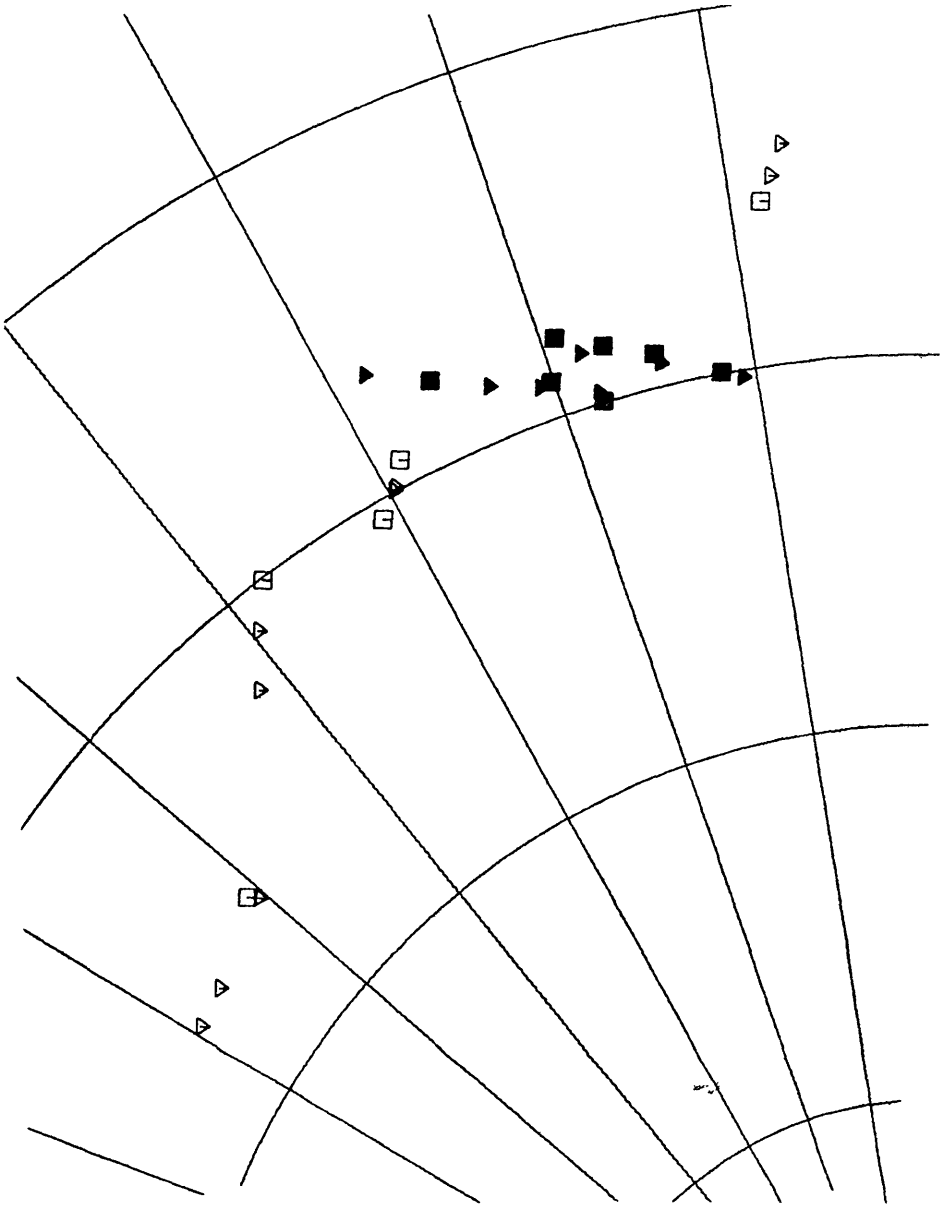

Figure 5k

Anomaly 18 Reconstruction: 74.60,-53.00 (32.19)

Symbols and conventions same as Figure 4a.

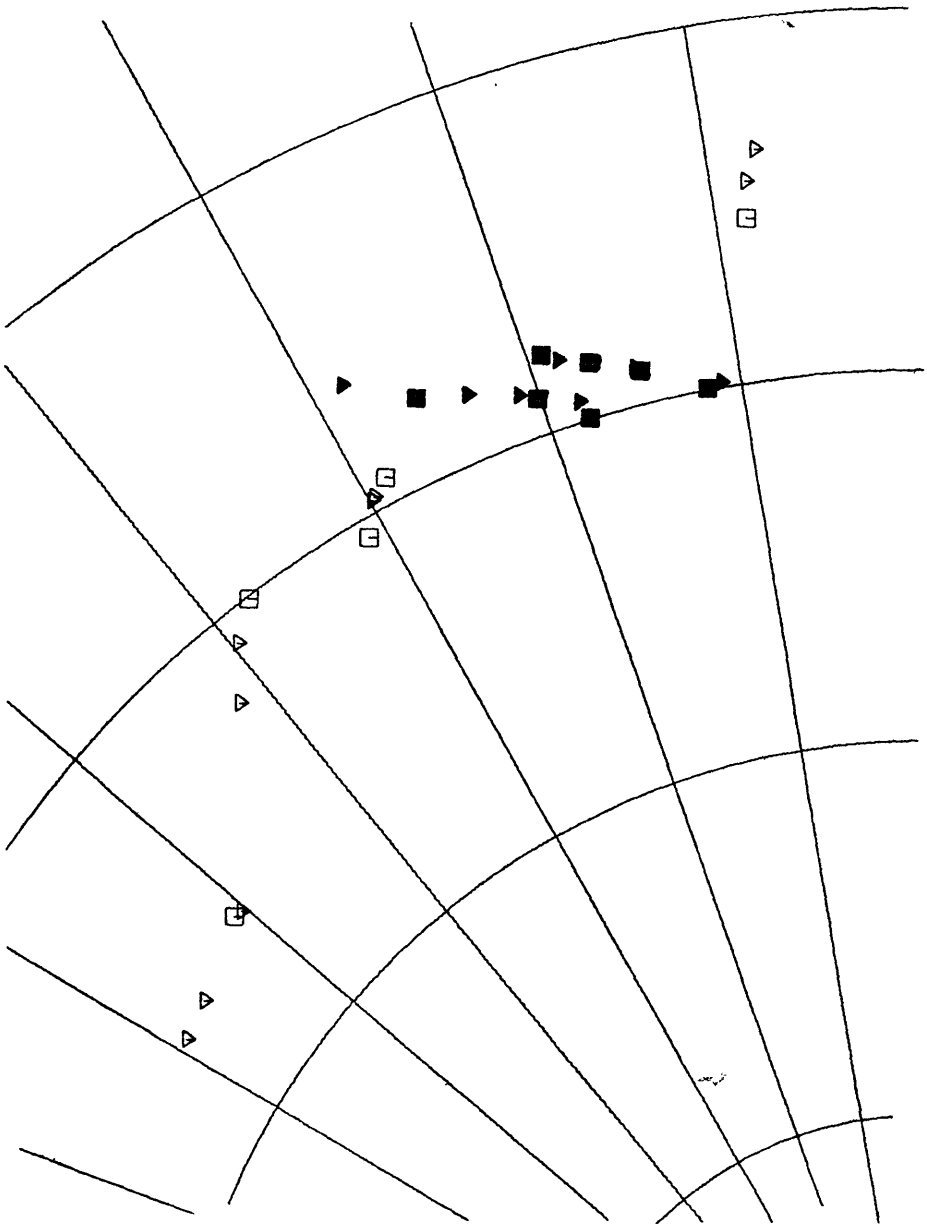

Figure 5L

Anomaly 18 Reconstruction: 74.80,-55.00 (31.63)

Symbols and conventions same as Figure 4a.

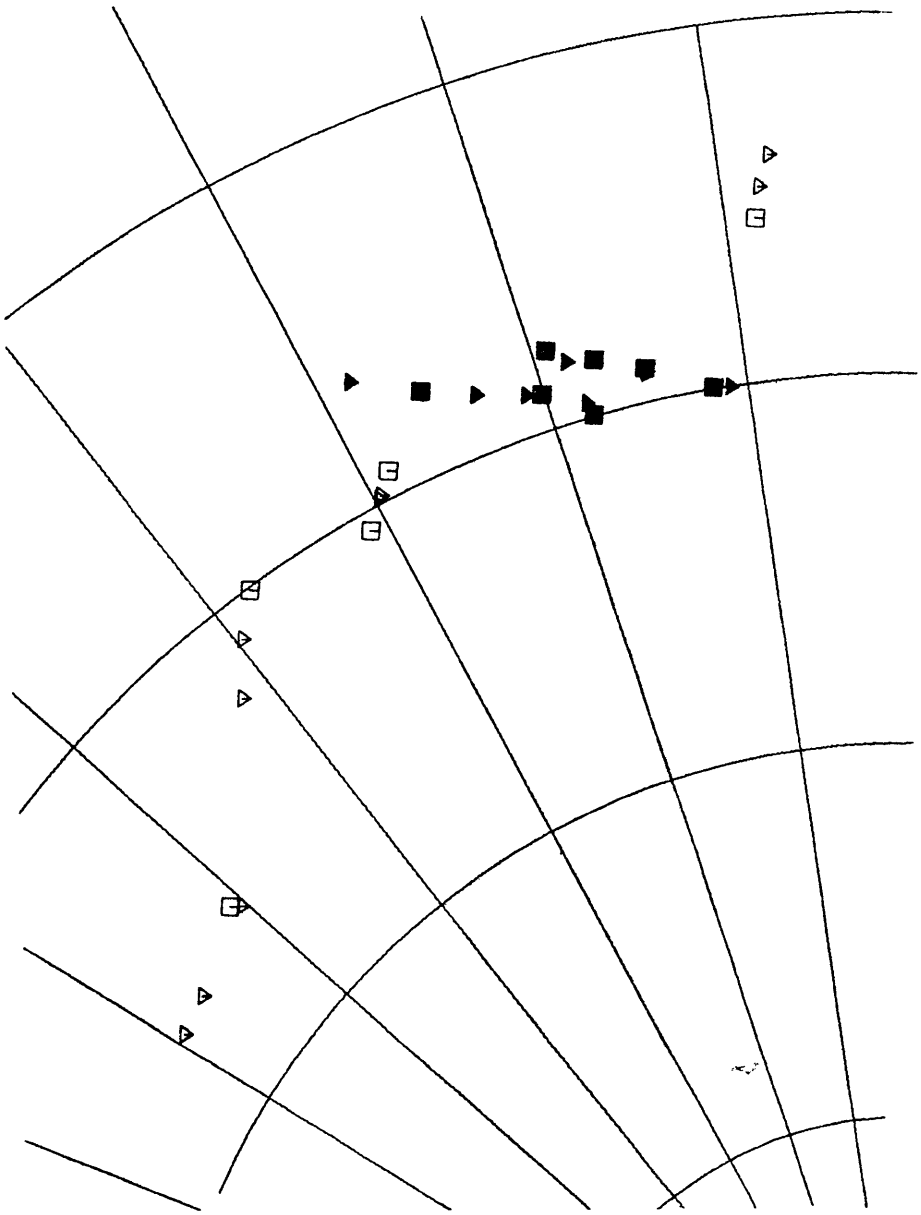

Figure 5m

Anomaly 18 Reconstruction: 74.50,-55.00 (31.68)

Symbols and conventions same as Figure 4a.

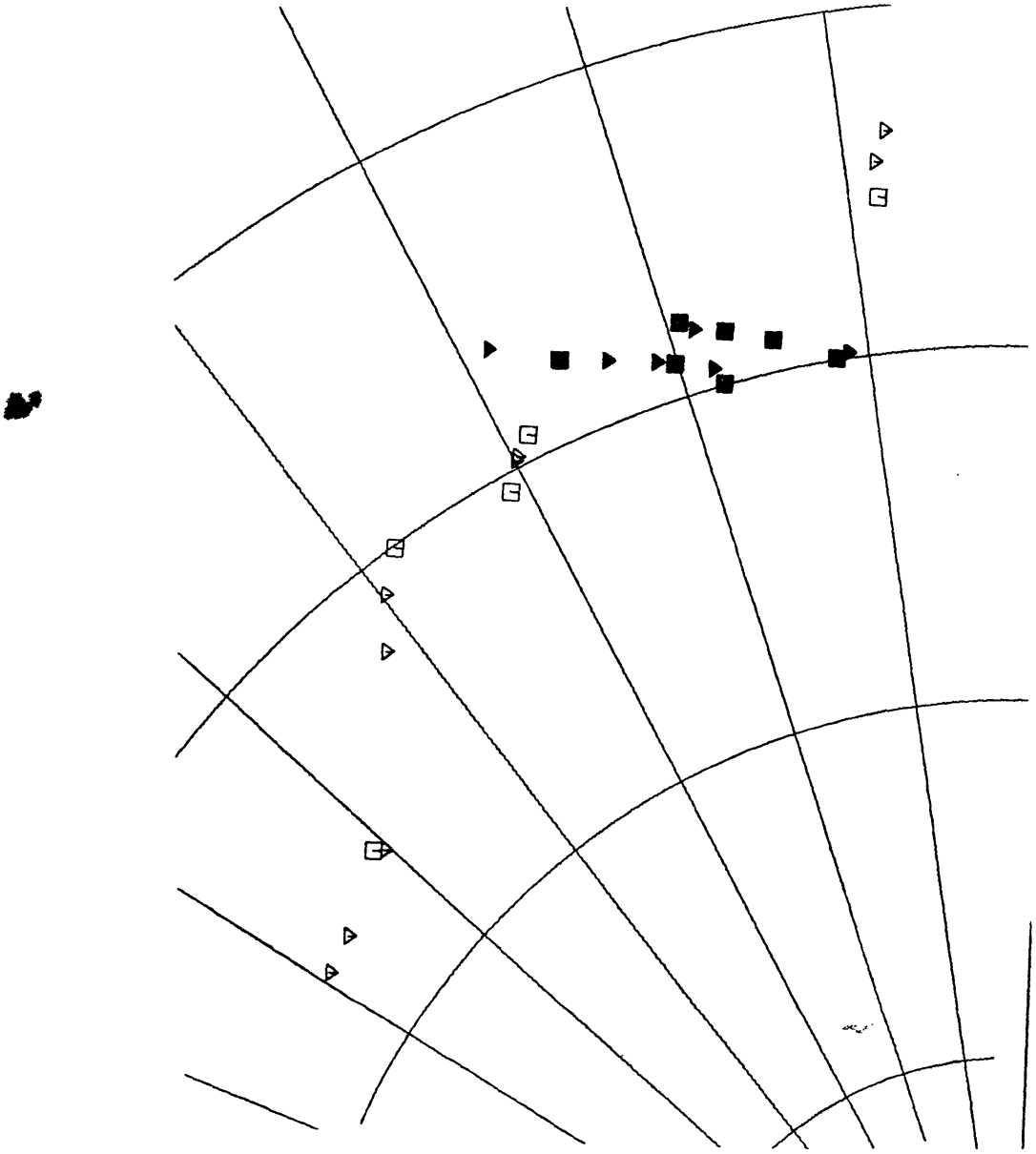

Figure 5n

Anomaly 18 Reconstruction: 74.30,-57.00 (31.17)

Symbols and conventions same as Figure 4a.